

SUPRAMOLECULAR CHEMISTRY ON CARBON DIOXIDE

by

HEXIANG ZHANG

Presented to the Faculty of the Graduate School of
The University of Texas at Arlington in Partial Fulfillment
of the Requirements
for the Degree of

MASTER OF SCIENCE IN CHEMISTRY

THE UNIVERSITY OF TEXAS AT ARLINGTON

December 2007

Copyright © by Hexiang Zhang 2007

All Rights Reserved

ACKNOWLEDGEMENTS

I would like to express my sincere appreciation to Professor Dmitry M. Rudkevich for his guidance and dedication to my education as a chemist. Dear Dr. Rudkevich, thank you for bringing me into this wonderful field of organic chemistry. I will never forget your encouragement and support; I am always proud of being your student.

I would also like to thank the members of my committee, Professors Carl Lovely, Daniel Armstrong, Martin Pomeranz, who challenged me and provided insight during the progress of this work.

I would like to thank all my colleagues in Dr. Rudkevich's group: Dr. Heng Xu, Dr. Valcav Stastny, Dr. Alexandre Leontyev, Dr. Organo Volaire, Mr. Anas Saleh, Mr. Eranda Wanigasekara, Mr. Luis Reyes, Mr. Zak Nixon for their assistance and friendship.

This work was supported by the Petroleum Research Fund and by NSF.

Finally, I would like to thank my parents and my fiancée, Jingyi Wei, for their unending love and support during the last several years; none of this would have been possible without them.

November 21, 2007

ABSTRACT

SUPRAMOLECULAR CHEMISTRY ON CARBON DIOXIDE

Publication No. _____

Hexiang Zhang, MS

The University of Texas at Arlington, 2007

Supervising Professor: Dr. Dmitry M. Rudkevich*, Dr. Martin Pomerantz

This dissertation describes approaches towards designs, syntheses, characterizations, and applications of supramolecular chemistry on carbon dioxide. Chapter 1 briefly overviews the field of supramolecular chemistry and highlights its horizons, also introduces the progress of sensing devices on chemical warfare agents. Chapter 2 introduces a modular approach to detect chemical warfare agent: phosgene by Fluorescence Resonance Energy Transfer (FRET). It combines the chemical reactivity between amines and phosgene with fluorescence properties of coumarin fluorophores, forms a fast, selective and reliable sensing system. Chapter 3 overviews the chemistry between amines and carbon dioxide and introduces the applications of this reaction in the molecular recognition, organic gelations and cation separations. A novel strategy for

alkali metal cation separations is demonstrated by introducing dibenzo-18-crown-6 and lysine derivatives, which successfully extract metal ions from aqueous solution. CO₂ was used to build reversible, supramolecular polymeric materials. Formation of cross-linked, porous supramolecular polymers leads to instant entrapment of organic guest species. These can be stored and then released upon changing solvent polarity, temperature, pH, and concentration. Chapter 4 presents a calix[4]arene based novel strategy for sodium cation separation. Because of high affinity towards sodium cations, calix[4]arene tetraester is selected and functionlized by ethylenediamine on the lower rims. After entrapment of sodium cations, CO₂ gas constructs these calix[4]arene sodium complexes into cross-linked supramolecular polymers. These polymers employ dynamic, thermally reversible carbamate bonds. This approach shows high efficiency and accuracy.

* Deceased August 4, 2007. Supervisorship is substituted by Dr. Martin Pomerantz

TABLE OF CONTENTS

ACKNOWLEDGEMENTS.....	iv
ABSTRACT	v
LIST OF ILLUSTRATIONS.....	ix
Chapter	
1. INTRODUCTION	1
1.1 Supramolecular Chemistry and Hydrogen Bonding	1
1.2 Fluorescence Sensor for the Detection of Chemical Warfare Agents.....	8
1.2.1 Chemically Reactive Sensors	11
2. SUPRAMOLECULAR SENSING DEVICES FOR PHOSGENE BY FRET	16
2.1 Design	16
2.1.1 Fluorescence Resonance Energy Transfer.....	16
2.1.2 Phosgene Sensor	18
2.2 Synthesis	18
2.3 Titrations and Discussions	21
3. CARBON DIOXIDE AND SUPRAMOLECULAR MATERIALS	25
3.1 Introduction to Supramolecular Chemistry of CO ₂	25
3.2 Separation Strategy by Using CO ₂	31

4. SEPARATION OF SODIUM BY CALIXARENE AND CARBON DIOXIDE	36
4.1 Design	36
4.2 Synthesis and Extractions	38
4.3 Results and Discussions.....	40
5. EXPERIMENTAL SECTION.....	44
5.1 General Information.....	44
5.2 Synthesis and Characterizations	45
Appendix	
A. NMR SPECTRA OF COMPOUNDS 1-9, 12-18	56
B. UV-VIS AND FLUORESCENCE SPECTRA	121
C. TITRATION RESULTS	133
REFERENCES	136
BIOGRAPHICAL INFORMATION.....	143

LIST OF ILLUSTRATIONS

Figure	Page
1.1 From molecular to supramolecular chemistry.....	2
1.2 Structures of crown ethers (A), cryptands (B), and cyclodextrins (C).....	3
1.3 Hydrogen-bonded self-assemblies	5
1.4 Major classes of chemical warfare agents, pesticides and nerve agent mimics and chemical structures of common representatives.....	9
1.5 Mechanism of the chemically reactive sensor developed by Pilato and co-workers (top), and by Swager and coworkers (bottom).....	12
1.6 The chemically reactive sensor developed by Rebek and coworkers	14
2.1 A FRET based approach to the detection of phosgene	17
2.2 Structures and spectral characteristics of the donor and acceptor dyes	18
2.3 Synthesis of donor amine 4 and acceptor amine 6	19
2.4 Fluorescence spectra of compound 4 and 6	20
2.5 Synthesis of ureas 7 , 8 , 9	21
2.6 Fluorescence spectrum of compound 9	22
2.7 Typical changes in fluorescence emission spectra upon titrations with triphosgene	23
2.8 The “naked eye” detection of triphosgene	24
3.1 Circulation of carbon dioxide: <i>Carbon Cycle</i>	26
3.2 Reversible covalent chemistry between CO ₂ and amines: self-assembly of molecular blocks.....	26

3.3	Structure of a CO ₂ -trapping ionic liquid	27
3.4	Model for fluorimetric sensing of CO ₂	28
3.5	Reversible covalent chemistry between CO ₂ and amines. Self-assembly of molecular blocks leads to linear (case A) and cross-linked polymers (case B) amines.....	30
3.6	Separation strategy uses CO ₂ as a cross-linking agent in the formation of supramolecular carbamate polymers	33
3.7	Potassium separation by dibenzo-18-crown-6 Lysine derivatives. Reaction with CO ₂ leads to the formation of insoluble in CHCl ₃ supramolecular polymeric materials b and d , which could be separated by simple filtration. Polymer d also separates K ⁺ Pic ⁻ by complexation. Polymers b and d can dissociate back to the corresponding monomers upon heating or addition of acid.....	34
4.1	Separation strategy using CO ₂	36
4.2	Separation of Na ⁺ involves calix[4]arene receptor 14 and CO ₂	37
4.3	Synthesis of calix[4]arene derivatives for sodium separation.....	39
4.4	Extraction, entrapment and separation of sodium ions	40
4.5	Portions of the ¹ H NMR spectra (500 MHz, rt, DMSO- <i>d</i> ₆) of: a) receptor 14 ; b) Na ⁺ -complex 17 . The residual Et ₃ N quartet is at ~2.8 ppm.....	41
4.6	The formation of polymeric carbamate using CO ₂	42

CHAPTER 1

INTRODUCTION

1.1 Supramolecular Chemistry and Hydrogen Bonding

Supramolecular chemistry has developed in the past decades as a borderline scientific field between chemistry, physics, and biology. The concept and term of supramolecular chemistry were introduced by Lehn et al. in 1978.¹ This chemistry was defined as “chemistry beyond the molecule”, based on the organized entities of higher complexity that result from the association of two or more chemical species held together by intermolecular forces.²

As molecular chemistry deals with molecules, supramolecular chemistry deals with supramolecular species, which are usually called “molecular receptor” and “substrate” (Figure 1.1). Binding of a substrate by a receptor yields supramolecules, and the binding process reflects molecular recognition. Numerous papers have appeared in this field. The substrates are usually cations, anions, neutral organic molecules, and even gases, while receptor molecules have complimentary molecular size, shape and architecture with the substrates, establishing non-covalent binding interactions.³ Macrocyclic compounds possess numerous branches, bridges and connections, and thus become the favorite receptors, which in most cases contain intramolecular cavities for a variety of substrates. Among these macrocyclic compounds, crown ethers, cyclodextrins, and calixarenes are most intensively investigated.

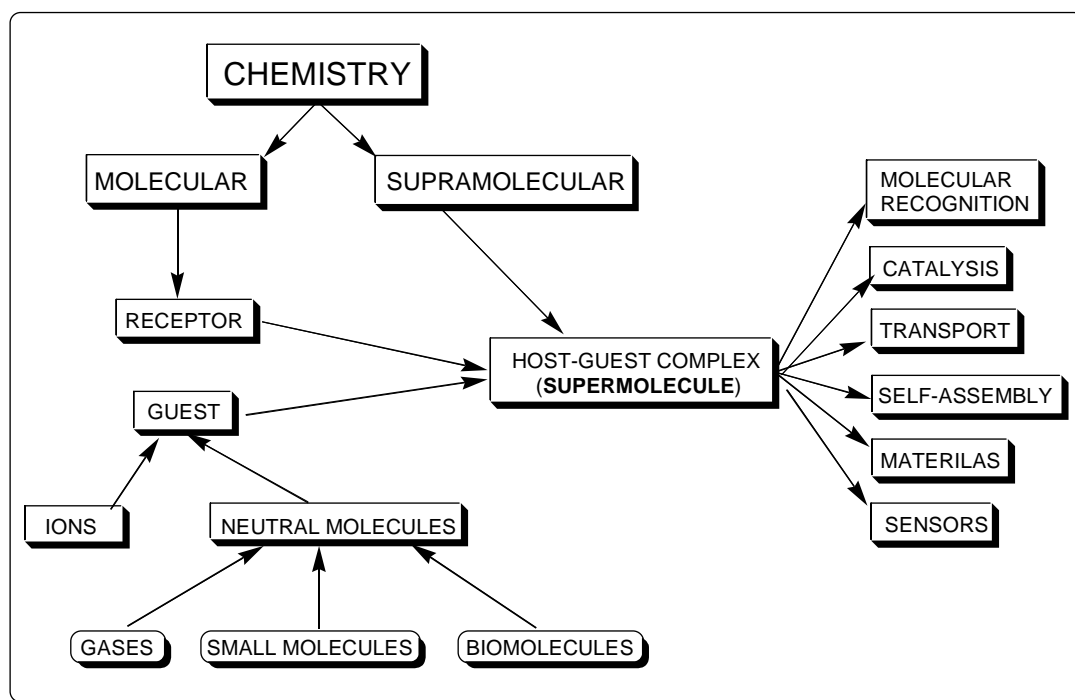


Figure 1.1 From molecular to supramolecular chemistry.

Crown ethers are macrocyclic compounds. They were discovered in the middle of 1960s by Charles Pedersen and are based on repeating $\text{-OCH}_2\text{CH}_2\text{-}$ units, derived from ethylene glycol.⁴ Varying the number of these units results in different size of the crown ether (Figure 1.2A). These compounds showed strong affinities for metal cations, such as Li^+ , Na^+ , K^+ . The applications of crown ethers led to phase-transfer catalysis, biological ion transfer, membrane transport, extractions, etc.⁵

Cryptands are another important class of macrocyclic compounds which contain three-dimensional, spherical cavities (Figure 1.2B). This work started in 1967 by Lehn⁶ shortly after discovery of crown ethers. Cryptands entirely surround the bound ions and form stronger complexes than the flat shaped macrocycles, thus displaying *spherical*

recognition of appropriate cations and anions. Numerous effects from these strong complexes have been brought about and studied in detail, such as: stabilization of alkalides and electrides, dissociation of ion pairs, anion activation, isotope separation, toxic metal binding, etc.⁷

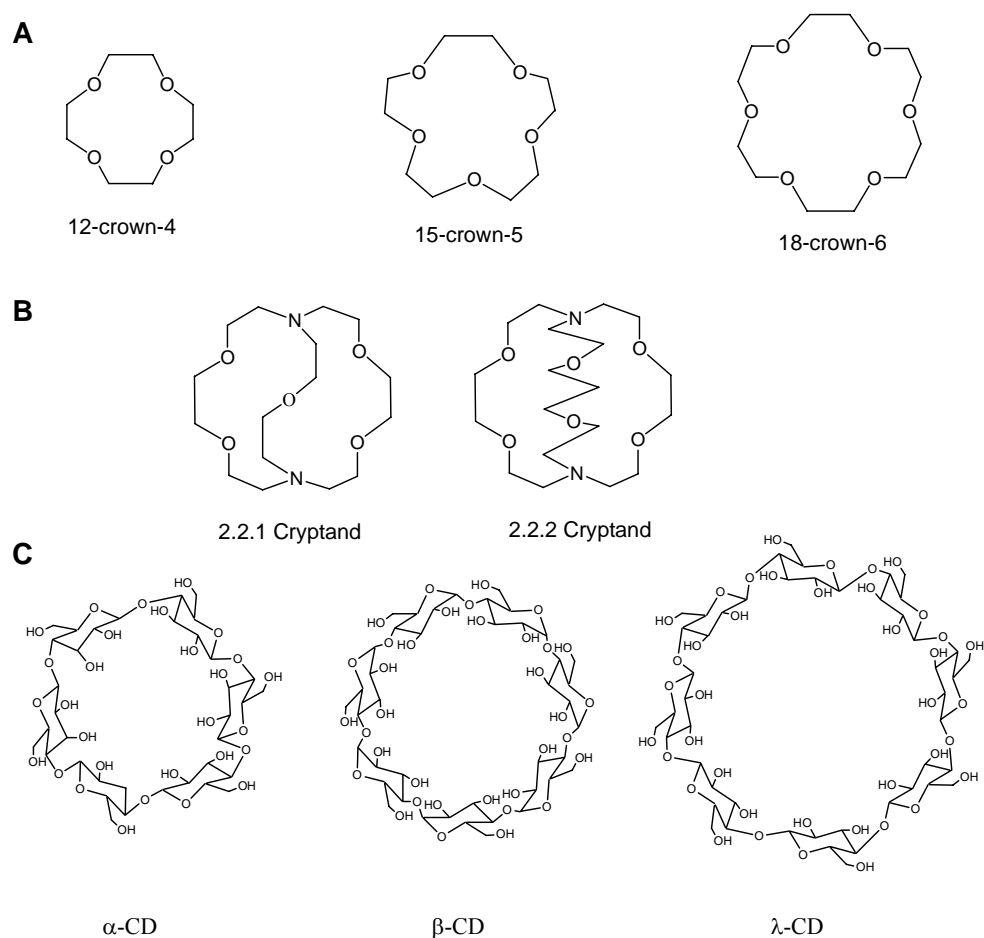


Figure 1.2 Structures of crown ethers (A), cryptands (B), and cyclodextrins (C)

Naturally occurring cyclodextrins are bucket-shaped oligosaccharides produced from starch (Figure 1.2C). Due to their molecular structure and shape, they possess a unique ability to act as molecular containers by entrapping guest molecules in

their internal cavities. The resulting inclusion complexes are one of most popular classes of host-guest supramolecules in academic research and they also offer a number of potential advantages in pharmaceutical formulations.⁸

Calixarenes were introduced in 1978 by C. D. Gutsche⁹ as cup-like shapes, capable of complexing guest molecules. Since then, calixarenes have attracted a lot of research attention in this field. Earlier work focused on functionalizing calixarenes on both its upper and lower rims to afford a variety of cavities of different shapes and sizes. Those calixarenes were mostly studied as receptors for metal cations. More recently, calixarenes have been utilized to construct cavitands, (hemi)carcerands and self-assembling capsules, in which larger neutral organic molecules, cations, anions, were bound.¹⁰

Besides binding of one molecule by another, supramolecular chemistry studies the self-assembly of multiple molecules into supramolecular structures. Self-assembly is the autonomous organization of components into patterns or structures without human intervention.¹¹ Since self-assembling processes are common throughout nature and technology, it was first studied in biology and physics.^{12,13} Supramolecular chemistry provides ways and means for chemical science to explore this area and apply its power of design and control. By self-assembly processes, receptors, transport agents, enzyme models, and extended arrays are constructed. These artificial assemblies are being utilized to mimic biological systems and applied to emerging scientific fields, especially nanotechnology. Self-assembly has become a rapidly growing field for two reasons. First, it is a crucial concept to understand many biologically important structures.

Second, it provides a solution to the problem of synthesizing larger structures. Although total synthesis of complex molecules can be achieved nowadays, synthesis of molecular structures with molecular weights >1000 Da through the stepwise formation of covalent bonds is still a formidable challenge.

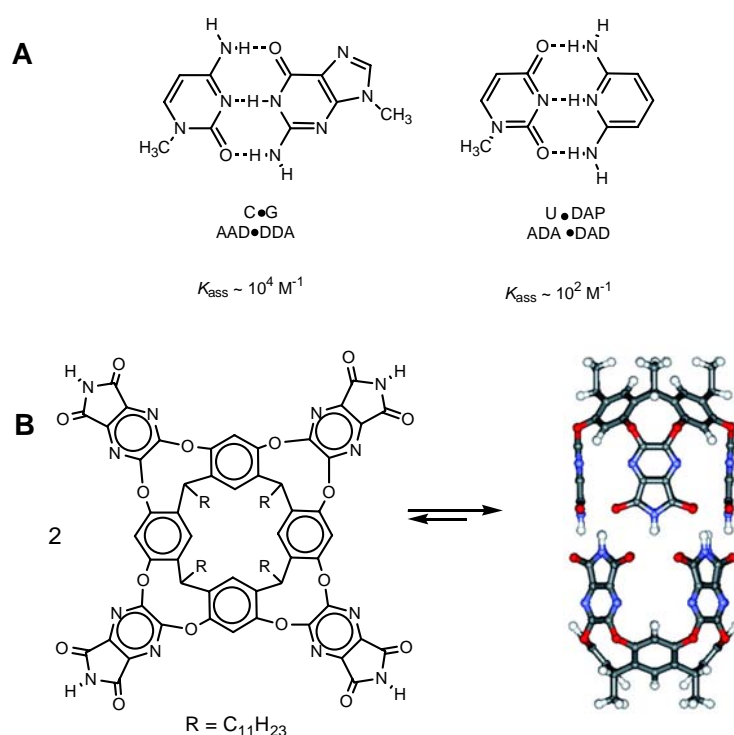


Figure 1.3 Hydrogen-bonded self-assemblies.

Hydrogen bonding is most frequently utilized in self-assembling systems, because it is directional, specific, and biologically relevant. Numerous self-assembly models on organic supramolecular structures have been reported in the literature, which can be categorized as dimers, multimers, capsules, polymers and nano-scale architectures, etc.¹⁴

Stable H-bond directed assemblies in most cases require multiple hydrogen bonds, while a variety of small organic functionalities, such as phenols, amines, and amides can dimerize through single H-bond. For stable assemblies, the number of hydrogen bonds is certainly not the only important parameter. “Cooperativity” is usually considered a key factor in increasing the stability of assemblies. The Jorgensen model was used as a basic rule to qualitatively predict the association constant between the individual units. These differences in stability can be largely attributed to attractive and repulsive secondary interactions. Stabilization arises from electrostatic attraction between positively and negatively polarized atoms in adjacent H-bonds, whereas destabilization is likewise the result of electrostatic repulsion between two positively or negatively polarized atoms (Figure 1.3 A).¹⁵ According to this model, AA•DD (A refers to Acceptor, D refers to Donor) in 2-H-bond modules and AAA•DDD in 3-H-bond modules were predicted to have highest association constant values. These predictions have been proven by experimental data.¹⁶ In 4-H-bond modules, AADD•DDAA arrays have been designed and demonstrated high stability with the association constant over $1 \times 10^6 \text{ M}^{-1}$.¹⁷ Apart from the expected increase in stability, the even number of H-bond donors and acceptors in 4-H-bond modules allows self-complementarity to be introduced in these motifs. Self-complementarity provides an attractive property for applications in polymeric materials or molecular capsules.

The development, characterization, and exploitation of novel materials based on the assembly of molecular components is an exceptionally active and rapidly expanding materials field. Electronic, magnetic, optical, structural, mechanical, and chemical

characteristics were considered. The formation of supramolecular entities from photoactive components may be expected to show the ground-state and excited-state properties of the individual species, giving rise to novel properties. Assembling individual components into supramolecular systems may initialize a number of processes: excitation energy migration, photo-induced charge separation by electron and proton transfer, perturbation of optical transitions and polarizabilities, modification of redox potentials, selective photochemical reactions, etc. For example, efficient energy transfer devices have been designed and synthesized based on a rigid linear array of porphyrin units.¹⁹ Self-assembled heterocyclic ribbons were shown to allow the directed long-range transfer of protons, thus functioning as proton-conducting channels.²⁰

Beyond the molecule, supramolecular chemistry aims at developing highly complex chemical systems from components interacting by noncovalent intermolecular forces. It has been growing into a major field over a quarter of the last century and fueled numerous developments at the interface with physics and biology. New horizons are still emerging to bring this field into a more complex, informational, selective, and practical world.²¹ Through appropriate manipulations of intermolecular noncovalent interactions, storage of information at the molecular level has become feasible and retrieval, transfer, and processing of the information can then be accomplished. This venture involves design and investigation of well pre-organized receptors, capable of binding to substrate with high efficiency and selectivity. Supramolecular chemistry opens new perspectives in materials science toward an area of supramolecular materials, “smart” materials whose features depend on molecular information. It allows the

design of materials and the control of their build-up from suitable units by self-organization. Supramolecular chemistry is gaining a lot of attention in the field of nanoscience. Indeed, the spontaneous but controlled generation of well-defined, functional supramolecular nanostructures through self-organization offers a very powerful alternative to nanofabrication and nanomanipulation, bypassing the implementation of tedious procedures and providing a chemical approach to nanoscience and technology.²²

1.2 Fluorescent Sensors for the Detection of Chemical Warfare Agents

Since early utilization in World War I, many different types of chemical warfare agents (CWAs) have been developed in laboratories around the world. Along with biochemical and nuclear threats, these weapons have become some of the most feared and least predictable mass destruction agents on the battlefield and in the hands of terrorists. CWAs were defined by one United Nations report at 1969 as "...chemical substances, whether gaseous, liquid, or solid, which might be employed because of their direct toxic effects on man, animals, and plants...". Some common representatives of the major classes of CWAs are shown in Figure 1.4. These include vesicants (blister or mustard agents), nerve agents (such as Sarin and Soman), blood agents (e.g. hydrogen cyanide), and pulmonary agents (choking agents such as phosgene). Another class of important chemical warfare agents includes natural toxins, such as the protein Ricin and the alkaloid Saxitoxin. The nerve agents represent one of the most important and lethal classes of chemical warfare agents. Their rapid and severe effects on human and animal health stem from their ability to block the action of acetylcholinesterase (AChE), a

critical central nervous system enzyme that is responsible for the breakdown of the neurotransmitter acetylcholine.

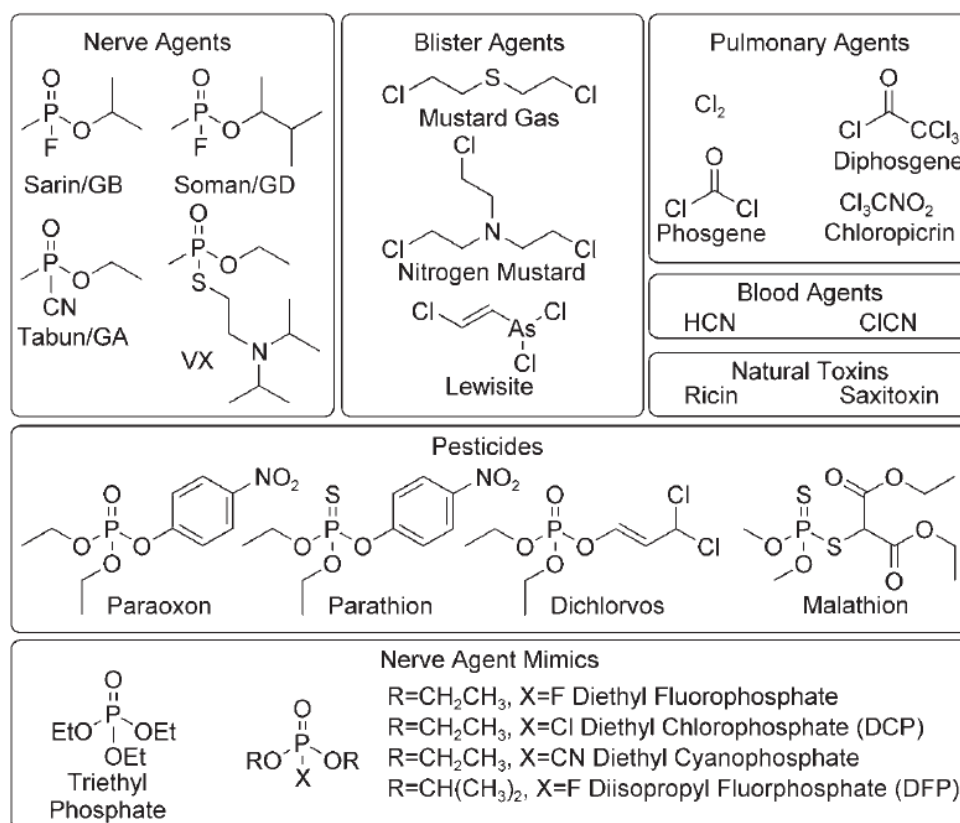


Figure 1.4 Major classes of chemical warfare agents, pesticides, and nerve agent mimics and chemical structures of common representatives.

Most of nerve agents are organophosphates (OPs) and capable of reacting with the esteratic site of the enzyme leading to a loss of enzyme function. Compared to the normal acylated intermediate complex, the phosphorylated enzyme is very stable and very slowly breaks down, leading to a loss of enzyme function.²³ This results in a build up of acetylcholine in the body, which can lead to organ failure and eventual death. The enzyme function can be restored with compounds that can dephosphorylate the enzyme

and as a consequence such compounds can be used as antidotes. Examples of such reactivating agents include oximes, such as Pralidoxime chloride.²³ OP nerve agents are generally stable, easy to disperse, and highly toxic. They can be absorbed through the skin, by ingestion, or by respiration and are generally classified into two groups, G-agents and V-agents. The G-series is older (developed in the World War II era) and encompasses compounds that are generally volatile, for example Tabun, Sarin, and Soman. The more modern V-series (developed in the 1950s) consists of nerve agents that are typically less volatile oils, such as VX. The V-agents generally degrade slower than G-agents, which along with their reduced volatility makes them more persistent. Furthermore, V-agents tend to be more toxic than representatives of the G-series (e.g. VX is about ten times more toxic than Sarin) and, as a consequence of their physicochemical properties, are primarily, although not exclusively, absorbed through the skin. Organophosphorus nerve agents were used in the Iraq–Iran war in the 1980s and as recently as 1995, in the Aum Shinrikyo terrorist attacks on the Tokyo subway system. In addition to CWAs, several organophosphorus derivatives, for example, paraoxon, parathion, dichlorvos, and malathion, have found commercial use as pesticides (Figure 1.4).²⁴ Their chemical structures closely resemble those of the above-discussed nerve agents, and hence, the development of detection systems for these compounds follows similar design principles.

In response to the serious threats to national and global security that result from the comparatively easy access to nerve agents, intense research efforts have been directed over the years to develop sensitive and selective schemes for the detection of

such organophosphorus derivatives.²⁵ Several different approaches have been used to detect organophosphorus compounds, including but not limited to: potentiometric methods,²⁶ colorimetric methods,²⁷ surface acoustic wave spectroscopy,²⁸ gas chromatography/mass spectrometry,²⁹ and interferometry.³⁰ One of the most convenient and simplest means of chemical detection is generating an optical event, such as a change in absorption or fluorescence intensity/color.³¹

1.2.1 Chemically Reactive Sensors

Chemically reactive sensors are compounds which alter specific properties (e.g., optical) upon reaction with an analyte of interest. The general reaction mechanism exploited by chemically reactive sensors for the detection of OP CWAs mimics the chemical framework of the AChE inhibition by CWAs, namely nucleophilic attack of the sensor molecule on the electrophilic OP analyte. Upon reaction with the OP, the reactive sensor molecules are converted into phosphate esters. This process can lead, either directly or through subsequent reactions that are enabled by the activating nature of the phosphate ester formation, to a change of the sensor molecule's fluorescence characteristics. The first fluorescent reactive chemosensors for the detection of organophosphates were reported by Pilato et al.³² A non-emissive platinum 1,2-enedithiolate complex with an appended primary alcohol was used as the chemosensor (Figure 1.5 top). Upon exposure to an electrophilic OP analyte and an activating agent (triazole) in dichloromethane, the alcohol is converted into the phosphate ester. This intermediate then undergoes a rapid intramolecular ring-closing reaction that is accompanied by the loss of a phosphate monoanion and affords a fluorescent cyclic

product. The rate-determining step of this reaction is the nucleophilic attack of the sensor on the OP analyte. When immobilized in plasticized cellulose acetate/triethylcitrate films, chemosensors based on platinum 1,2-enedithiolate complexes were able to detect $\text{PO}(\text{OEt})_2\text{X}$, ($\text{X} = \text{Cl}$, F , and CN) vapor in a nitrogen atmosphere. The fastest response time reported for such sensors was 15 s. The main limitation of this particular series of sensor molecules appears to be the fact that the fluorescence of the cyclic platinum complexes is quenched by oxygen, which, of course, stifles the use of these sensors in ambient conditions.

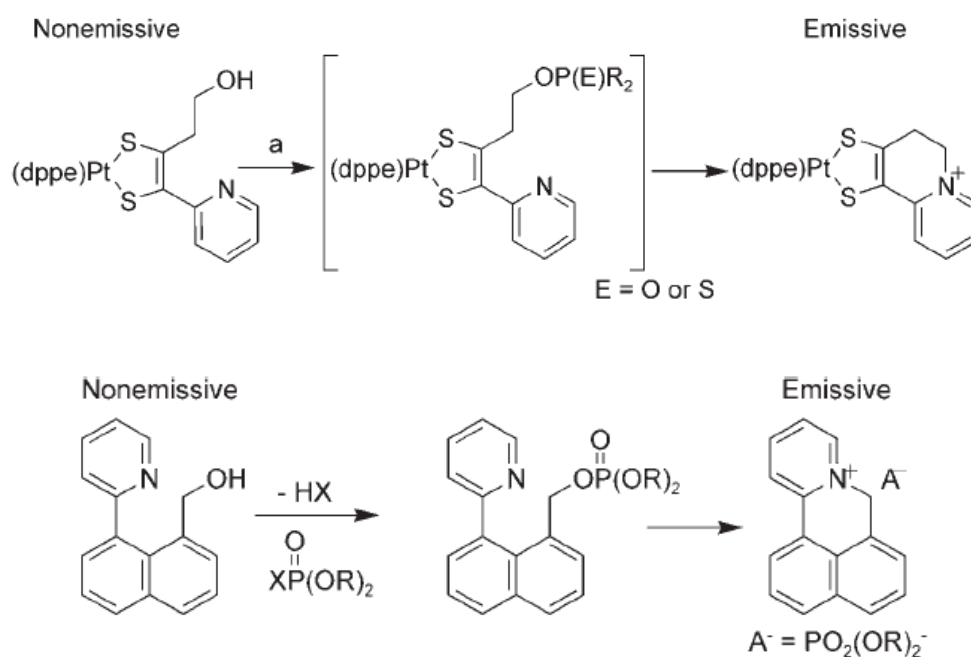


Figure 1.5 Mechanism of the chemically reactive sensor developed by Pilato and co-workers (top), and by Swagger and coworkers (bottom).

Utilizing a similar concept, Swagger and co-workers³³ developed an organophosphate sensor that can be used in an ambient atmosphere. In this case a

naphthalene scaffold (Figure 1.5 bottom) effectively replaces the platinum complex utilized by Pilato and co-workers. As in Pilato's system, the mechanism involves the reaction of the alcohol group of the sensor molecule with the analyte to yield a phosphate ester intermediate that is converted into a fluorescent cyclic product. The naphthylpyridyl sensor molecule studied by Swager was found to react with the analyte under pseudo-first-order kinetics in CH_2Cl_2 with an observed rate constant (k_{obs}) > 0.024 s^{-1} . Chemosensors produced by impregnating a cellulose acetate film with this sensor molecule showed a complete response to 10 ppm diisopropylfluorophosphate (DFP) vapor within five minutes.

Recently, Rebek and co-workers³⁴ reported a reactive chemical sensor that utilizes a similar reaction mechanism as the sensor molecules designed by Pilato and Swager. Rebek's sensor relies on the suppression of a photo-induced electron transfer (PET) process to trigger a fluorescent signal (Figure 1.6).³⁵ In this case, as in the previous examples, a hydroxyl group reacts with the analyte to yield a reactive intermediate which undergoes an intramolecular reaction with a tertiary amine that is part of the sensor molecule. The system is designed so that the electron pair of the unreacted tertiary amine quenches the emission of a fluorescent moiety attached to the sensor compound by way of PET. As the chemosensor is exposed to the OP analyte (diethylchlorophosphate, DCP), an intramolecular cyclization reaction occurs. In the case of the sensor molecules designed by Rebek et al., a quaternary azaadamantane ammonium salt is formed. Upon loss of the lone electron pair on the nitrogen atom, the PET is suppressed and the fluorophore (pyrene) is rendered fluorescent. A maximum

increase of the fluorescence intensity of up to 22 times of the original signal was observed upon exposure of the sensor molecules to DCP. Interestingly, minor structural variations proved to have rather significant effects; maximum “contrast” was achieved if one methylene unit was used as the spacer between the nitrogen and the fluorophore, while a butylene spacer only displayed a 1.1-fold increase in fluorescence upon exposure to DCP. The sensor complexes investigated by Rebek and co-workers were deposited on a piece of filter paper. The simple solid-state sensors thus produced displayed a practical instantaneous (5 s) fluorescence upon exposure to vapor comprising 10 ppm of DCP. This sensor system offers the distinct advantage of being useful in conjunction with many existing fluorophores.

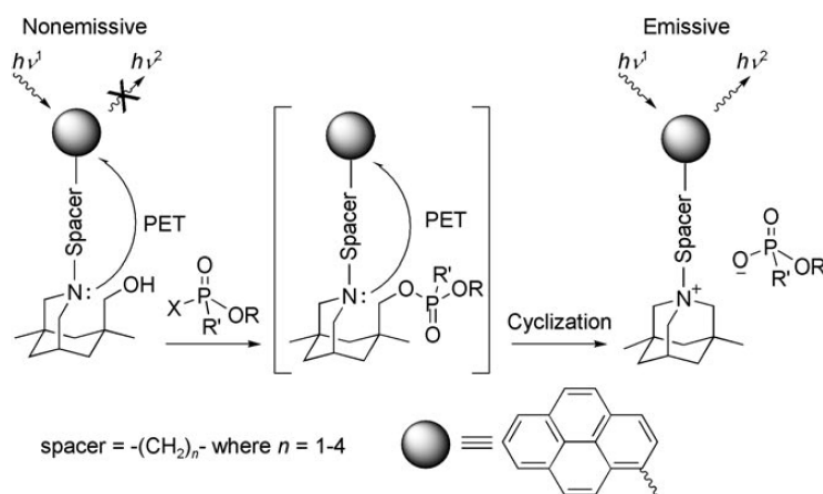


Figure 1.6 The chemically reactive sensor developed by Rebek and coworkers.

The severe threat of exposure to chemical warfare agents on both the battlefield and through terrorist attacks has lead to a recent surge in the research aimed at the detection of these highly toxic compounds. Focusing on fluorescent sensors developed

to counter the threat of nerve agents, a wide variety of approaches are being studied, many of which are also applicable to transduction schemes involving effects other than fluorescence changes, for example, changes of optical absorption, electrical conductivity, and so on. Fluorescence sensing offers a number of benefits from the perspective of detecting chemical warfare agents, such as high sensitivity, large signal changes, and even on-off responses. This is a field that is going to continue to grow over the next decade as more and more researchers commit resources to this issue.

CHAPTER 2

SUPRAMOLECULAR SENSING DEVICES FOR PHOSGENE BY FRET

2.1 Design

2.1.1. Fluorescence Resonance Energy Transfer

Förster Resonance Energy Transfer (FRET), named after the German scientist Theodor Förster, describes an energy transfer mechanism between two chromophores. A donor chromophore in its excited state can transfer energy by a nonradiative, long-range dipole-dipole coupling mechanism to an acceptor chromophore in close proximity (typically <10 nm). This energy transfer mechanism is termed "Förster resonance energy transfer" (FRET). When both molecules are fluorescent, the term "fluorescence resonance energy transfer" is often used, although the energy is not actually transferred by fluorescence.³⁶ Here we design phosgene sensors based on FRET.³⁷ It includes a selective chemical reaction between phosgene and donor and acceptor fluorophores, which bring them together, within the appropriate Förster distance (Figure 2.1). Phosgene serves here as a cross-linking agent. When the emission spectrum of the donor overlaps with the absorption spectrum of the acceptor, FRET occurs upon irradiation of the donor and strong emission of the acceptor can be detected.

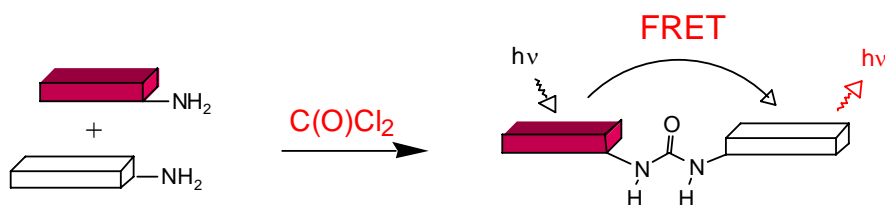


Figure 2.1 A FRET based approach to the detection of phosgene.

To realize this concept we review carefully the properties of the chromophores currently available from commercial sources. We eventually choose the laser dye coumarin 2 as the donor terminal chromophore, and coumarin 343 as the acceptor chromophore (Figure 2.2). A favorable intramolecular charge transfer takes place in the excited state of these molecules, and accounts for their high extinction coefficients and high dipole moments, which are necessary for a strong dipole – dipole interaction. This pair of chromophores meets the basic requirement for energy transfer: the donor emission band strongly overlaps the acceptor absorption band (resonance condition). In addition, the emission of coumarin 2 displays a large Stokes shift, which lowers the probability of self-quenching between the numerous peripheral chromophores. Furthermore, because of their high fluorescence quantum yields and their solubility—a decisive advantage for building multichromophoric macromolecules—these coumarins are used extensively in dye lasers and are therefore commercially available in high purity (>99%).

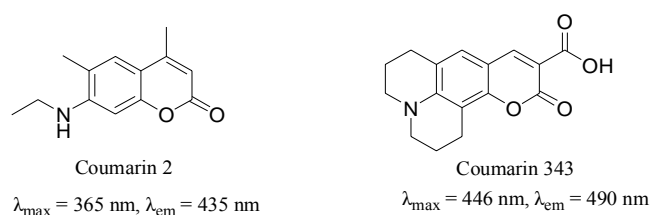


Figure 2.2 Structures and spectral characteristics of the donor and acceptor dyes.

2.1.2. Phosgene Sensor

Phosgene ($\text{C}(\text{O})\text{Cl}_2$) is a highly toxic and chemically reactive gas that has been used as a chemical warfare agent.³⁸ It is a lung irritant and a very insidious poison, which does not irritate immediately, even when fatal concentrations are inhaled. Inhalation of phosgene causes severe lung injury, the full effects appearing several hours after exposure. Phosgene first came into battlefield during World War I, when it was used, either alone or mixed with chlorine, against troops. A renewed interest occurs in the development of phosgene sensors due to the increased threat of weapons deployment by terrorists. Sensing methods for phosgene are typically electrochemical or based on remote spectroscopic detection techniques.³⁹ At the same time, optical sensors for this gas are very rare.⁴⁰ This is interesting since reactive chromophores and fluorophores are now actively used for sensing other chemical agents.³³⁻³⁵ Such sensors utilize a change of absorption or fluorescence upon detection and better address the needs of military and homeland security in that they are simple, fast and reliable.

2.2 Synthesis

To take advantage of this chemical property, commercially available laser

dyes⁴¹ coumarin 2 and coumarin 343 were functionalized with primary amino groups (Figure 2.3). Coumarin 2 refluxed with methyl 4-(bromomethyl)benzoate, potassium carbonate in CH₃CN, to obtain compound **1**. **1** was hydrolyzed by tetrabutylammonium hydroxide (TBA⁺OH⁻) in H₂O/THF to get free carboxylic acid **2**. Coupling reaction between **2** and Boc-ethylenediamine was carried on in CH₂Cl₂ in presence of *N*-ethyl-*N'*-(3-dimethylaminopropyl)carbodiimide (EDC), 1-hydroxybenzotriazole (HOBT) and *N*-methylmorpholine (NMM), to give compound **3**. Donor amine **4** was obtained by deprotection of **3** in trifluoroacetic acid (TFA) and CHCl₃. Analogously, acceptor amine **6** was also obtained. Fluorescence studies showed donor amine **4** excitation wavelength $\lambda_{\text{ex}} = 343$ nm, emission wavelength $\lambda_{\text{em}} = 425$ nm. As for **6**, $\lambda_{\text{ex}} = 435$ nm, $\lambda_{\text{em}} = 468$ nm. Moreover, no strong emission was detected for acceptor amine **6** when the excitation wavelength was 343 nm (Figure 2.4). Measurements were taken in CHCl₃ at rt, [c] = 1×10^{-6} M.

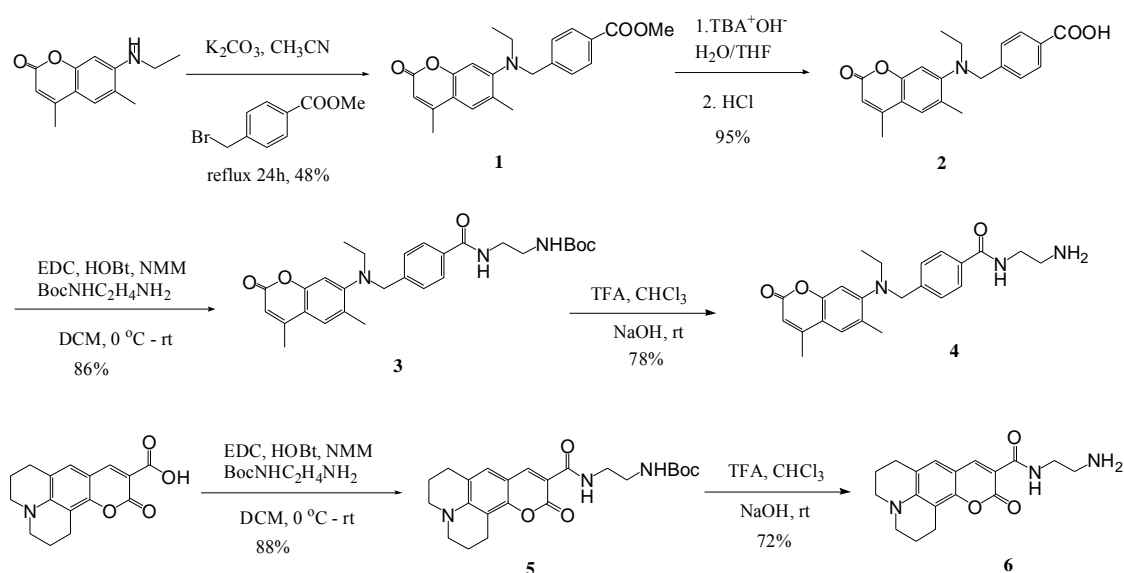


Figure 2.3 Synthesis of donor amine **4** and acceptor amine **6**.

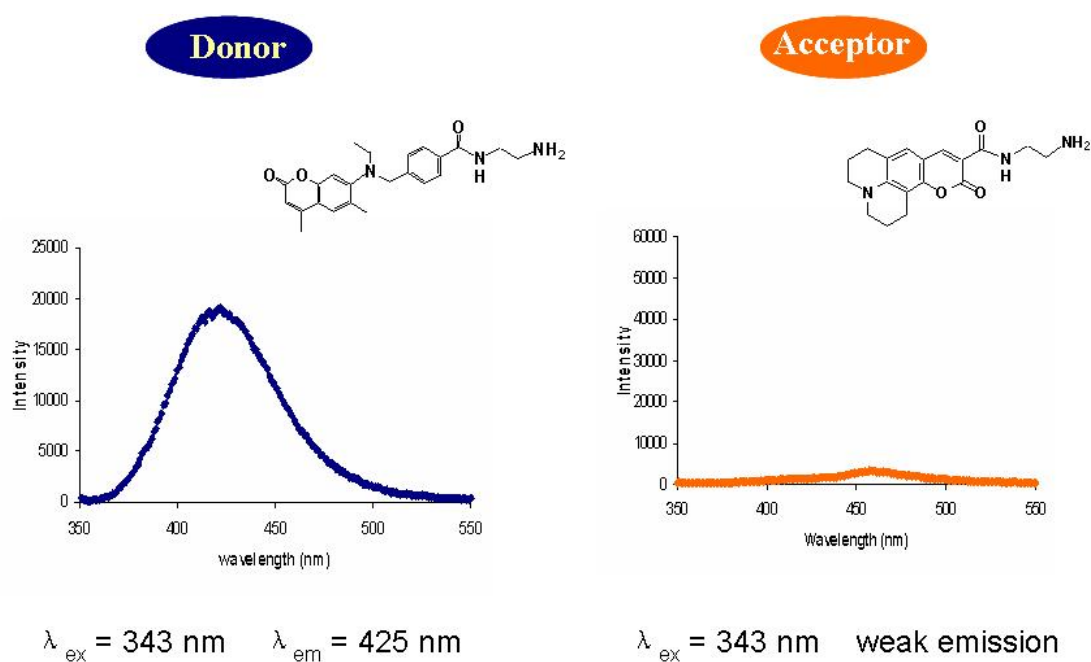
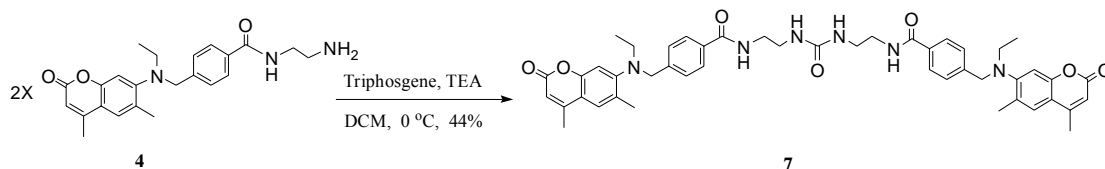


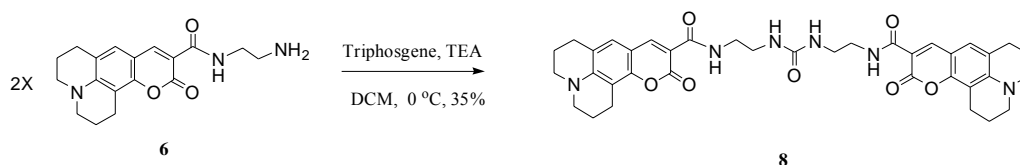
Figure 2.4 Fluorescence spectra of compound **4** and **6**.

For the laboratory synthesis of ureas, triphosgene ($\text{CCl}_3\text{OC(O)OCCL}_3$) was used as a phosgene simulant. It is less toxic and easier to handle. In organic chemistry, triphosgene has been utilized as a safe reagent for making ureas.⁴² Taken separately, thus prepared coumarin derivatives **4** and **6** smoothly reacted with triphosgene at room temperature in CHCl_3 in the presence of triethylamine (TEA) with the formation of the corresponding ureas (Figure 2.5). In molecule **9**, Macromodel calculation shows the donor and acceptor units are covalently linked and positioned within $\sim 20 \text{ \AA}$ of one another. Similarly to urea **9**, donor-donor urea **7** and acceptor-acceptor urea **8** were synthesized and fully characterized.

Donor-Donor Urea **7**



Acceptor-Acceptor Urea **8**



Donor- Acceptor Urea **9**

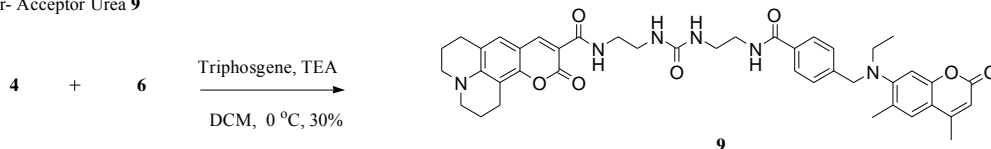


Figure 2.5 Synthesis of ureas **7**, **8**, **9**.

In the fluorescence studies of **7-9**, all measurements were taken in dried CHCl_3 at rt, $[c] = 1 \times 10^{-6}$ M. **7** showed a similar result as donor amine **4**, $\lambda_{\text{ex}} = 344$ nm, $\lambda_{\text{em}} = 424$ nm, as for acceptor-acceptor urea **8**, wavelengths are 435 nm and 462 nm, respectively. The absorption spectrum of **9** showed two strong bands at 343 and 438 nm which belong to the coumarin 2 and coumarin 343 units, respectively.

2.3 Titrations and Discussions

The phosgene sensing titration experiment involves the formation of urea **9** and its fluorescence. Coumarins **4** and **6** were mixed in a 1:1 ratio at the concentration range between 5×10^{-4} and 10^{-2} M in CHCl_3 , TEA (~ 10 eq) was added and then triphosgene was introduced. Addition of TEA prevented protonation of the amino groups. Control

experiments confirmed that TEA did not affect the fluorescence. Aliquots were taken and diluted to 10^{-6} M, and the emission was recorded upon excitation at $\lambda_{\text{ex}} = 343$ nm.

For compound **9**, more important is that at low concentrations of $\leq 5 \times 10^{-5}$ M, the donor excitation at $\lambda_{\text{em}} = 343$ nm leads to the acceptor emission at $\lambda_{\text{em}} = 464$ nm (Figure 2.6). The shoulder around 424 nm still represents the emission of donor chromophore, but it is obviously less strong than emission at 464 nm. In a control experiment only utilizing donor amine **4** and acceptor amine **6**, no emission was detected around 460 nm upon the same conditions. This implied a FRET phenomenon in urea **9**.

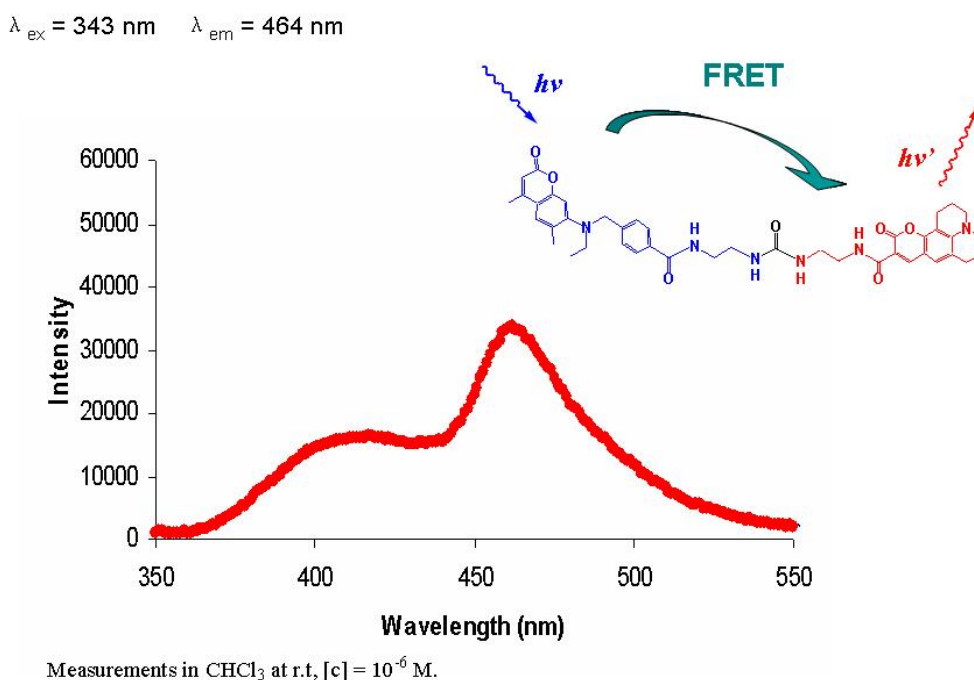


Figure 2.6 Fluorescence spectrum of compound **9**.

In the phosgene sensing titration experiment, significant fluorescence enhancement at $\lambda_{\text{em}2} = 464$ nm was detected (Figure 2.7). Coumarins **4** and **6** were

mixed in a 1:1 ratio at 10^{-3} M in CHCl_3 , TEA (10 eq) was added and then triphosgene (0.03 to 5 eq) was introduced. Aliquots were taken and diluted to 10^{-6} M, and the emission was recorded upon excitation at 343 nm. The arrows indicate the fluorescence changes upon increasing the triphosgene concentration.

This is particularly important since the acceptor unit alone does not emit under those conditions. The fluorescence increase is obviously due to the formation of urea **9**.⁴³ Simultaneously, the fluorescence from the donor unit at $\lambda_{\text{eml}} = 424$ nm decreased. This is due to the quenching, indicating that efficient energy transfer took place from the donor to the acceptor. The fluorescence changes were clearly seen already upon addition of as little as ~ 0.1 eq of phosgene (recalculated from 0.03 eq triphosgene), which places the detection limit for this particular FRET system at $\sim 5 \times 10^{-5}$ M.

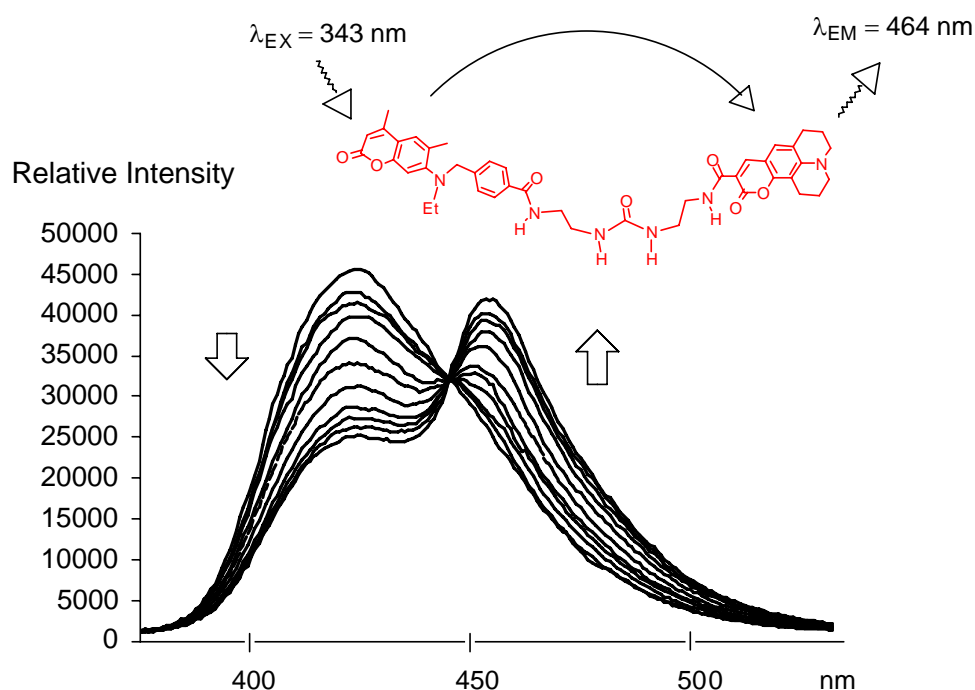


Figure 2.7 Typical changes in fluorescence emission spectra upon titrations with triphosgene.

In addition to fluorescence spectroscopy, the response of compounds **4** and **6** to triphosgene can be conveniently followed even with the naked eye (Figure 2.8). Left: coumarins **4** and **6** in CHCl_3 before addition of triphosgene. Right: after addition of ~ 5 eq of triphosgene. The experiments were performed at 10^{-3} M, and the solutions were then diluted to 10^{-6} M. Both vials are irradiated at $\lambda = 365$ nm with a laboratory UV lamp. The increased fluorescence intensity was clearly observed within seconds after the addition of triphosgene.



Figure 2.8 The “naked eye” detection of triphosgene.

It is now possible to detect phosgene utilizing a designed FRET system. This systems is selective, since no other gas can serve as a cross-linking agent.⁴⁴ This sensor design is clearly not limited to coumarins: the dyes do not react with phosgene but rather report on its presence. In principle, any other FRET acceptors and donors can be used. Further synthetic modification is also possible, to achieve more colorful responses. It would also be important to modify the system for phosgene detection at the gas-solid interface.

CHAPTER 3

CARBON DIOXIDE AND SUPRAMOLECULAR MATERIALS

3.1 Introduction to Supramolecular Chemistry of CO₂

Carbon dioxide is one of the major greenhouse gases.⁴⁵ It circulates in the environment through a variety of processes known as the *carbon cycle* (Figure 3.1). Large-scale industrial processes, volcanoes and living systems release huge quantities of CO₂ into the atmosphere. On the other hand, plants and also oceans, lakes, and rivers collect it. Although the concentration of CO₂ in the earth's atmosphere is low (~0.04% by volume), CO₂ is a very important component, because it absorbs infrared radiation and enhances the greenhouse effect. CO₂ in the atmosphere is accumulating much faster than the Earth's natural processes can absorb it. The CO₂ levels in the atmosphere have risen by more than 30% over the last 250 years and these concentrations may well double or even triple in the next century. Such extensive CO₂ circulation in the atmosphere, industry and agriculture requires not only its systematic monitoring under a variety of conditions, but more importantly, necessitates the development of improved methods of the CO₂ chemical utilization.

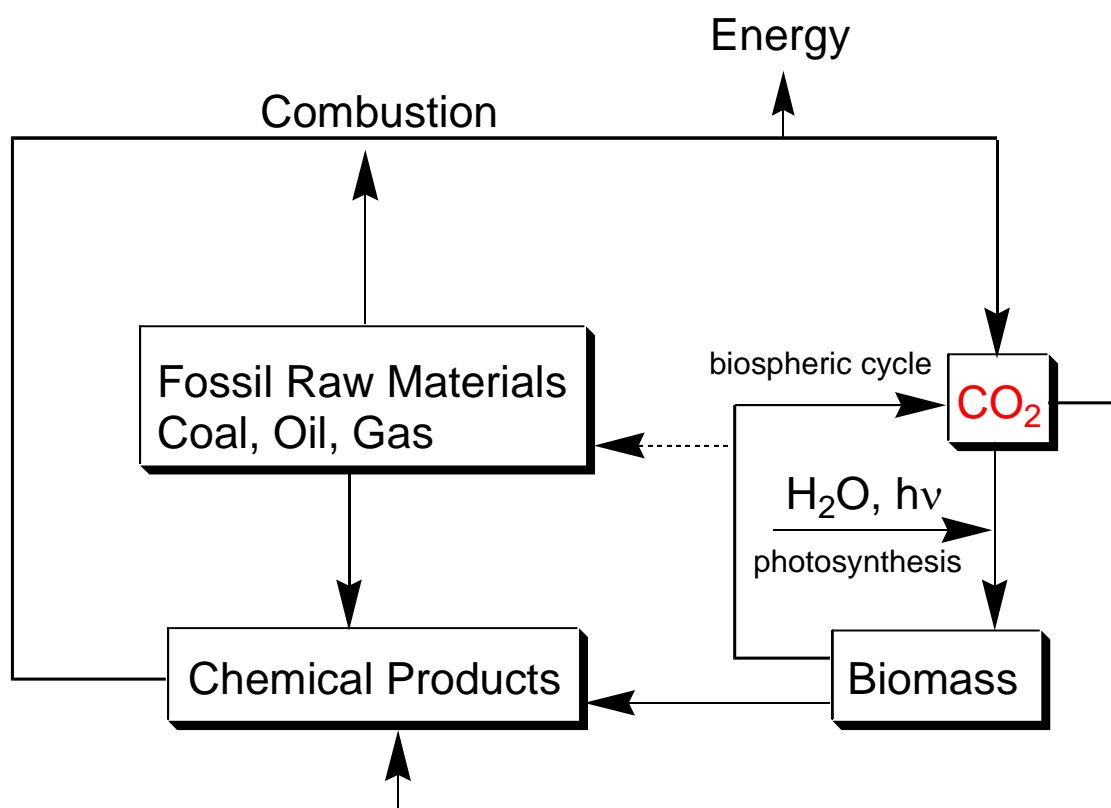


Figure 3.1 Circulation of carbon dioxide: *Carbon Cycle*.

The reactions between CO₂ and amines readily occur at ordinary temperatures and pressures to yield carbamates, presumably by way of the corresponding carbamic acids. Notably, carbamates are thermally unstable and release CO₂ upon heating (Figure 3.2).⁴⁶

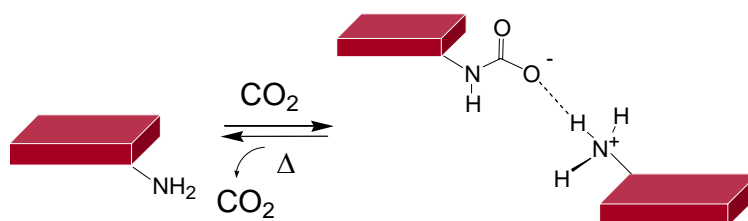


Figure 3.2 Reversible covalent chemistry between CO₂ and amines: self-assembly of molecular blocks.

Accordingly, polymer-bound amines have been employed in industry as reusable CO₂ scrubbers, removing CO₂ from industrial exhaust streams.⁴⁷ It has been demonstrated that amines containing ionic liquid also trap CO₂ (Figure 3.3).⁴⁸ Imprinted polymers have been introduced, in which a template can be attached and then removed through a carbamate linker.⁴⁹

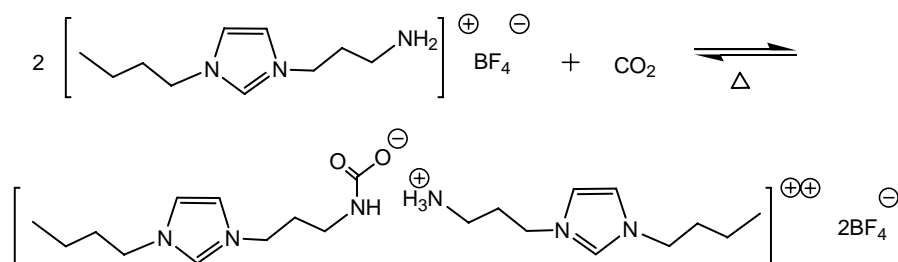


Figure 3.3 Structure of a CO₂-trapping ionic liquid.

Finally, reactions between CO₂ and immobilized amines have been employed by our laboratory for the gas sensing (Figure 3.4).⁵⁰ Specifically, 1-aminomethylpyrene readily reacts with CO₂ in polar aprotic solvent to form the corresponding carbamic acid, which exhibits at least 10 times more fluorescence emission than the amine. Here, the disruption of proton induced electron transfer quenching by resonance between the lone pair on nitrogen atom and carbonyl oxygen is responsible for the increased fluorescence.

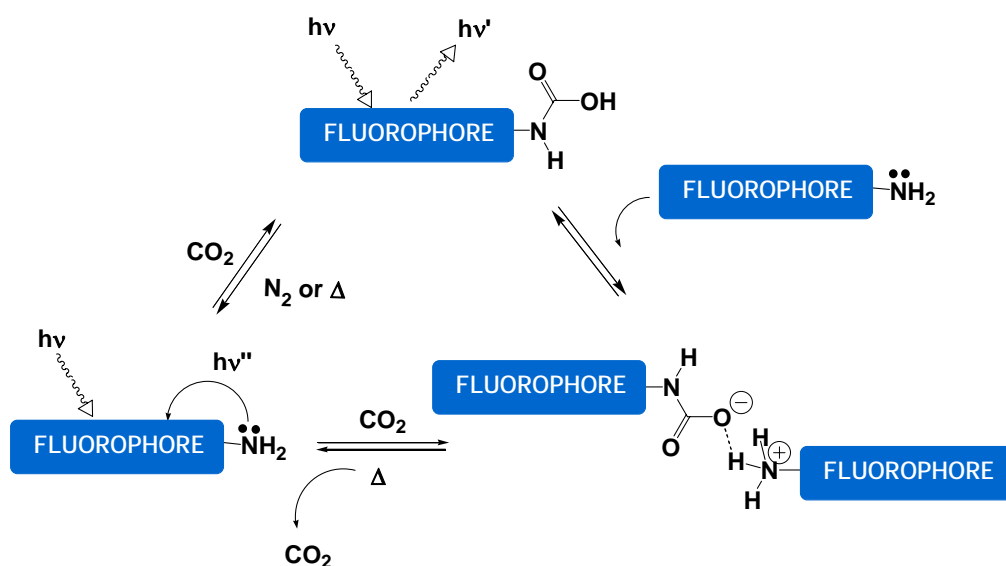


Figure 3.4 Model for fluorimetric sensing of CO₂.

Dynamic covalent chemistry (DCC) is now quickly emerging as a promising alternative to noncovalent self-assembly.⁵¹ It simply offers an elegant opportunity to perform supramolecular chemistry with covalent bonds. One of the most important advantages here is the robustness of covalently organized structures, which on the other hand can be reversibly broken, at will. Our research has proposed, that carbamate bonds could be employed for wider variety of DCC experiments.⁵⁰

Non-covalent self-assembly has been very well explored in the past two decades and leads to well defined nano-scale structures, such as capsules, supramolecular polymers, etc. Covalent, still reversible, assembly is only at the beginning in supramolecular chemistry. This carbamate chemistry, simply introduced from CO₂ and alkyl amines, could offer us a good opportunity to quickly assemble a variety of robust

nanostructures and “smart” materials. Furthermore, the reversible nature of carbamate bonds may lead to possibilities of switching structures and properties.

Simultaneously with us, Weiss and co-workers demonstrated that chemically reversible organogels could be prepared with CO₂ and aliphatic amines as latent gelators.⁵² The organogelation process was simple and reliable. Rapid uptake of CO₂ by aliphatic amines produced the ammonium carbamate-based gel, while thermal release of CO₂ transformed the gel into the amine solutions. The gel-solution cycles can be repeated for at least 10 times without losing efficiency. Gels are viscoelastic liquid-like or viscoelastic solid-like materials. Due to their thermo-reversibility and great diversity of structures on the microscale and mesoscale, gels will attract more attention in the field of supramolecular chemistry.⁵³

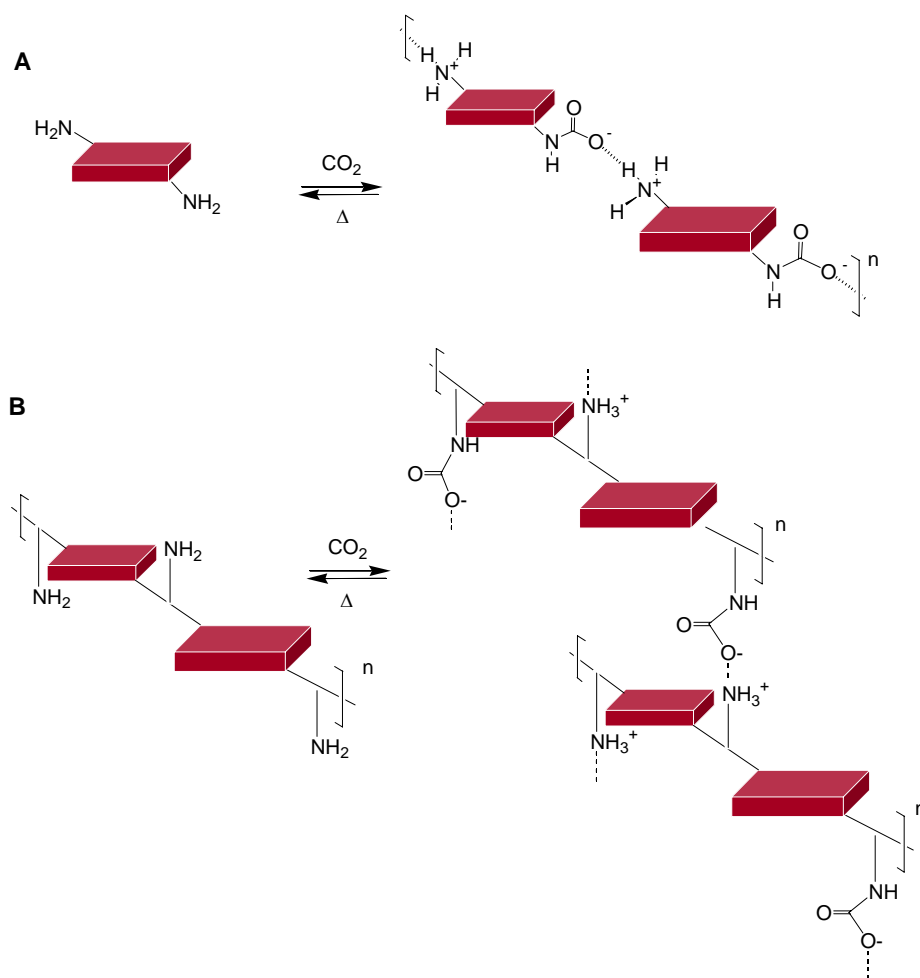


Figure 3.5 Reversible covalent chemistry between CO₂ and amines. Self-assembly of molecular blocks leads to linear (case A) and cross-linked polymers (case B).

The reactions between CO₂ and di- or even polyamines are very interesting, since they can lead to reversibly formed polymeric chains or even cross-linked 3D networks (Figure 3.5A and 3.5B). In one case, such structures have been proposed for polycarbamate $[\text{---H}_3\text{N}^+(\text{CH}_2)_{12}\text{NHC}(\text{O})\text{O}^-\text{---H}_3\text{N}^+(\text{CH}_2)_{12}\text{NHC}(\text{O})\text{O}^-\text{---}]_n$, which forms thermally reversible organogels.⁵²

With this in mind, we employed CO₂ as a cross-linking agent to build supramolecular polymeric materials.⁵⁴⁻⁵⁶ Supramolecular polymers represent a novel class of macromolecules, in which monomeric units are held together by reversible forces. Supramolecular polymers combine features of conventional polymers with properties resulting from the bonding reversibility. Structural parameters of supramolecular polymeric materials, in particular their two- and three-dimensional architectures, can be switched “on-off” through the main chain assembly dissociation processes. On the other hand, their strength and degree of polymerization relies on how tight the monomeric units are aggregated. In this chapter, we introduce a strategy to build supramolecular polymers for cation separation, which utilizes hydrogen bonding and takes advantage of dynamic, reversible chemistry between CO₂ and amines. These polymers are also functional. We demonstrate that macrocyclic receptor and CO₂-amine chemistry leads to switchable materials, which selectively trap, store and then release alkali metal cations. And finally using CO₂, we convert linear supramolecular polymeric chains into supramolecular, three-dimensional polymeric networks.

3.2 Separation Strategy by Using CO₂

Separation processes are central to the chemical, materials, energy, and pharmaceutical industries. Generally speaking, distillation, filtration, extraction, membrane transport process, crystallization and various chromatography are the most traditional separation techniques. Nowadays molecular recognition is becoming a new area which gets more attention. The impact of molecular receptors and molecular containers in chemistry and chemical technology has been very impressive.^{57,58} A great

number of chemically, industrially and biologically significant molecules and ions have been complexed. However, most of these “host-guest” complexes exist in solution and often break or dissociate upon separation. Another severe problem is the usage of large quantities of solvents, which may very often be toxic and generate environmental problems. Polymers and materials, functionalized with molecular recognition sites, have also been prepared. In these cases, recognition/complexation events take place not in homogenic solution but at the solid-liquid or gas-solid interface, which means not effective.

Recently we described a novel separation strategy,⁵⁹ which combined selective complexation by macrocyclic receptors and CO₂-induced molecular switching,⁵⁶ leading to effective precipitation. Earlier, we established that unique materials could be prepared from CO₂ and primary amines, especially derived from amino acids.^{55,56} CO₂ reacts rapidly with amine building blocks, at normal temperatures and pressures, with the formation of alkylammonium - N⁺H₃ ••• O⁻C(O)NH - carbamate salts.^{46,50,52} The carbamate formation is rapid at room temperature, and loss of CO₂ from the formed ammonium salt can be readily achieved upon gentle heating (~60 °C) or by simply adding HCl or TFA.⁶⁰ These carbamate materials can be called supramolecular. Supramolecular polymers represent a novel class of macromolecules, in which monomeric units are held together by reversible forces.⁶¹

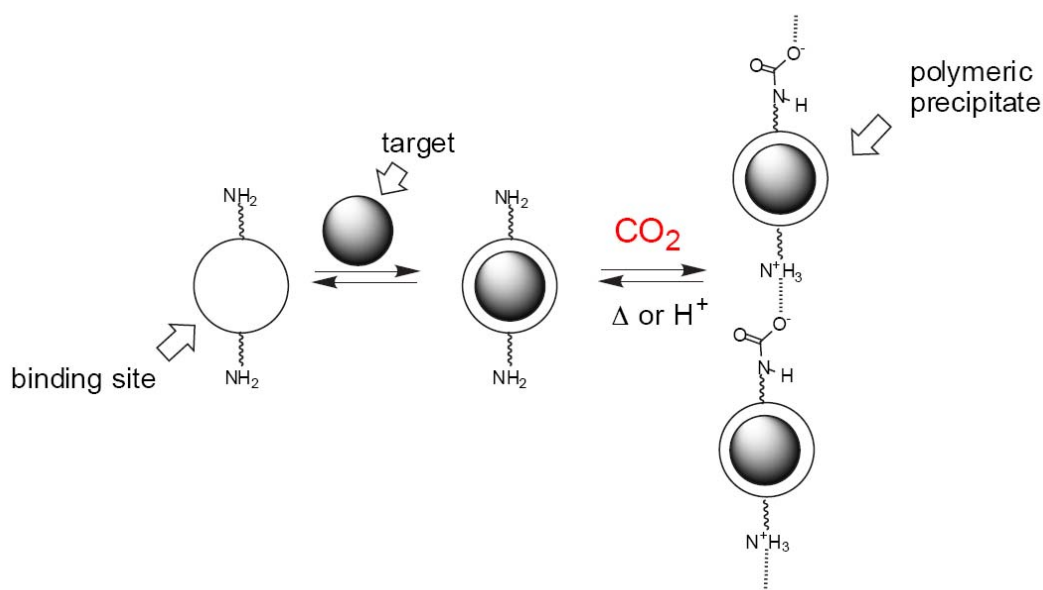


Figure 3.6 Separation strategy uses CO_2 as a cross-linking agent in the formation of supramolecular carbamate polymers.

Our separation strategy involves supramolecular polymers and is presented on Figure 3.6. Receptors can be prepared, which also possess multiple primary amino groups capable of reacting with CO_2 . After complexation of target species by these receptors, CO_2 is introduced (rt, 1 atm), which reacts with the terminal amino groups of the receptors. As the result, cross-linked carbamate polymers will form and precipitate. These polymers incorporate the target complexes within their structures. The process will separate the complexed species from the bulk solution and uncomplexed species. The precipitated materials can be collected and stored. On the other hand, they can release CO_2 and dissociate back to monomers upon heating or addition of acid, and subsequently release the complexed species in their pure form.

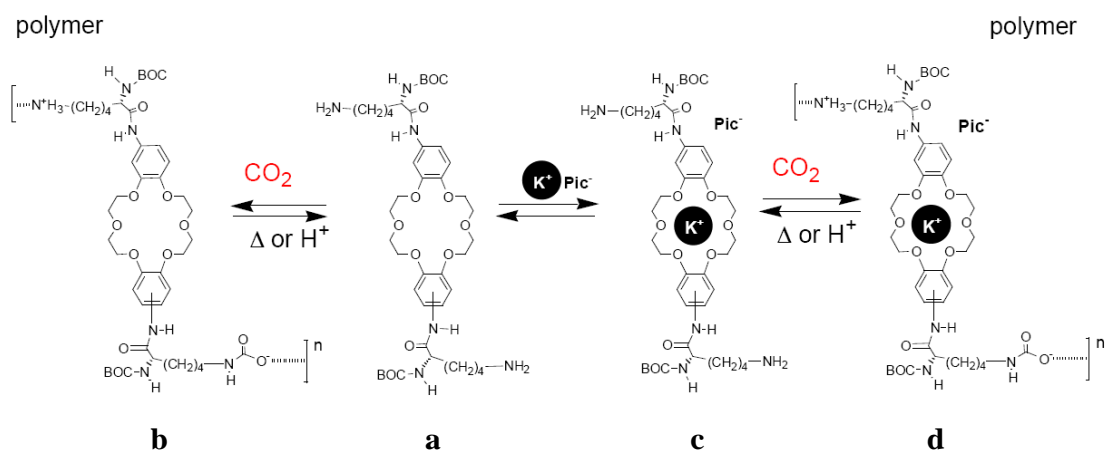


Figure 3.7 Potassium separation by dibenzo-18-crown-6 Lysine derivatives. Reaction with CO_2 leads to the formation of insoluble in CHCl_3 supramolecular polymeric materials **b** and **d**, which could be separated by simple filtration. Polymer **d** also separates K^+Pic^- by complexation. Polymers **b** and **d** can dissociate back to the corresponding monomers upon heating or addition of acid.

It was established already by C. J. Pedersen that potassium (K^+) cations could be selectively extracted by dibenzo-18-crown-6 ether in the presence of other cations.⁶² Our research group combined the dibenzo-18-crown-6 with two *L*-lysine fragments on the periphery (Figure 3.7), since preliminary results showed recently that the free lysine ϵ -amino groups readily react with CO_2 in apolar solution.⁵⁴⁻⁵⁶ Receptor **a** was then used for the extraction of potassium picrate (K^+Pic^-) from water to CHCl_3 . Then CO_2 was introduced, which quickly reacted with the lysine ϵ -amino groups and cross-linked complex **c** into insoluble polymeric carbamate **d**.

This strategy is unique in all respects. It involves structural switching, which works together with complexation. The architecture and recognition properties of the separating materials can be programmed through synthesis at the stage of their monomers. In contrast to known separating polymers and materials, which impose

significant phase-transfer restrictions on complexation, the proposed receptors complex guests in solution, as monomers, and only polymerize upon reaction with CO₂. Due to effective precipitation, large quantities of solvent can be recovered and reused. The storage is accomplished without the use of solvent, which is economically preferred. For the first time CO₂ gas can be used as a building block for separating materials. Considering the huge significance of CO₂ in industry and environment, the strategy offers means for creating environmentally responsive processes for separation.

CHAPTER 4

SEPARATION OF SODIUM BY CALIXARENE AND CARBON DIOXIDE

4.1 Design

Preliminary results from our lab showed switchable, supramolecular polymers could be prepared by CO₂.⁵⁶ More recently, we found that such polymers can be employed for metal ion separation.⁵⁹ Separation of ions through molecular recognition typically involves extraction. Macrocyclic receptors have been synthesized that selectively complex metal salts and solubilize them in organic solvents. Polymer-supported macrocyclic receptors have also been introduced. One significant problem here is the handling and storage of large quantities of organic solvents that are often expensive and/or environmentally toxic. This is particularly important for storage of toxic metal wastes in solution after the extraction. On the other hand, when polymers with appended receptors are used, the complexation takes place not in homogeneous solution but at the solid-liquid interface, which is often not effective. We are developing an approach, which eliminates these problems. It combines solution complexation/extraction by macrocyclic receptors and subsequent CO₂-induced precipitation of the complexes (Figure 4.1).⁵⁹

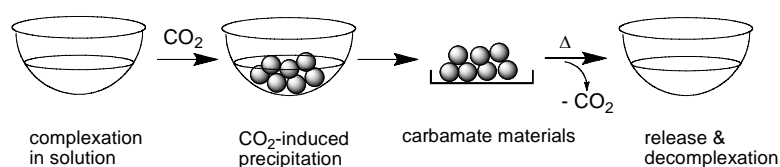


Figure 4.1 Separation strategy using CO₂.

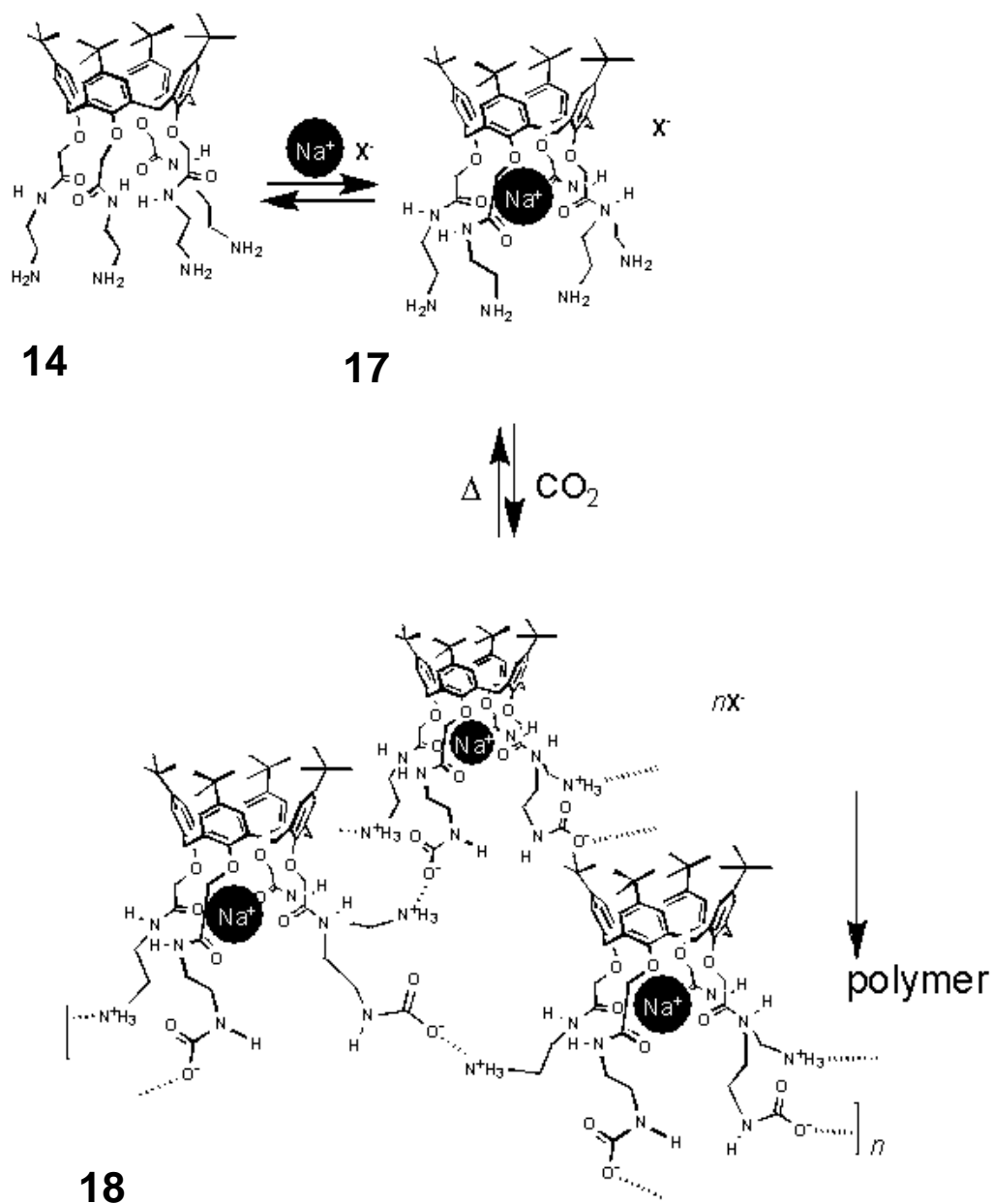


Figure 4.2 Separation of Na^+ involves calix[4]arene receptor **14** and CO_2 .

There is a significant interest in Na^+ separation in industry, including nuclear waste treatments and desalination of seawater, and therefore we demonstrate selective separation of Na^+ salts using CO_2 and calix[4]arene based receptors.

Calix[4]arene **14** has four CH₂C(O)NH amide groups at the lower rim (Figure 4.2). The carbonyl oxygen atoms and four ether oxygens provide eight preorganized coordination sites for binding Na⁺. According to the literature, such structural arrangement offers a very high affinity towards sodium cation; the binding constants over 10⁵ M⁻¹ and selectivities levels of Na⁺/K⁺ >10⁴ have been documented.⁶³ Receptor **14** also possesses four primary amino groups on the periphery that are capable of reacting with CO₂ to form cross-linked ammonium carbamates.^{46a}

4.2 Synthesis and Extractions

Parent tetrahydroxycalix[4]arene **10** was prepared according to the published procedures.⁶⁴ Then it was functionalized to introduce the four ester group as Na⁺ binding sites and primary amino groups as sites to be linked with CO₂ (Figure 4.3). Compound **11** was prepared by refluxing tetrahydroxycalix[4]arene with ethyl bromoacetate and sodium carbonate in dried CH₃CN. Calix[4]arene tetraacid **12** was obtained by LiOH hydrolysis in H₂O/THF. Boc protected tetraamide **13** was prepared by coupling reaction with *N*-ethyl-*N*-(3-dimethylaminopropyl)carbodiimide (EDC), boc-ethylenediamine, and *N*-methylmorpholine (NMM). After deprotection by trifluoroacetic acid (TFA), calix[4]arene tetraamine module **14** was ready for extraction and separation. CO₂ was introduced to DMSO-*d*₆ and CDCl₃ solutions in the presence of triethylamine (TEA), calix[4]arene tetraamine carbamic acid **15** and carbamate **16** were obtained respectively.

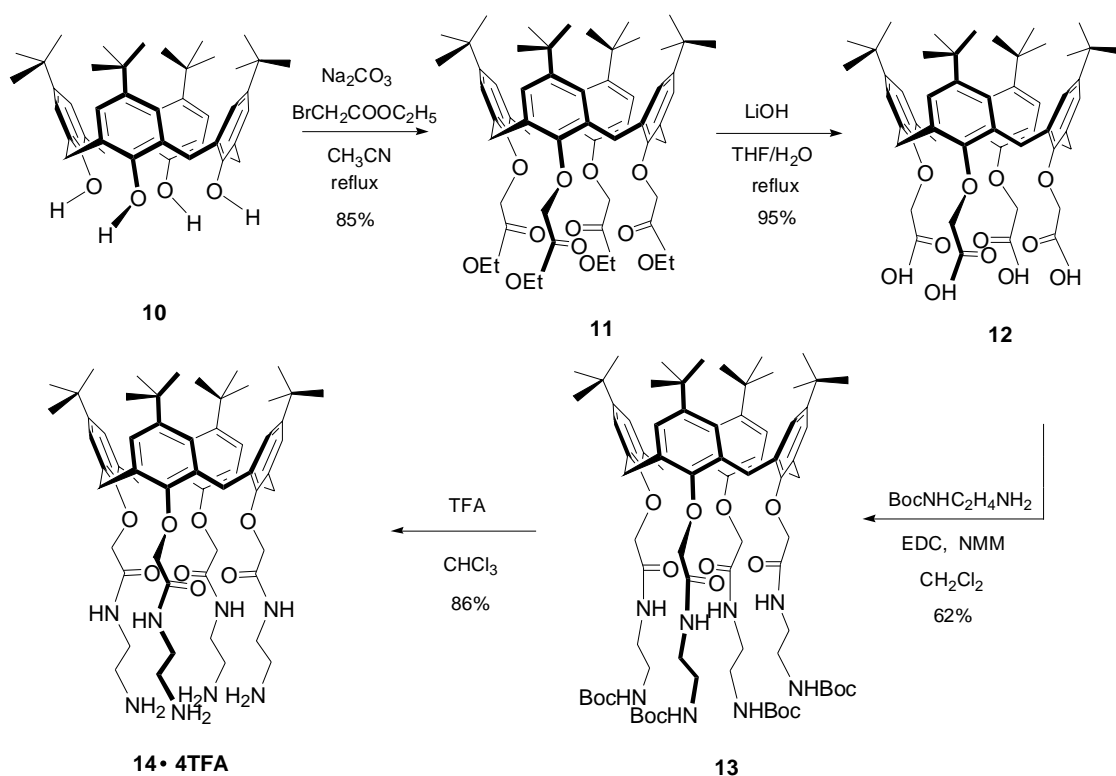


Figure 4.3 Synthesis of calix[4]arene derivatives for sodium separation.

The general procedure for extraction of alkali-metal perchlorates (M^+ClO_4^-) and picrates (M^+Pic^-) by calixarene **14** (Figure 4.4) was as follows. Compound **14** was stirred with alkali-metal perchlorate in CHCl_3 in the presence of TEA overnight and the solution was separated. CO_2 (or $^{13}\text{CO}_2$) was then introduced and the precipitate was collected and dried. The ^{13}C NMR spectrum of calixarene- Na^+ carbamate polymer **18** was measured with $^{13}\text{CO}_2$ gas.

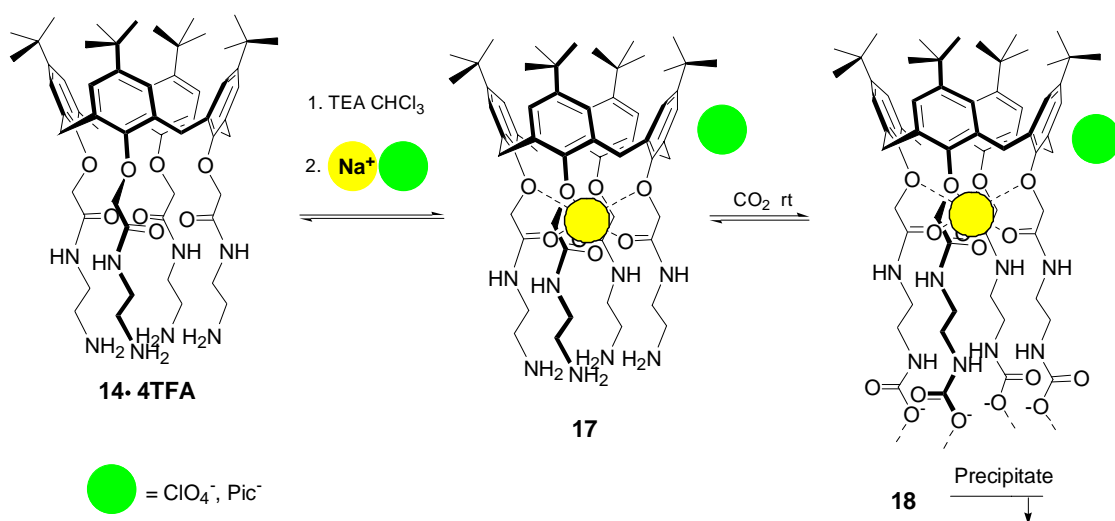


Figure 4.4 Extraction, entrapment and separation of sodium ions.

4.3 Results and Discussions

We found that receptor **14** selectively extracts Na^+ salts vs K^+ and Cs^+ and complex **17** can subsequently be precipitated upon reacting with CO_2 (Figure 4.2). In detail, the TFA salt of calixarene **14** was dissolved in CHCl_3 in the presence of triethylamine (TEA) (~ 15 eq) and, as expected, quantitatively extracted $\text{Na}^+\text{ClO}_4^-$ from the solid phase. Complex **17** was characterized by ^1H NMR spectroscopy in $\text{DMSO}-d_6$, showing significant changes compared to free receptor **14** (Figure 4.5). For example, the aromatic protons shifted from 6.83 in free **14** to 7.12 ppm in **17**, which is attributed to the electron-withdrawing nature of Na^+ . The CH_2 protons of the methylene bridges between the aromatic rings shifted from 4.52 and 3.22 in **14** to 4.34 and 3.34 ppm in **17**, respectively. This phenomenon is known and caused by fixation of Na^+ cation at the lower rim.⁶⁵ Under the same conditions, no extraction of K^+ClO_4^- and $\text{Cs}^+\text{ClO}_4^-$ was observed; no

changes in the ^1H NMR spectra were detected. Similar selectivity was also observed for Na^+Pic^- over K^+Pic^- and Cs^+Pic^- .

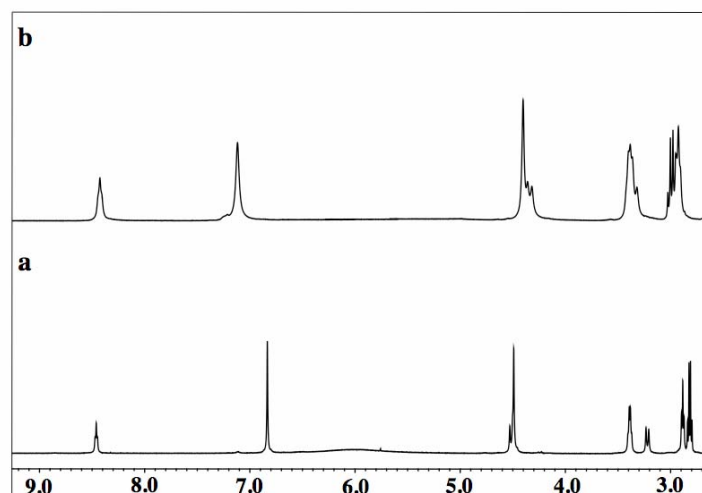


Figure 4.5 Portions of the ^1H NMR spectra (500 MHz, rt, $\text{DMSO-}d_6$) of: a) receptor **14**; b) Na^+ -complex **17**. The residual Et_3N quartet is at ~ 2.8 ppm.

After the extraction, the solution was separated and CO_2 gas was introduced (rt, 1 atm). A fine white precipitate quickly formed (Figure 4.6), which was identified as cross-linked carbamate polymer **18**. The right tube: Na^+ -complex **17** in CHCl_3 after the extraction. The left tube: same solution after bubbling CO_2 . While the ^1H NMR spectrum was broad, ^{13}C NMR spectroscopy provided an unambiguous proof of the carbamate formation. Specifically, when ^{13}C -labeled CO_2 was used, a strong carbamate $\text{C}=\text{O}$ signal at ~ 160 ppm was clearly seen (in $\text{DMSO-}d_6$). In additional experiments, metal-free receptor **14** also reacted with CO_2 both in CHCl_3 and DMSO , forming the corresponding carbamate precipitate and carbamic acid, respectively. For example, when CO_2 was bubbled through the $\text{DMSO-}d_6$ solution of **14**, the carbamic $\text{CH}_2\text{NHC(O)}$ methylene and

NH signals were detected at 3.03 and 6.68 ppm in the ^1H NMR spectrum, respectively. In the COSY spectrum, a cross-peak between these two signals was observed. These data agree well with the published spectra for alkylammonium carbamates.^{50, 52a}

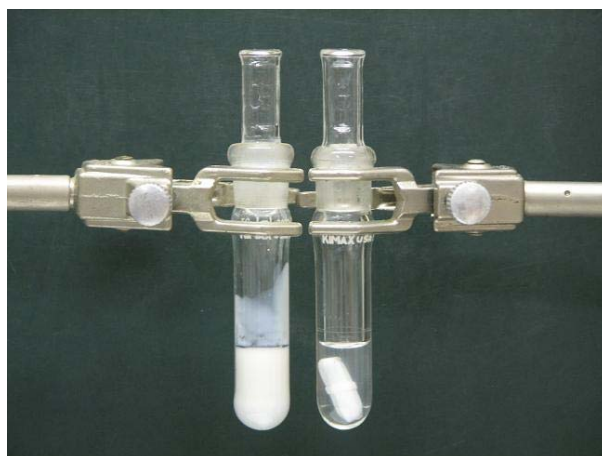


Figure 4.6 The formation of polymeric carbamate using CO_2 .

More important, polymer **18** incorporates the Na^+ cations. Control experiments, involving the use of KClO_4 and CsClO_4 , revealed no entrapment of these cations. The process thus separates the complexed species from the bulk solution. Considering that neither K^+ nor Cs^+ were complexed under the described conditions, this approach offers a selective Na^+ separation. Precipitate **18** was collected and stored for several weeks. On the other hand, it released CO_2 and dissociated back to the monomers simply upon heating and flushing with nitrogen (40-50 $^\circ\text{C}$). The Na^+ can subsequently be released in the pure form simply upon washing with water.

It is possible to selectively separate Na^+ -salts through binding in solution and subsequent precipitation with CO_2 . The Na^+ -storage can now be accomplished without solvent, which is economically preferred and prevents environmentally dangerous

leaching. Combined with the increasing role of CO₂ in separations⁶⁶ and green chemistry,⁶⁷ our approach offers means for creating environmentally responsive processes.

CHAPTER 5

EXPERIMENTAL SECTION

5.1 General Information

Melting points were determined on a Mel-Temp apparatus (Laboratory Devices, Inc.) and are uncorrected. ^1H , ^{13}C NMR, COSY and HMBC NMR spectra were recorded at $295 \pm 1^\circ\text{C}$ on JEOL 300 and 500 MHz spectrometers. Chemical shifts were measured relative to residual non-deuterated solvent resonances. FTIR spectra were recorded on a Bruker Vector 22 FTIR spectrometer. UV-vis spectra were measured on a Varian Cary-50 spectrophotometer. Fluorescence spectra were recorded on a JOBIN YVON FluoroMax-3 spectrofluorometer. Mass spectra were recorded at the Scripps Center for Mass Spectrometry (La Jolla, CA). High Resolution MALDI FT mass spectra were obtained on an IonSpec Ultima FTMS. MALDI TOF mass spectra were obtained on an Applied Biosystems Voyager STR (2). Elemental analysis was performed on a Perkin-Elmer 2400 CHN analyzer.

All experiments with moisture- and/or air-sensitive compounds were run under a dried nitrogen atmosphere. For column chromatography, Silica Gel 60 Å (Sorbent Technologies, Inc.; 200–425 mesh) was used. Parent tetrahydroxycalix[4]arene **10**⁶⁴ was prepared according to the published procedures. Calixarenes **11**⁶⁸ and **12**⁶⁹ were

prepared by known protocols, and their data matched literatures. Molecular modeling was performed using commercial MacroModel 7.1.

5.2 Synthesis and Characterizations

Methyl 4-[[(4,6-dimethyl-2-oxo-2H-1-benzopyran-7-yl)ethylamino**]methyl]benzoate (**1**)**

This compound was prepared according to a modification of the literature procedure.^{41c} Coumarin 2 (217 mg, 1.0 mmol), methyl 4-(bromomethyl)benzoate (275 mg, 1.2 mmol) and potassium carbonate (690 mg, 5.0 mmol) were mixed in distilled acetonitrile (30 mL) and refluxed under nitrogen for 72 hours. The solvent was evaporated and the residue was subject to column chromatography (CH₂Cl₂/CH₃OH 50:1) to give **1** as slightly yellow power (175 mg, 48%), mp 92-93 °C. ¹H NMR (DMSO-*d*₆, 500 MHz): δ 7.87 (d, *J* = 8 Hz, 2H), 7.54 (s, 1H), 7.46 (d, *J* = 8 Hz, 2H), 7.01 (s, 1H), 6.18 (s, 1H), 4.36 (s, 2H), 3.81 (s, 3H), 3.07 (q, *J* = 7 Hz, 2H), 2.37 (s, 3H), 2.36 (s, 3H), 1.05 (t, *J* = 7 Hz, 3H). ¹³C NMR (DMSO-*d*₆, 500 MHz): δ 170.0, 161.6, 153.4, 152.7, 152.4, 143.7, 129.9, 129.8, 129.6, 128.1, 126.7, 126.5, 115.1, 112.8, 109.4, 64.6, 56.4, 52.1, 47.0, 18.7, 18.6, 11.9. Elemental analysis: C₂₂H₂₅NO₄, calcd. C, 71.91; H, 6.86; N, 3.81; O, 17.42; found C, 71.81; H, 6.90; N, 3.78; O, 17.51.

4-[[(4,6-Dimethyl-2-oxo-2H-1-benzopyran-7-yl)ethylamino**]methyl]benzoic acid (**2**).**

Compound **1** (175 mg, 0.48 mmol), and tetrabutylammonium hydroxide (40% w/w 0.78 mL, 1.2 mmol) were added to a solution of THF (5 mL) and water (5 mL), stirred 2 hours and treated with hydrochloric acid (1 M) until weakly acidic. The precipitate was

filtrated and washed with water (3×20 mL). White powder (160 mg, >95%) was obtained after drying, mp 203-204 °C. UV-vis spectrum showed the maximum absorption is 342 nm, which matched the literature.^{41c} ^1H NMR (DMSO- d_6 , 500 MHz): δ 7.85 (d, $J = 8$ Hz, 2H), 7.54 (s, 1H), 7.43 (d, $J = 7$ Hz, 2H), 7.01 (s, 1H), 6.18 (s, 1H), 4.35 (s, 2H), 3.08 (q, $J = 7$ Hz, 2H), 2.38 (s, 3H), 2.37 (s, 3H), 1.05 (t, $J = 7$ Hz, 3H). ^{13}C NMR (DMSO- d_6 , 500 MHz): δ 167.7, 160.8, 153.6, 152.6, 144.4, 130.1, 129.9, 129.6, 128.6, 127.6, 114.8, 112.4, 109.1, 55.3, 47.6, 18.8, 18.5, 12.4.

***N*-[2-[(1,1-dimethylethoxy)-formylamido]ethyl]-4-[[[(4,6-dimethyl-2-oxo-2H-1-benzopyran-7-yl)ethylamino]methyl]benzamide (3)**

N-Boc ethylenediamine (0.126 mL, 0.8 mmol), compound **2** 140 mg, 0.4 mmol) were mixed with EDC•HCl (153 mg, 0.8 mmol), HOBT (108 mg, 0.8 mmol) and NMM (0.1 mL) in dry CH_2Cl_2 (25 mL) and stirred at 0 °C overnight. The solution was evaporated to dryness. The solid was dissolved in CH_2Cl_2 (50 mL) and washed with 5% aqueous HCl (50 mL). The organic layer was separated, washed with water (3×50 mL), and evaporated. Column chromatography ($\text{CH}_2\text{Cl}_2/\text{CH}_3\text{OH}$, 50:1) afforded the product as yellow powder. Yield 169 mg (86%), mp 86–87 °C. ^1H NMR (DMSO- d_6 , 500 MHz) δ 8.40-8.30 (br. s, 1H), 7.73 (d, $J = 7$ Hz, 2H), 7.52 (s, 1H), 7.38 (d, $J = 7$ Hz, 2H), 6.98 (s, 1H), 6.90-6.82 (br. s, 1H), 6.17 (s, 1H), 4.32 (s, 2H), 3.25 (q, $J = 6$ Hz, 2H), 3.15-3.00 (m, 4H), 2.37 (s, 3H), 2.36 (s, 3H), 1.05 (m, 3H). ^{13}C NMR (DMSO- d_6 , 500 MHz) δ 166.7, 160.8, 156.3, 153.7, 153.6, 152.6, 142.4, 133.8, 129.6, 128.3, 127.8, 127.6, 114.7,

112.3, 109.2, 78.2, 55.5, 55.1, 47.7, 28.8, 18.8, 18.6, 12.4. ESI-TOF high-res. MS: calcd. for $[MH^+]$ $C_{28}H_{38}N_3O_5$ 496.2810, found 496.2816.

***N*-(2-aminoethyl)-4-[[*(4,6*-dimethyl-2-oxo-2H-1-benzopyran-7-yl)ethylamino]methyl]benzamide (4)**

Compound **3** (148 mg, 0.3 mmol) and trifluoroacetic acid (5 mL, 0.067 mol) were dissolved in dry CH_2Cl_2 (10 mL) and stirred overnight. The solvent was evaporated and the residue was washed with 5% aqueous NaOH (25 mL) and water (3×25 mL). The organic layer was dried by Na_2SO_4 and evaporated to obtain yellowish powder (92 mg, 78%), mp 97-98 °C. 1H NMR (DMSO- d_6 , 300 MHz): δ 8.27 (t, $J = 6$ Hz, 1H), 7.71 (d, $J = 8$ Hz, 2H), 7.50 (s, 1H), 7.35 (d, $J = 8$ Hz, 2H), 6.96 (s, 1H), 6.14 (s, 1H), 4.30 (s, 2H), 3.31-3.15 (m, 2H), 3.04 (q, $J = 7$ Hz, 2H), 2.60 (t, $J = 6$ Hz, 2H), 2.34 (s, 3H), 2.33 (s, 3H), 1.02 (t, $J = 7$ Hz, 3H). ^{13}C NMR (DMSO- d_6 , 500 MHz): δ 166.8, 160.8, 153.7, 152.6, 142.3, 134.0, 129.6, 128.3, 127.8, 127.6, 114.7, 112.3, 109.1, 55.5, 55.1, 47.6, 43.5, 41.8, 18.8, 18.6, 12.4. IR (KBr, cm^{-1}): ν 3361, 2928, 2869, 1718, 1612, 1540, 1502, 1390, 1350, 1268, 1158, 1060. ESI-TOF high-res. MS, $[MH^+]$ calcd for $C_{23}H_{28}N_3O_3$ 394.2125, found 394.2130. Fluorescence: $\lambda_{ex} = 343$ nm, $\lambda_{em} = 422$ nm in $CHCl_3$, $[c] = 1 \times 10^{-6}$ M.

{2-[4-[[*(4,6*-dimethyl-2-oxo-2H-1-benzopyran-7-yl)ethylamino]methyl]benzoylamido]ethyl}carbamic acid (4a)

CO₂ was introduced to the NMR sample of compound **4** for 5 mins. ¹H NMR (DMSO-*d*₆, 500 MHz): δ 8.39 (t, *J* = 5 Hz, 1H), 7.73 (d, *J* = 8 Hz, 2H), 7.52 (s, 1H), 7.38 (d, *J* = 8 Hz, 2H), 6.98 (s, 1H), 6.79 (t, *J* = 6 Hz, 1H), 6.16 (s, 1H), 4.32 (s, 2H), 3.29-3.25 (q, *J* = 6 Hz, 2H), 3.10-3.04 (m, 4H), 2.37 (s, 3H), 2.35 (s, 3H), 1.05 (t, *J* = 7 Hz, 3H). ¹³C NMR (DMSO-*d*₆, 500 MHz): δ 166.7, 160.8, 157.8, 153.8, 153.7, 153.6, 152.5, 142.4, 133.7, 129.5, 128.3, 127.7, 127.6, 124.7 (CO₂), 114.7, 112.3, 109.0, 55.0, 47.6, 18.8, 18.5, 12.4.

***N*-[2-(1,1-dimethylethoxy-formylamido)ethyl]-2,3,6,7-tetrahydro-11-oxo-1H,5H,11H-[1]benzopyrano[6,7,8-ij]quinolizine-10-carboxamide (5)**

Similarly to compound **3**, bright yellow *N*-boc acceptor amine **5** was also synthesized. Compound **5**: mp 220 °C. ¹H NMR (DMSO-*d*₆, 500 MHz): δ 8.72 (t, *J* = 6 Hz, 1H), 8.47 (s, 1H), 7.20 (s, 1H), 6.91 (t, *J* = 5 Hz, 1H), 3.36-3.30 (m, 6H), 3.08 (q, *J* = 6 Hz, 2H), 2.72-2.68 (m, 4H), 1.89-1.84 (m, 4H), 1.37 (s, 9H). ¹³C NMR (DMSO-*d*₆, 500 MHz): δ 163.3, 162.2, 156.3, 152.6, 148.5, 148.0, 127.6, 119.9, 108.4, 107.8, 105.1, 78.2, 50.1, 49.5, 28.7, 27.3, 21.0, 20.1.

***N*-(2-aminoethyl)-2,3,6,7-tetrahydro-11-oxo-1H,5H,11H-[1]benzopyrano[6,7,8-ij]quinolizine-10-carboxamide (6)**

Similarly to compound **4**, brown acceptor amine **5** was also synthesized. mp > 300 °C (dec.). ¹H NMR (CDCl₃, 500 MHz): δ 9.05 (t, *J* = 6 Hz, 1H), 8.52 (s, 1H), 6.96 (s, 1H), 3.59-3.52 (m, 2H), 3.34-3.27 (m, 4H), 3.02 (t, *J* = 5 Hz, 2H), 2.89-2.79 (m, 2H), 2.78-

2.71 (m, 2H), 2.02-1.88 (m, 4H). ^{13}C NMR (CDCl_3 , 500 MHz): δ 164.5, 163.1, 152.8, 148.3, 148.2, 127.2, 119.7, 108.8, 108.3, 105.7, 50.3, 49.9, 41.8, 41.7, 27.5, 21.2, 20.3, 20.2. IR (KBr, cm^{-1}) ν 3320, 2938, 2854, 1692, 1616, 1517, 1367, 1309, 1212, 1174. ESI-TOF high-res. MS, $[\text{MH}^+]$ calcd. for $\text{C}_{18}\text{H}_{22}\text{N}_3\text{O}_3$: 328.1656, found 328.1653. Fluorescence: λ_{ex} = 435 nm, λ_{em} = 462 nm in CHCl_3 , $[\text{c}] = 1 \times 10^{-6}$ M.

{2-[2,3,6,7-Tetrahydro-11-oxo-1H,5H,11H-[1]benzopyrano[6,7,8-ij]quinolizine-10-formylamido]ethyl}carbamic acid (6a)

CO_2 was introduced to the NMR sample of compound **6** for 5 mins. ^1H NMR ($\text{DMSO}-d_6$, 500 MHz): δ 8.73 (t, J = 6 Hz, 1H), 8.52 (s, 1H), 7.26 (s, 1H), 6.80 (t, J = 5 Hz, 1H), 3.11-3.07 (q, J = 6 Hz, 2H), 2.76-2.70 (m, 4H), 1.92-1.85 (m, 4H). ^{13}C NMR ($\text{DMSO}-d_6$, 500 MHz): δ 163.3, 162.3, 157.8, 152.6, 148.5, 148.0, 127.6, 127.4 (CO_2), 119.9, 108.3, 107.8, 105.1, 50.1, 49.5, 27.3, 21.0, 20.1.

1,3-Bis{2-[4-[(4,6-dimethyl-2-oxo-2H-1-benzopyran-7-yl)ethylamino]methyl]benzoylamido]-ethyl}urea (7).

To a dried CH_2Cl_2 (10 mL) solution of coumarin **4** (40 mg, 0.1 mmol) and dried TEA (0.1 mL), triphosgene (9.89 mg, 0.033 mmol) were added. The mixture was stirred at 0 $^\circ\text{C}$ for 30 min after another equivalent of coumarin **4** was added in CH_2Cl_2 (5 mL). The reaction mixture was stirred for an hour, the solvent was removed in vacuo, and the residue was applied to column chromatography, ($\text{CH}_2\text{Cl}_2/\text{MeOH}$, 20:1) to give product **7** as a pale yellow powder. Yield 35mg (44%), mp >300 $^\circ\text{C}$ (decomp). IR (KBr, cm^{-1}): ν

3382, 2926, 2855, 1717, 1613, 1547, 1502, 1391, 1267, 1158, 1060. ^1H NMR (CDCl_3 , 500 MHz): δ 7.71 (d, J = 8 Hz, 4H), 7.67 (br. s, 2H), 7.33 (s, 2H), 7.25 (m, 4H), 6.79 (s, 2H), 6.08 (s, 2H), 5.79 (br. s, 2H), 4.20 (s, 4H), 3.48-3.36 (m, 4H), 3.36-3.26 (m, 4H), 3.02 (q, J = 7 Hz, 4H), 2.38 (s, 6H), 2.35 (s, 6H), 1.05 (t, J = 7 Hz, 6H). ^{13}C NMR (CDCl_3 , 500 MHz): δ 167.9, 161.7, 160.5, 153.4, 152.7, 152.6, 141.8, 133.1, 129.6, 128.3, 127.3, 126.7, 114.9, 112.6, 109.3, 56.1, 53.5, 47.1, 41.9, 40.1, 39.9, 29.8, 18.7, 18.6, 12.0. ESI-TOF high-res. MS: calcd. for $[\text{MH}^+]$ $\text{C}_{47}\text{H}_{53}\text{N}_6\text{O}_7$ 813.3970, found 813.3966.

1,3-Bis{2-[2,3,6,7-tetrahydro-11-oxo-1H,5H,11H-[1]benzopyrano[6,7,8-ij]quinolizine-10-formylamido]ethyl}urea (8)

To a dried CH_2Cl_2 (10 mL) solution of coumarin **6** (33 mg, 0.1 mmol) and dried TEA (0.1 mL), triphosgene (9.89 mg, 0.033 mmol) was added. The mixture was stirred at 0 $^\circ\text{C}$ for 30 mins after which another equivalent of coumarin **6** was added in CH_2Cl_2 (5 mL). The reaction mixture was stirred for an hour, the solvent was removed in vacuo, and the residue was applied to column chromatography, ($\text{CH}_2\text{Cl}_2/\text{MeOH}$, 15:1) to give compound **8** as a bright yellow powder. Yield 26mg (35%), mp >300 $^\circ\text{C}$ (decomp). IR (KBr, cm^{-1}): ν 3337, 2941, 2845, 1687, 1616, 1519, 1457, 1367, 1309, 1211, 1176. ^1H NMR (CDCl_3 + 10 % CD_3OD , 500 MHz): δ 8.40 (s, 2H), 6.91 (s, 2H), 3.50-3.43 (m, 8H), 3.32-3.26 (m, 8H), 2.83-2.62 (m, 8H), 2.01-1.82 (m, 8H). ^{13}C NMR (CDCl_3 + 10 % CD_3OD , 500 MHz): δ 164.9, 163.1, 159.3, 152.7, 148.5, 148.1, 127.2, 119.9, 108.2,

107.7, 105.5, 50.7, 50.2, 49.8 (CD₃OD), 40.0, 39.8, 29.6, 27.4, 21.0, 20.0, 19.9. ESI-TOF high-res. MS: calcd for [MH⁺] C₃₇H₄₁N₆O₇ 681.3031, found 681.3032.

***N*-{2-[4-[(4,6-dimethyl-2-oxo-2H-1-benzopyran-7-yl)ethylamino]methyl]benzoylamido]ethyl}-*N*'-{2-[2,3,6,7-tetrahydro-11-oxo-1H,5H,11H-[1]benzopyrano[6,7,8-ij]quinolizine-10-formylamido]ethyl}urea (**9**)**

To a dried CH₂Cl₂ (10 mL) solution of coumarin **4** (40 mg, 0.1 mmol) and TEA (0.1 mL), triphosgene (9.89 mg, 0.033 mmol) were added. The mixture was stirred at 0 °C for 15 min after which coumarin **6** (33 mg, 0.1 mmol) was added in CH₂Cl₂ (5 mL). The reaction mixture was stirred for an hour, the solvent was removed in vacuo, and the residue was applied to column chromatography, (CH₂Cl₂/ MeOH, 15:1) to give product **9** as a yellow powder. Yield 23 mg (30%), mp >300 °C (decomp.); IR (KBr, cm⁻¹): ν 3295, 2928, 2490, 1689, 1616, 1531, 1309, 1175, 1062. ¹H NMR (CDCl₃, 500 MHz): δ 9.06 (t, *J* = 6 Hz, 1H), 8.38 (s, 1H), 8.18 (t, *J* = 4 Hz, 1H), 7.77 (d, *J* = 8 Hz, 2H), 7.68 (s, 2H), 7.33 (s, 1H), 7.27 (d, *J* = 8 Hz, 2H), 7.09 (br., 6H), 6.86 (s, 1H), 6.82 (s, 1H), 6.10 (s, 1H), 6.02 (br., 1H), 5.81 (br., 1H), 4.15 (s, 2H), 3.54-3.45 (m, 4H), 3.45-3.40 (m, 2H), 3.39-3.34 (m, 2H), 3.34-3.24 (m, 4H), 3.00 (q, *J* = 7 Hz, 2H), 2.76 (t, *J* = 6 Hz, 2H), 2.71 (t, *J* = 6.0 Hz, 2H), 2.36 (s, 3H), 2.35 (s, 3H), 2.01-1.87 (m, 4H), 1.01 (t, *J* = 7 Hz, 3H). ¹³C NMR (CDCl₃, 500 MHz): δ 167.8, 164.8, 163.1, 161.8, 160.0, 153.7, 152.7, 152.6, 148.5, 148.0, 141.8, 135.4, 133.3, 129.7, 128.2, 127.4, 127.2, 126.7, 122.1, 121.9, 119.9, 114.9, 112.6, 109.2, 108.2, 105.6, 56.3 50.3, 49.9, 46.7, 42.5, 40.8, 39.9,

39.8, 31.0, 29.8, 27.5, 21.1, 20.2, 20.1, 18.7, 18.8, 11.9. ESI-TOF high-res. MS: calcd. for $[MH^+]$ $C_{42}H_{47}N_6O_7$ 747.3501, found 747.3492.

5,11,17,23-Tetra-*tert*-butyl-25,26,27,28-tetra-{[[*N*-[2-(1,1-dimethylethoxy)formylamido)]ethyl]carbonylimino]methyl}calix[4]arene (13)

N-*boc*-ethylenediamine (0.24 mL, 1.5 mmol) and *t*-Bu-calixarene tetraacid **12** (220 mg, 0.25 mmol) were mixed with EDC•HCl (191 mg, 1.0 mmol), HOBt (135 mg, 1.0 mmol) and NMM (0.1 mL) in dry CH_2Cl_2 (25 mL) and stirred at 0 °C overnight. The solution was evaporated to dryness. The solid was dissolved in CH_2Cl_2 (50 mL) and washed with 5% aq HCl (50 mL) and water (3 x 50 mL) and evaporated. The residue was recrystallized from MeOH to give tetraamide **13** as a white solid (259 mg, 62 %); m.p. > 240 °C (decomp); IR (KBr, cm^{-1}): ν 2964, 2880, 1692, 1534, 1480, 1392, 1365, 1251, 1174, 1126, 1043, 871; 1H NMR ($CDCl_3$, 500 MHz): δ 7.98 (br., 4H), 6.78 (s, 8H), 5.48 (br., 4H), 4.53 (m, 4H), 4.50 (s, 8H), 3.50 (m, 8H), 3.29 (m, 8H), 3.24 (d, J = 13 Hz, 4H), 1.41 (s, 36H), 1.07 (s, 36H); ^{13}C NMR ($CDCl_3$, 500 MHz): δ 170.4, 156.6, 152.8, 146.0, 132.7, 126.0, 79.2, 74.3, 45.0, 40.8, 39.5, 34.0, 31.4, 28.5; ESI-TOF m/z 1449.8880, ($[M + H^+]$, calcd for $C_{80}H_{120}N_8O_{16}$ 1449.8895); Calcd for $C_{80}H_{120}N_8O_{16}$: C, 66.27; H, 8.34; N, 7.73. Found: C, 66.36; H, 8.17; N, 7.96.

5,11,17,23-Tetra-*tert*-butyl-25,26,27,28-tetra-[[*N*-(2-aminoethyl)carbonylimino]methyl]calix[4]arene TFA salt (14•4TFA)

Tetraamide **13** (145 mg, 0.1 mmol) and TFA (0.5 mL, 6.5 mmol) were dissolved in dry CH₂Cl₂ (10 mL) and stirred overnight. The solvent was removed, and Et₂O (20 mL) was added to precipitate tetraamine **14** as a TFA salt (129 mg, 86 %); m.p. 182-185 °C (decomp); IR (KBr, cm⁻¹): ν 2964, 2083, 1659, 1535, 1461, 1392, 1363, 1300, 1178, 1135, 1052, 872 cm⁻¹; ¹H NMR (DMSO-*d*₆, 300 MHz): δ 8.43 (br t, 4H), 7.90 (br, 12H), 6.81 (s, 8H), 4.49 (m, 4H), 4.47 (s, 8H), 3.40-3.38 (m, 8H), 3.20 (d, *J* = 13 Hz, 4H), 2.90 (br, 8H), 1.02 (s, 36H); ¹³C NMR (DMSO-*d*₆, 300 MHz): δ 170.6, 159.4 (q, *J* = 125 Hz, CF₃C=O), 151.8, 146.8, 134.3, 126.3, 117.6 (q, *J* = 1185 Hz, CF₃C=O), 74.8, 42.8, 41.8, 34.1, 31.6; ESI-TOF *m/z* 1049.6782, ([Free amine + H⁺], calcd. for C₆₀H₈₉N₈O₈ 1449.6803); Calcd for C₆₈H₉₂F₁₂N₈O₁₆: C, 54.25; H, 6.16; N, 7.44. Found: C, 54.36; H, 6.17; N, 7.36.

5,11,17,23-Tetra-*tert*-butyl-25,26,27,28-tetra-[[*N*-(2-aminoethyl)carbonylimino]methyl]calix[4]arenecarbamic acid (15**)**

Compound **14**•**4TFA** (15 mg, 0.01 mmol) was dissolved in DMSO-*d*₆ (0.5 mL), TEA (0.02 mL) was added. Then CO₂ was introduced for 5 mins to form carbamic acid **15**: ¹H NMR (DMSO-*d*₆, 300 MHz): δ 8.34 (br, 4H), 6.81 (s, 8H), 6.70 (br, 4H), 4.53 (d, *J* = 13.0 Hz, 4H), 4.46 (s, 8H), 3.20 (d, *J* = 13.0 Hz, 4H), 3.03 (br., 8H), 1.04 (s, 36H).

5,11,17,23-tetra-*tert*-butyl-25,26,27,28-tetra-[[*N*-(2-aminoethyl)carbonylimino]methyl]calix[4]arene carbamate (16**)**

Compound **14•4TFA** (15 mg, 0.01 mmol) was suspended in 1 mL CHCl₃. TEA (0.02 mL) was added to dissolve **14**. Then CO₂ was introduced for 10 mins to form white precipitate **16**, which was isolated and dried in vacuo. ¹H NMR (DMSO-*d*₆, 500 MHz): δ 8.50 (br t, 4H), 6.83 (s + br. s, 12H), 6.80-6.00 (br), 4.46-4.53 (m, 12H), 3.42 (br., 8H), 3.21 (d, *J* = 12 Hz, 4H), 2.90-2.85 (m, 24H), 1.02 (m, 60H). ¹³C NMR (DMSO-*d*₆, 300 MHz): δ 170.5, 159.1 (q, *J* = 121 Hz, CF₃C=O), 153.3, 145.1, 133.4, 125.9, 117.7 (q, *J* = 1187 Hz, CF₃C=O), 74.4, 46.2, 37.6, 34.1, 31.6, 10.1. Due to the low concentration, the carbamate C=O singlet could not be detected.^{52b,e}

Extraction of alkali-metal perchlorates (MClO₄) by calixarene (14); a general procedure

Compound **14** (15.0 mg, 0.01 mmol) was dissolved in 1 mL of CHCl₃ in the presence of TEA (0.02 mL). Alkali-metal perchlorate (0.01 mmol) was added and the suspension was stirred overnight. The solution was separated. CO₂ (or ¹³CO₂) was then introduced and the precipitate was collected and dried. The ¹³C NMR spectrum of calixarene-Na⁺ carbamate polymer **18** was measured with ¹³CO₂ gas.

5,11,17,23-Tetra-*tert*-butyl-25,26,27,28-tetra-[[*N*-(2-aminoethyl)carbonylimino]methyl]calix[4]arene NaClO₄ complex (17):

¹H NMR (DMSO-*d*₆, 300 MHz): δ 8.43 (br, 4H), 7.12 (s, 8H), 4.40 (s, 8H), 4.34 (d, *J* = 12.0 Hz, 4H), 3.40-3.32 (m, 12H), 3.03-2.88 (m, 14H), 1.12 (m, 45H); ¹³C NMR

(DMSO- d_6 , 300 MHz): δ 170.6, 160.0 (q, $\text{CF}_3\text{C}=\text{O}$), 151.8, 147.0, 134.3, 126.3, 117.6 (q, $\text{CF}_3\text{C}=\text{O}$), 74.8, 46.2, 34.4, 31.5, 30.6, 9.4.

5,11,17,23-tetra-*tert*-butyl-25,26,27,28-tetra-[[*N*-(2-

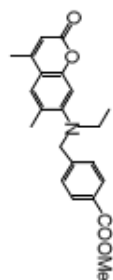
aminoethyl)carbonylimino]methyl]calix[4]arene NaClO_4 complex carbamate (18**):**

Carbamate **18** was obtained from **17** using ^{13}C -labeled CO_2 . ^{13}C NMR (DMSO- d_6 , 300 MHz): δ 160.4 ($^{13}\text{C}=\text{O}$), 159.7 (m, $\text{CF}_3\text{C}=\text{O}$), 151.6, 147.0, 134.5, 126.3, 117.7 (m, $\text{CF}_3\text{C}=\text{O}$), 74.9, 46.2, 37.8, 34.5, 31.5, 30.6, 10.1

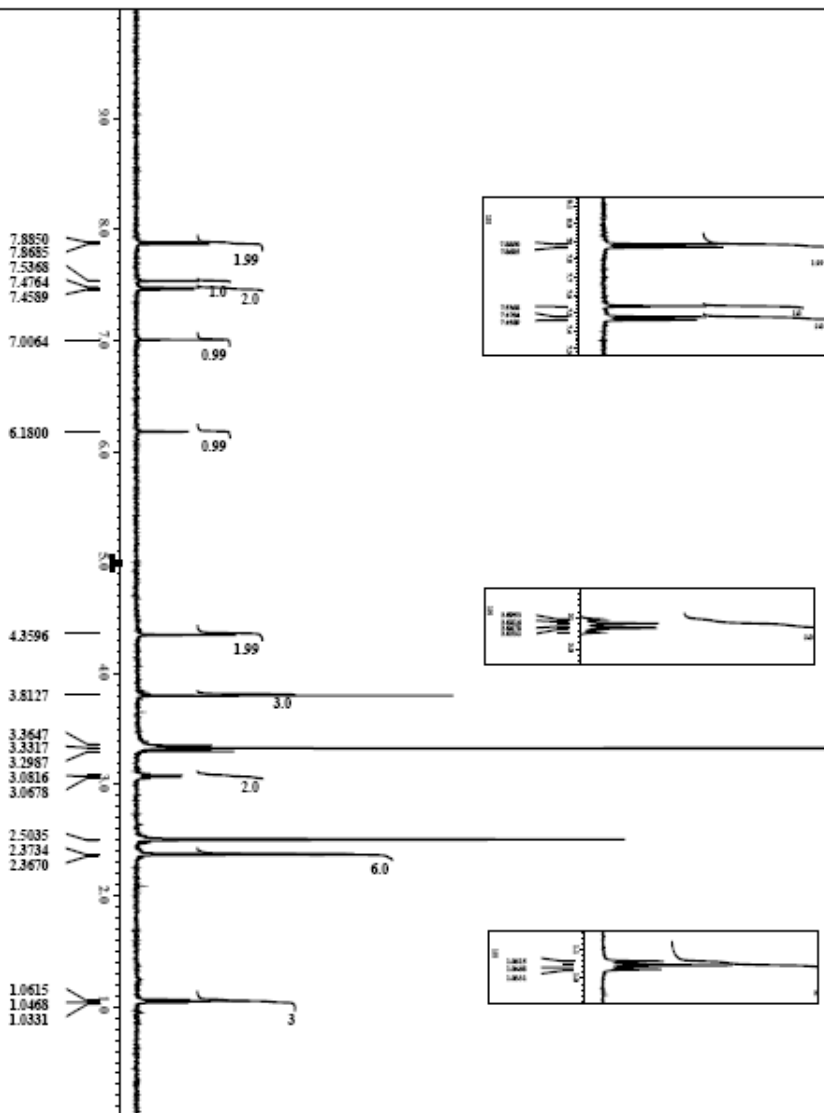
APPENDIX A

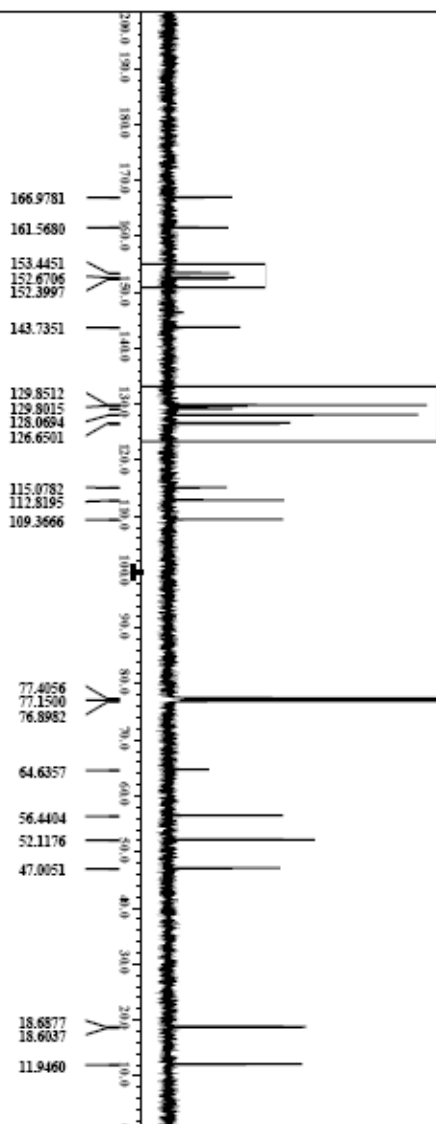
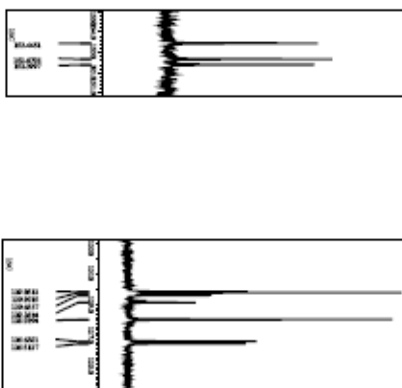
NMR SPECTRA OF COMPOUNDS **1-9,12-18**

¹H NMR in CDCl₃ for compound 1



P1: Name = 0631_Cou2CH2PhCOOMe_1D
 P1: Date = 2013-04-15
 Experiment = 81001.e_Pulse-exp
 Sample_ID = 81005.427
 Solvent = DMSO-D6
 Creation_time = 31-AUG-2005 17:39:01
 Revision_time = 11-NOV-2007 20:55:10
 Current_time = 11-NOV-2007 21:04:19
 Content = Cou2CH2PhCOOMe_1mol1
 Data_format = 1D_COMPLEX
 Data_size = 1.6384
 Data_file = 18901
 Data_extensions = 18901
 Site = B111peak_500
 Spectrometer = DMSO_1HMR
 P1: old_ftlength = 11.7473576(17) (5001MHz)
 X: acq_date = 21-08-2005 08:10
 X: obsain = 1 H
 X: freq = 500.15091521 (MHz)
 X: offset = 5 (ppm)
 X: pulseprog = 18901
 X: resolution = 0.45822189 (Hz)
 X: meap = 7.50750751 (kHz)
 C1: ppd = P_AUGR
 Mod: return = 1
 Secans = 24
 TO: 121_secs = 24
 X: 90_width = 1.85 (us)
 X: acq_time = 2.1823488 (s)
 X: angle = 45 (deg)
 X: pulse = 9.25 (us)
 P1: 121_yield = 1 (s)
 P1: 121_peak = 1 (s)
 Power_gain = 22 (us)
 Relaxation_delay = 4 (s)
 Temp_get = 25.4 (C)
 Unblank_time = 2 (us)



CCN(Cc1ccc(cc1)C(=O)O)C2=CC=C3C(=C2)OC(=O)C3



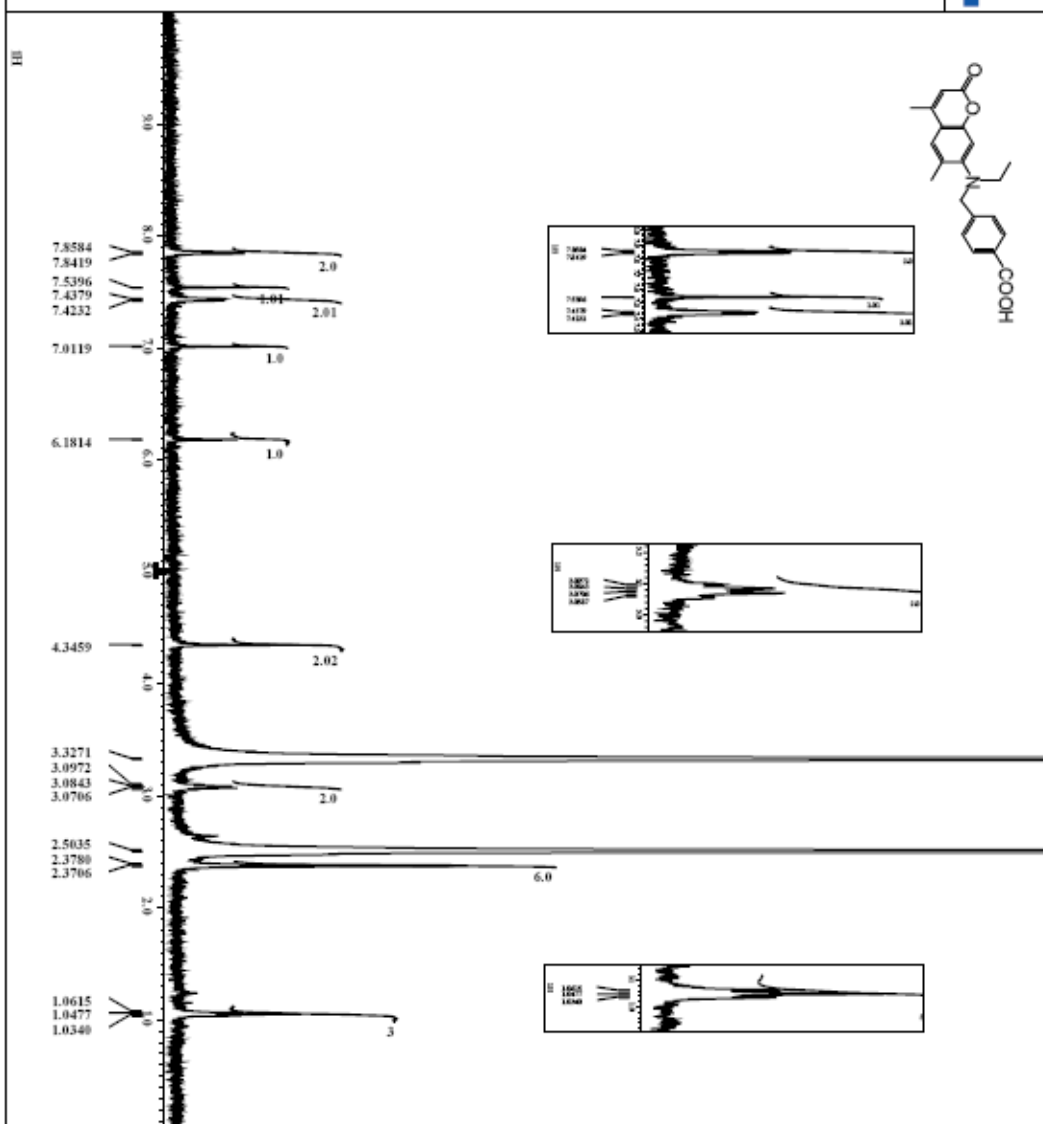
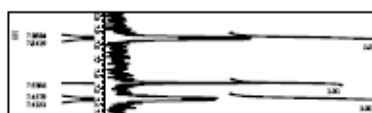
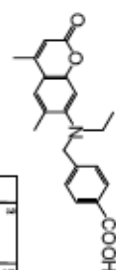
```

file_name      = 0003_C002C02PhocOOH_1H
dir_path       = /home/aveol/1H/0003_C002C02PhocOOH_1H
experiment     = 1d
sample_id      = C0020714
solvent        = DMSO-d6
creation_time   = 2-SEP-2005 18:05:49
revision_time   = 11-NOV-2007 21:07:28
current_time    = 11-NOV-2007 21:12:41

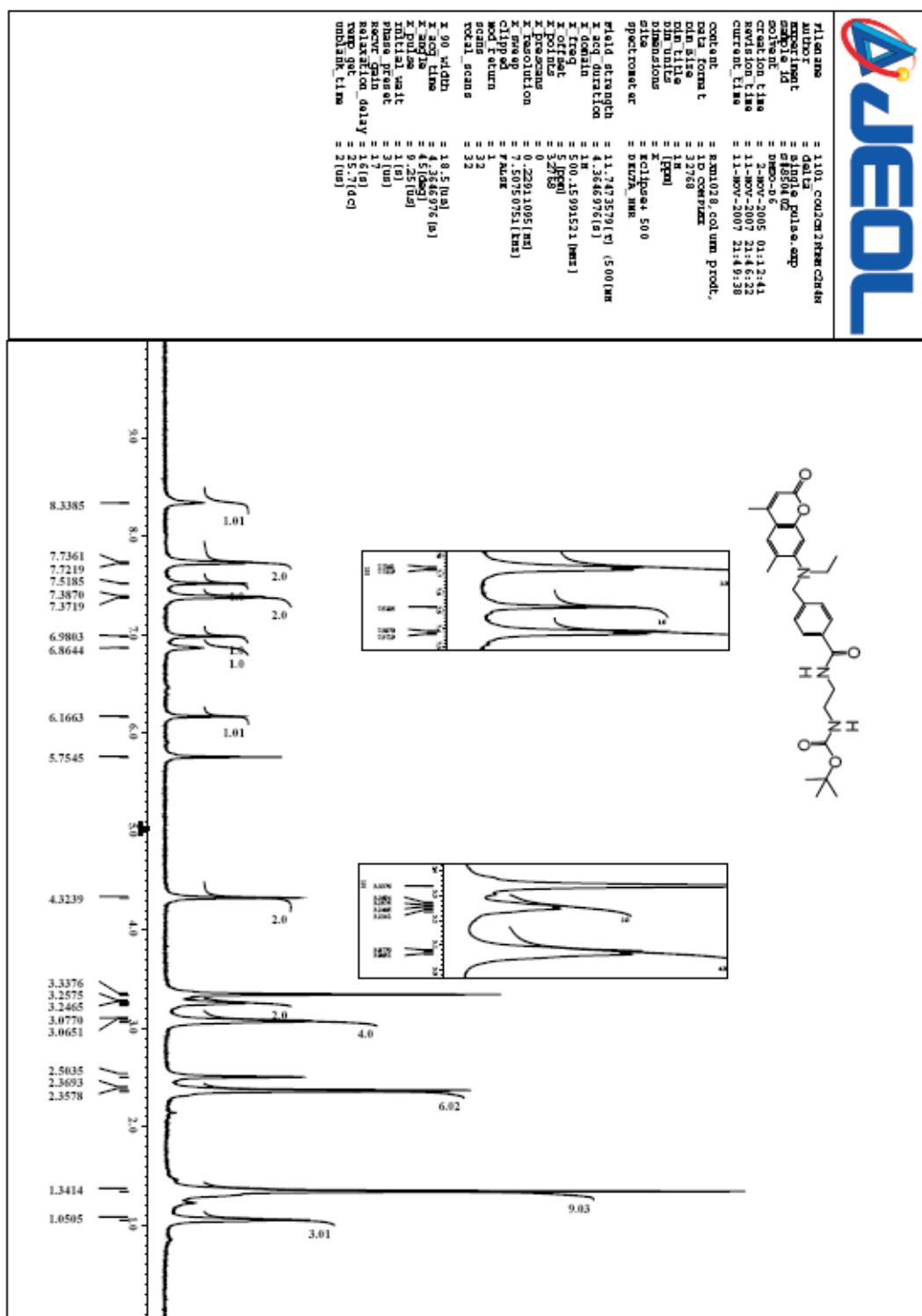
content        = COMBUSTION-CPHOCOOH, 4
data_format    = 1D COMBUSTION
data_size      = 16384
data_title     = 1H
data_subtitle   = C0020714
dimensions     = 1K
acquisition     = KClipped, 500
site           = DELTA, NMR

spectrometer    =

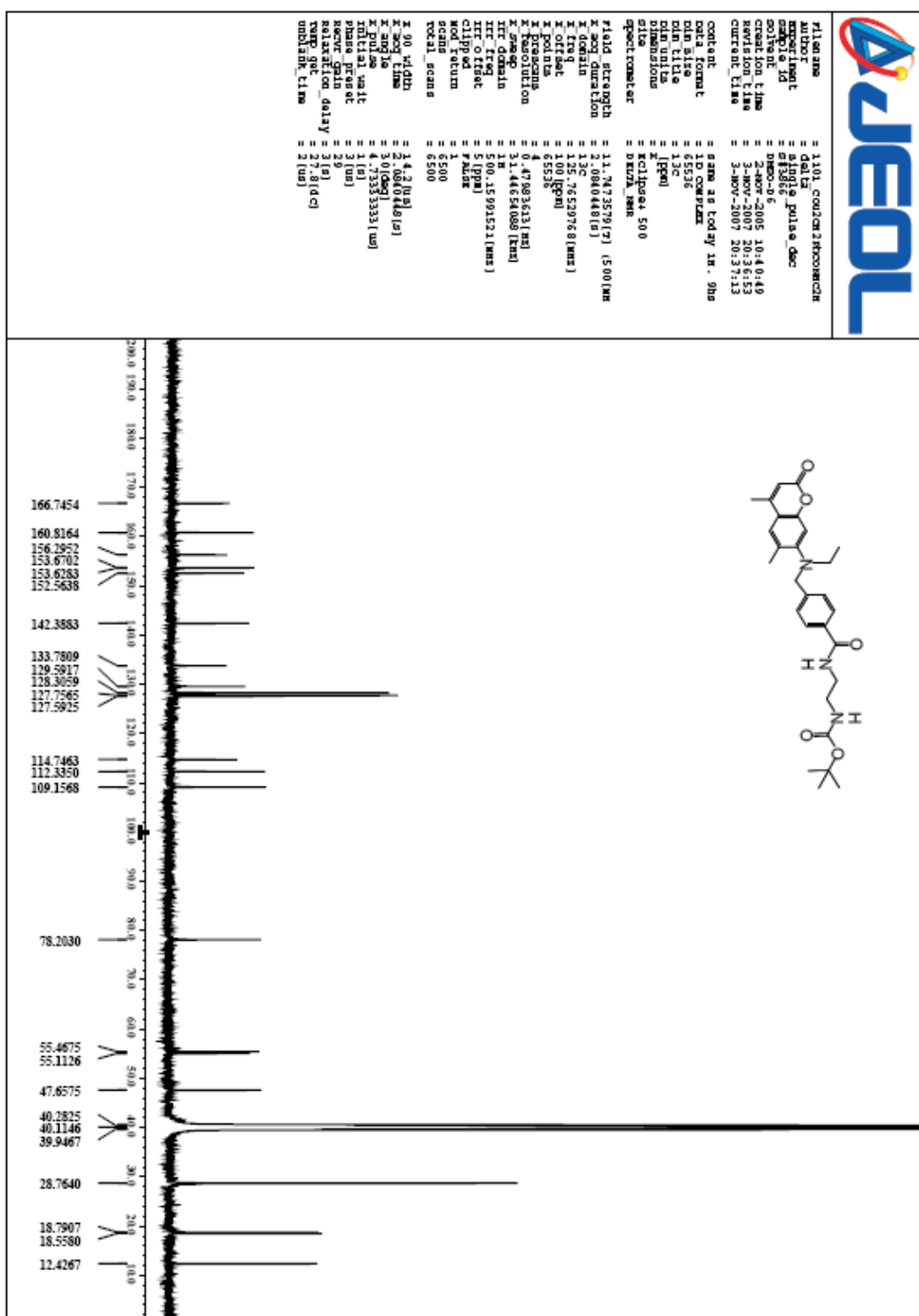
field_strength  = 11.7473579 [G] (500 [MHZ])
freq            = 123.408 [MHz]
x_coord         = 500.15991521 [mm:ss]
x_freq          = 5 [ppm]
x_offset        = 16384
x_points        = 0
x_resolution    = 4.6823489 [Hz]
x_resolution    = 7.50750751 [Hz]
x_resolution    = 1
x_resolution    = 20
mod_f_return    = 1
scans           = 20
total_scans     = 20
x_90_pulch     = 10.5 [us]
x_acq_time      = 2.1823488 [s]
x_acq_size      = 45 [kbytes]
x_pulse         = 9.25 [us]
initial_pulch   = 1 [us]
initial_pulch   = 1 [us]
initial_pulch   = 2 [us]
initial_pulch   = 4 [us]
relaxation_delay = 25 [s]
temp_get        = 25 [C]
unblank_time    = 2 [us]
    
```



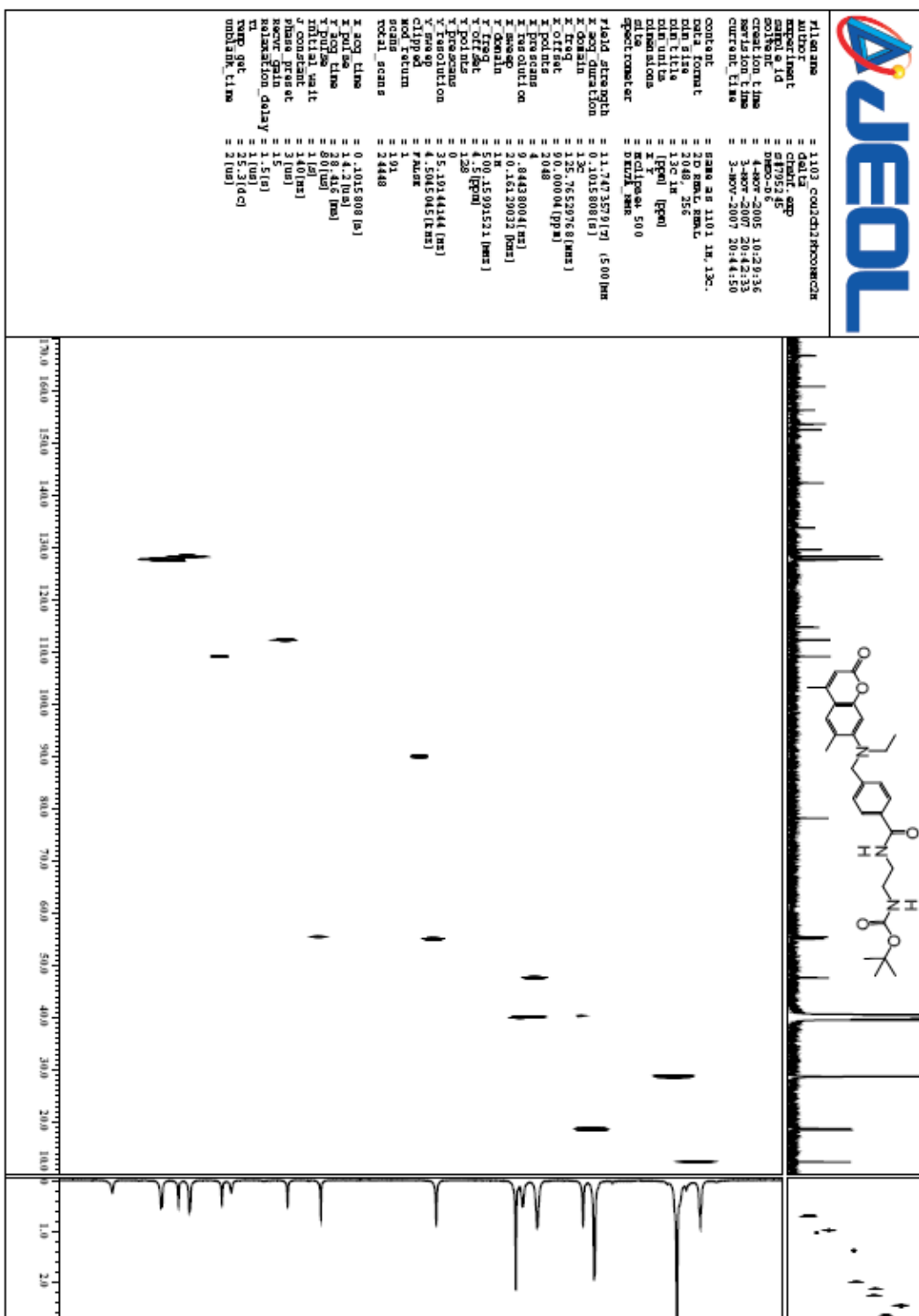
¹H NMR in DMSO-*d*₆ for compound 3



¹³C NMR in DMSO-*d*₆ for compound 3



^{13}C - ^1H HETCOR NMR in $\text{DMSO}-d_6$ for compound 3



¹³C NMR in DMSO-*d*₆ for compound 4

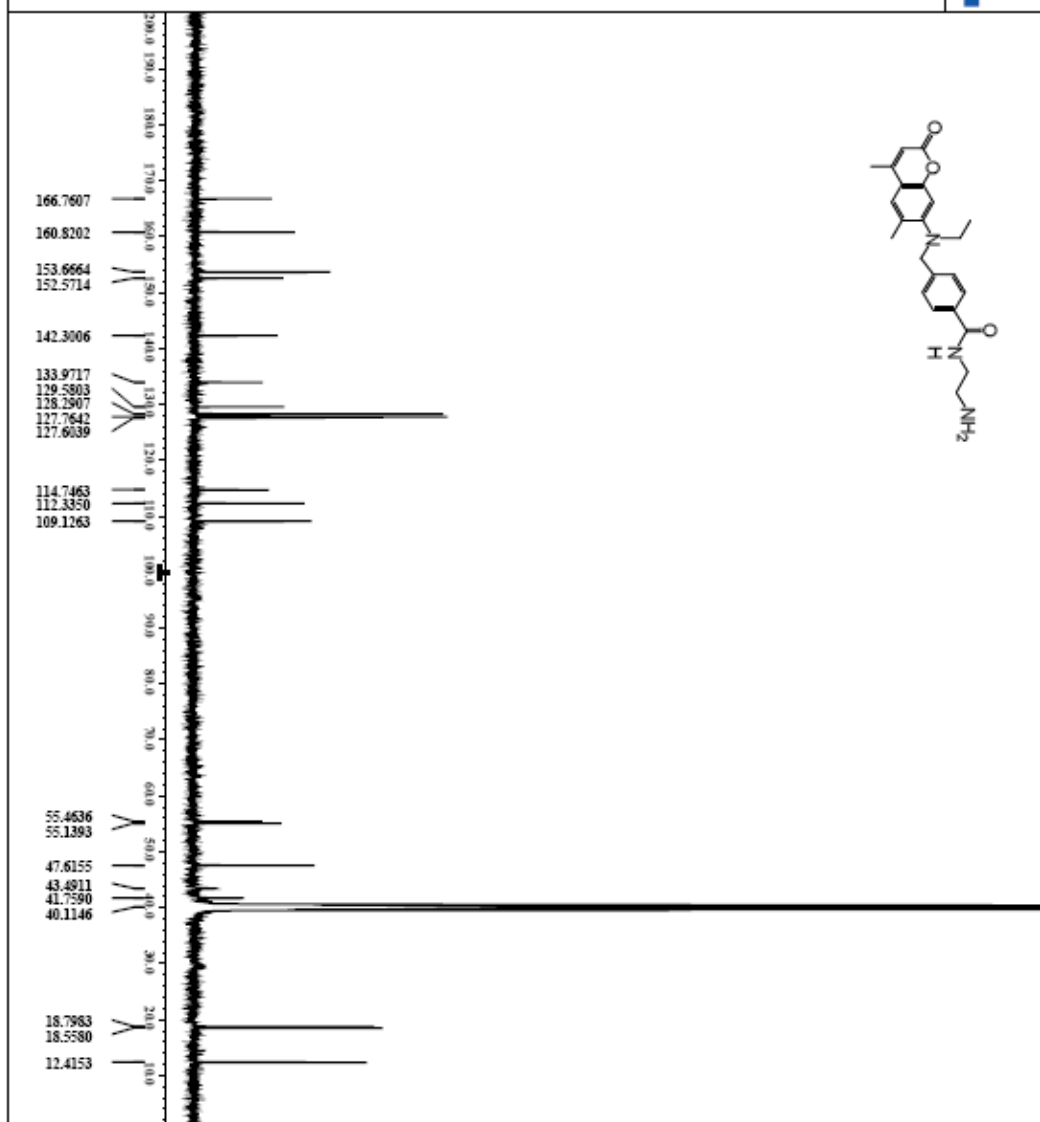
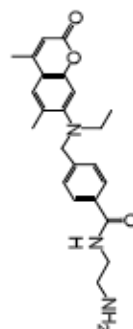


```

=====
file name      = 1108_C0410212R000002R
author        = Delta
experiment    = 1300
date_ymdhms   = 20051103_1340
solvent       = DMSO-d6
creation_time = 9-Nov-2005 06:44:25
revision_time = 3-Nov-2007 20:59:19
current_time  = 3-Nov-2007 21:00:21

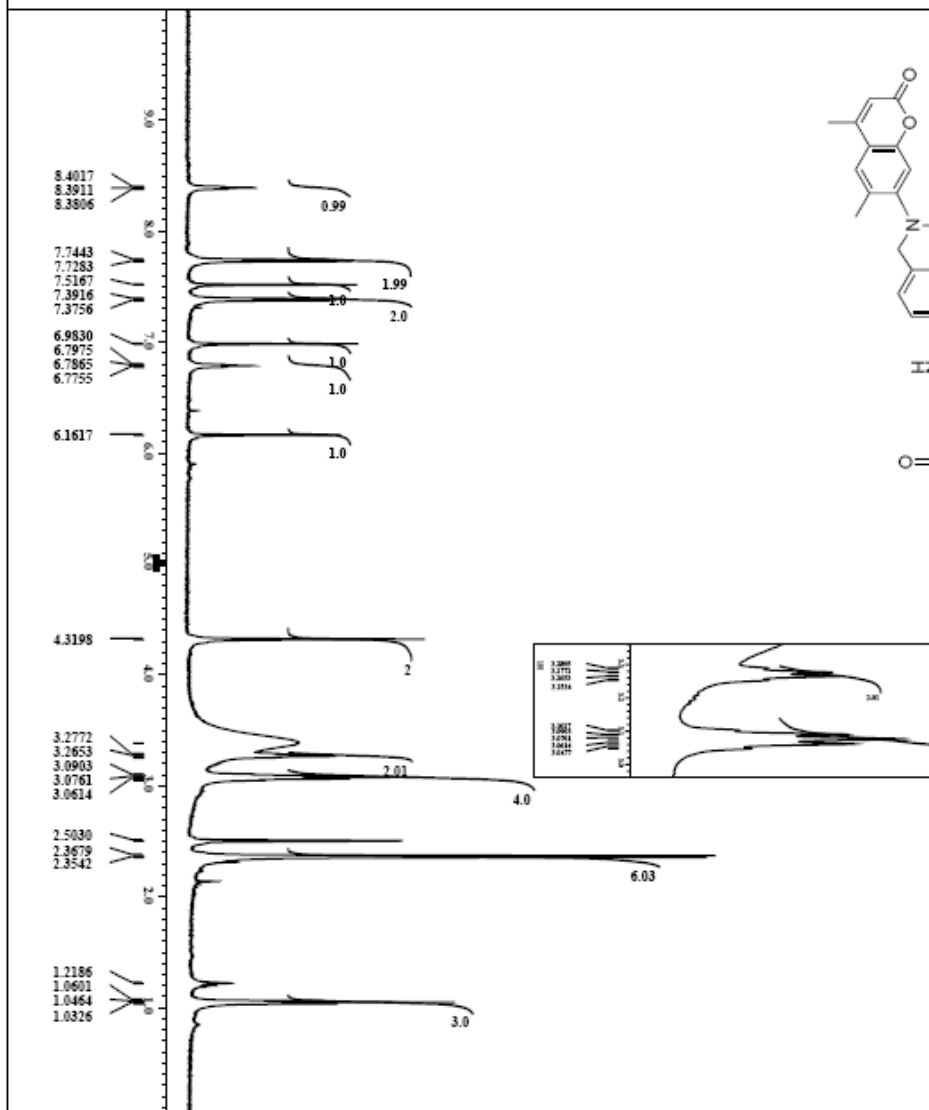
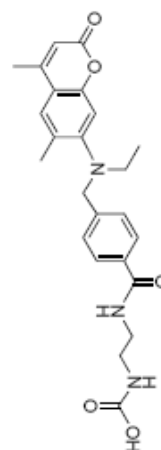
content
data format   = 1D COMPLEX
data size     = 65536
data title    = 13c
data unit     = [ppm]
data version  = 2.010004.500
=====
spectrometer  = spect
f1d1_freq     = 125.7633533 (MHz)
f1d1_p1       = 1.00 (ppm)
f1d1_p2       = 1.00 (ppm)
f1d1_p3       = 1.00 (ppm)
f1d1_p4       = 1.00 (ppm)
f1d1_p5       = 1.00 (ppm)
f1d1_p6       = 1.00 (ppm)
f1d1_p7       = 1.00 (ppm)
f1d1_p8       = 1.00 (ppm)
f1d1_p9       = 1.00 (ppm)
f1d1_p10      = 1.00 (ppm)
f1d1_p11      = 1.00 (ppm)
f1d1_p12      = 1.00 (ppm)
f1d1_p13      = 1.00 (ppm)
f1d1_p14      = 1.00 (ppm)
f1d1_p15      = 1.00 (ppm)
f1d1_p16      = 1.00 (ppm)
f1d1_p17      = 1.00 (ppm)
f1d1_p18      = 1.00 (ppm)
f1d1_p19      = 1.00 (ppm)
f1d1_p20      = 1.00 (ppm)
f1d1_p21      = 1.00 (ppm)
f1d1_p22      = 1.00 (ppm)
f1d1_p23      = 1.00 (ppm)
f1d1_p24      = 1.00 (ppm)
f1d1_p25      = 1.00 (ppm)
f1d1_p26      = 1.00 (ppm)
f1d1_p27      = 1.00 (ppm)
f1d1_p28      = 1.00 (ppm)
f1d1_p29      = 1.00 (ppm)
f1d1_p30      = 1.00 (ppm)
f1d1_p31      = 1.00 (ppm)
f1d1_p32      = 1.00 (ppm)
f1d1_p33      = 1.00 (ppm)
f1d1_p34      = 1.00 (ppm)
f1d1_p35      = 1.00 (ppm)
f1d1_p36      = 1.00 (ppm)
f1d1_p37      = 1.00 (ppm)
f1d1_p38      = 1.00 (ppm)
f1d1_p39      = 1.00 (ppm)
f1d1_p40      = 1.00 (ppm)
f1d1_p41      = 1.00 (ppm)
f1d1_p42      = 1.00 (ppm)
f1d1_p43      = 1.00 (ppm)
f1d1_p44      = 1.00 (ppm)
f1d1_p45      = 1.00 (ppm)
f1d1_p46      = 1.00 (ppm)
f1d1_p47      = 1.00 (ppm)
f1d1_p48      = 1.00 (ppm)
f1d1_p49      = 1.00 (ppm)
f1d1_p50      = 1.00 (ppm)
f1d1_p51      = 1.00 (ppm)
f1d1_p52      = 1.00 (ppm)
f1d1_p53      = 1.00 (ppm)
f1d1_p54      = 1.00 (ppm)
f1d1_p55      = 1.00 (ppm)
f1d1_p56      = 1.00 (ppm)
f1d1_p57      = 1.00 (ppm)
f1d1_p58      = 1.00 (ppm)
f1d1_p59      = 1.00 (ppm)
f1d1_p60      = 1.00 (ppm)
f1d1_p61      = 1.00 (ppm)
f1d1_p62      = 1.00 (ppm)
f1d1_p63      = 1.00 (ppm)
f1d1_p64      = 1.00 (ppm)
f1d1_p65      = 1.00 (ppm)
f1d1_p66      = 1.00 (ppm)
f1d1_p67      = 1.00 (ppm)
f1d1_p68      = 1.00 (ppm)
f1d1_p69      = 1.00 (ppm)
f1d1_p70      = 1.00 (ppm)
f1d1_p71      = 1.00 (ppm)
f1d1_p72      = 1.00 (ppm)
f1d1_p73      = 1.00 (ppm)
f1d1_p74      = 1.00 (ppm)
f1d1_p75      = 1.00 (ppm)
f1d1_p76      = 1.00 (ppm)
f1d1_p77      = 1.00 (ppm)
f1d1_p78      = 1.00 (ppm)
f1d1_p79      = 1.00 (ppm)
f1d1_p80      = 1.00 (ppm)
f1d1_p81      = 1.00 (ppm)
f1d1_p82      = 1.00 (ppm)
f1d1_p83      = 1.00 (ppm)
f1d1_p84      = 1.00 (ppm)
f1d1_p85      = 1.00 (ppm)
f1d1_p86      = 1.00 (ppm)
f1d1_p87      = 1.00 (ppm)
f1d1_p88      = 1.00 (ppm)
f1d1_p89      = 1.00 (ppm)
f1d1_p90      = 1.00 (ppm)
f1d1_p91      = 1.00 (ppm)
f1d1_p92      = 1.00 (ppm)
f1d1_p93      = 1.00 (ppm)
f1d1_p94      = 1.00 (ppm)
f1d1_p95      = 1.00 (ppm)
f1d1_p96      = 1.00 (ppm)
f1d1_p97      = 1.00 (ppm)
f1d1_p98      = 1.00 (ppm)
f1d1_p99      = 1.00 (ppm)
f1d1_p100     = 1.00 (ppm)
=====

```





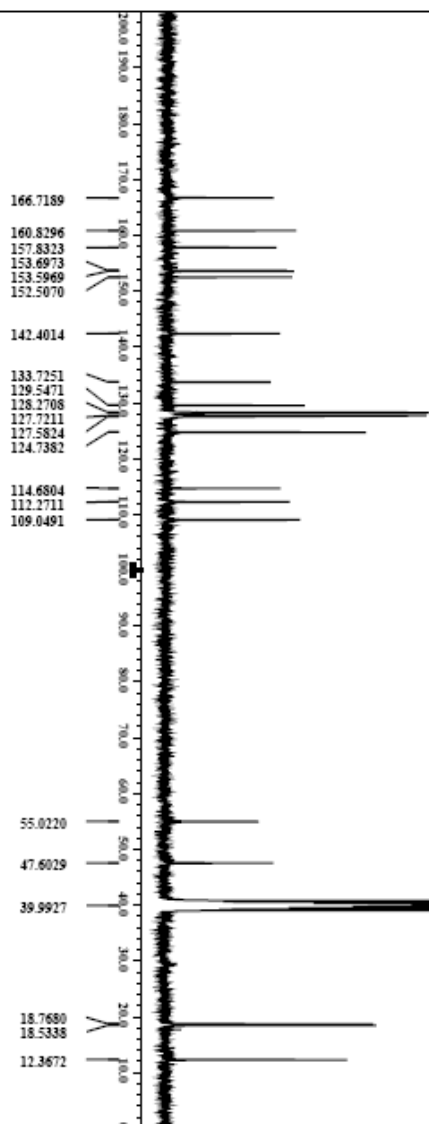
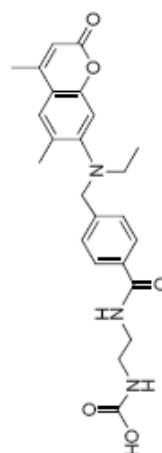
Filename = 1109_Denocx_NMR_A_TMR80
Author = delta
Experiment = single_pulse.scf
Date_YYYYMMDD = 20051118
Solvent = DMSO-d6
Creation_time = 9:40V-2005 18:23:46
Acquisition_time = 11-Nov-2007 22:13:44
Purification_time = 11-Nov-2007 22:13:54
Current_time = 11:08 18 20mg - CD2
Content = 1D CPMG
Data_format = 32768
Data_size = 32768
Data_title = H
Data_units = [ppm]
Dimensions = 2 311564 500
Name = 1109_Denocx_NMR
Spectrometer = JEOL_NMR
P1_pulse_length = 11.7473579 [μs] (500 [MHz])
P1_pulse_delay = 4.3844976 [μs]
P2_pulse_length = 500.15991521 [μs]
P2_pulse_delay = 51 [μs]
P3_pulse_length = 32768
P3_pulse_delay = 0.22011005 [μs]
P4_pulse_length = 7.50750751 [μs]
P4_pulse_delay = 1
Mod_Factor = 1
Scan = 32
P1_pulse_echo = 32
P2_pulse_echo = 18.5 [μs]
P3_pulse_echo = 4.3844976 [μs]
P4_pulse_echo = 45 [μs]
P5_pulse_echo = 9.25 [μs]
Initial_wait = 1 [μs]
Initial_wait = 31 [μs]
Initial_wait = 31 [μs]
Initial_wait = 31 [μs]
Relaxation_delay = 25.5 [s]
Temp_get = 21 [μs]
Unit_mn_time = 21 [μs]

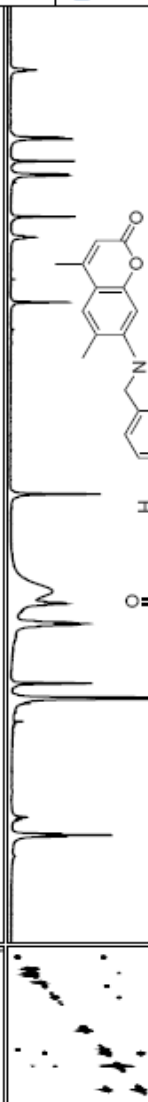
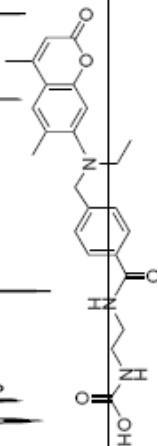
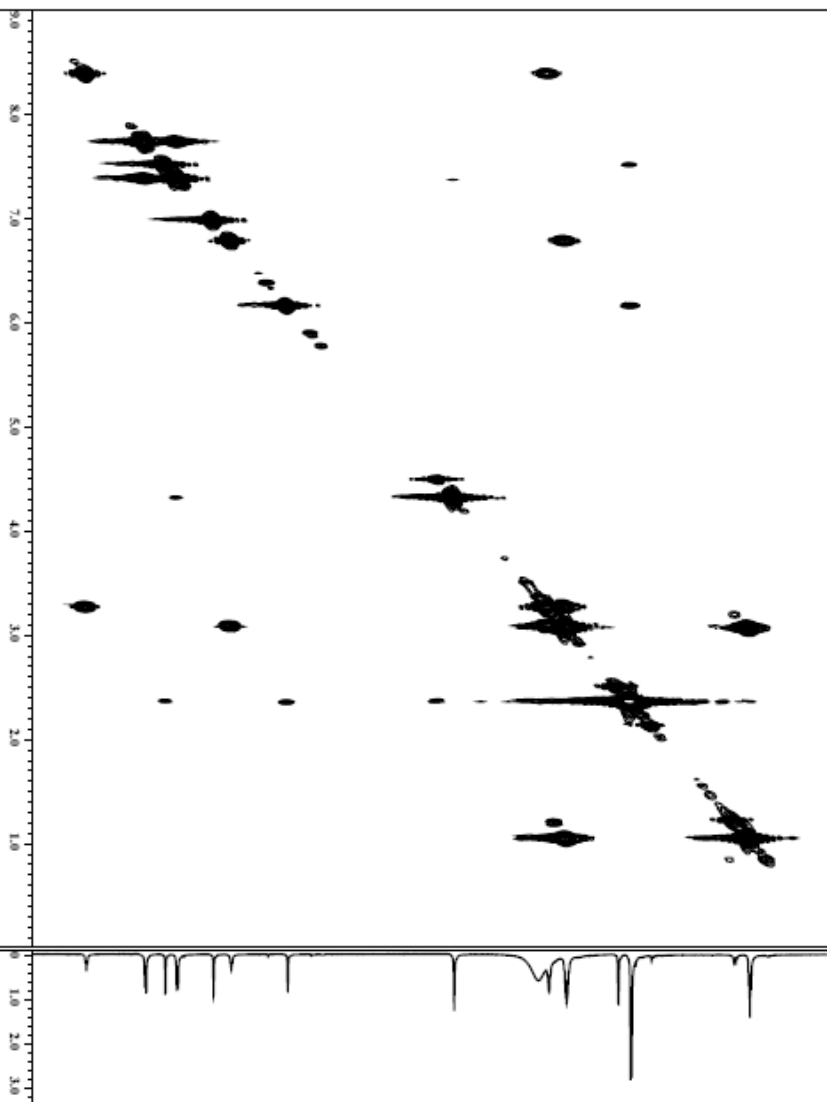


¹³C NMR in DMSO-*d*₆ for compound 4a

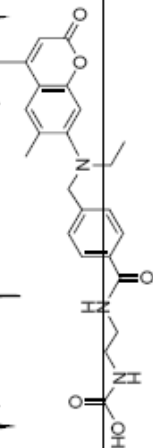


Filename = 1115_DMSO-NH2_CA_DM80
 Author = da1ta
 Experiment = 13Cqpt1e_pul_00_dec
 Sample_ID = 1115
 Solvent = DMSO-*d*₆
 Creation_time = 16-NOV-2005 04:27:18
 Revision_time = 3-NOV-2007 21:27:48
 Current_Etime = 3-NOV-2007 21:28:19
 Comment = ac 1100 DMSO-NH2CA_P
 Data_Filename = 1D_CompLex
 Data_Grupo = 52428
 Data_title = 13C
 Data_units = [ppm]
 Data_instrument = spect 300
 Data_location = DMU7A2_NMR
 Spectrometer =
 P1.q1d_acq_length = 7.058601377 (300 MHz
 P1.q1d_acq_duration = 2.76824054 [s]
 P1.q1d_resolution = 12.0
 P1.q1d_f1_offset = 71.6583442 [MHz]
 P1.q1d_f2_offset = 100.1 [ppm]
 P1.q1d_f3_offset = 65.53 [ppm]
 P1.q1d_p1_offset = 4
 P1.q1d_p2_offset = 0.36124027 [Hz]
 P1.q1d_p3_offset = 22.6782824 [Hz]
 P1.q1d_p4_offset = 30.5205592 [MHz]
 P1.q1d_p5_offset = 5 [ppm]
 P1.q1d_p6_offset = PALER
 P1.q1d_p7_offset = 10
 P1.q1d_p8_offset = 4000
 P1.q1d_p9_offset = 4000
 P1.q1d_p10_offset = 9.75 [Hz]
 P1.q1d_p11_offset = 2.76824054 [s]
 P1.q1d_p12_offset = 30 [dB]
 P1.q1d_p13_offset = 3 [dB]
 P1.q1d_p14_offset = 25 [dB]
 P1.q1d_p15_offset = 25 [dB]
 P1.q1d_p16_offset = 60.475
 P1.q1d_p17_offset = 7700
 P1.q1d_p18_offset = 7700
 P1.q1d_p19_offset = 2 [s]
 P1.q1d_p20_offset = 50
 P1.q1d_p21_offset = 21 [s]
 P1.q1d_p22_offset = 4.76824054 [s]
 P1.q1d_p23_offset = 22.8 [dB]
 P1.q1d_p24_offset = 22.8 [dB]

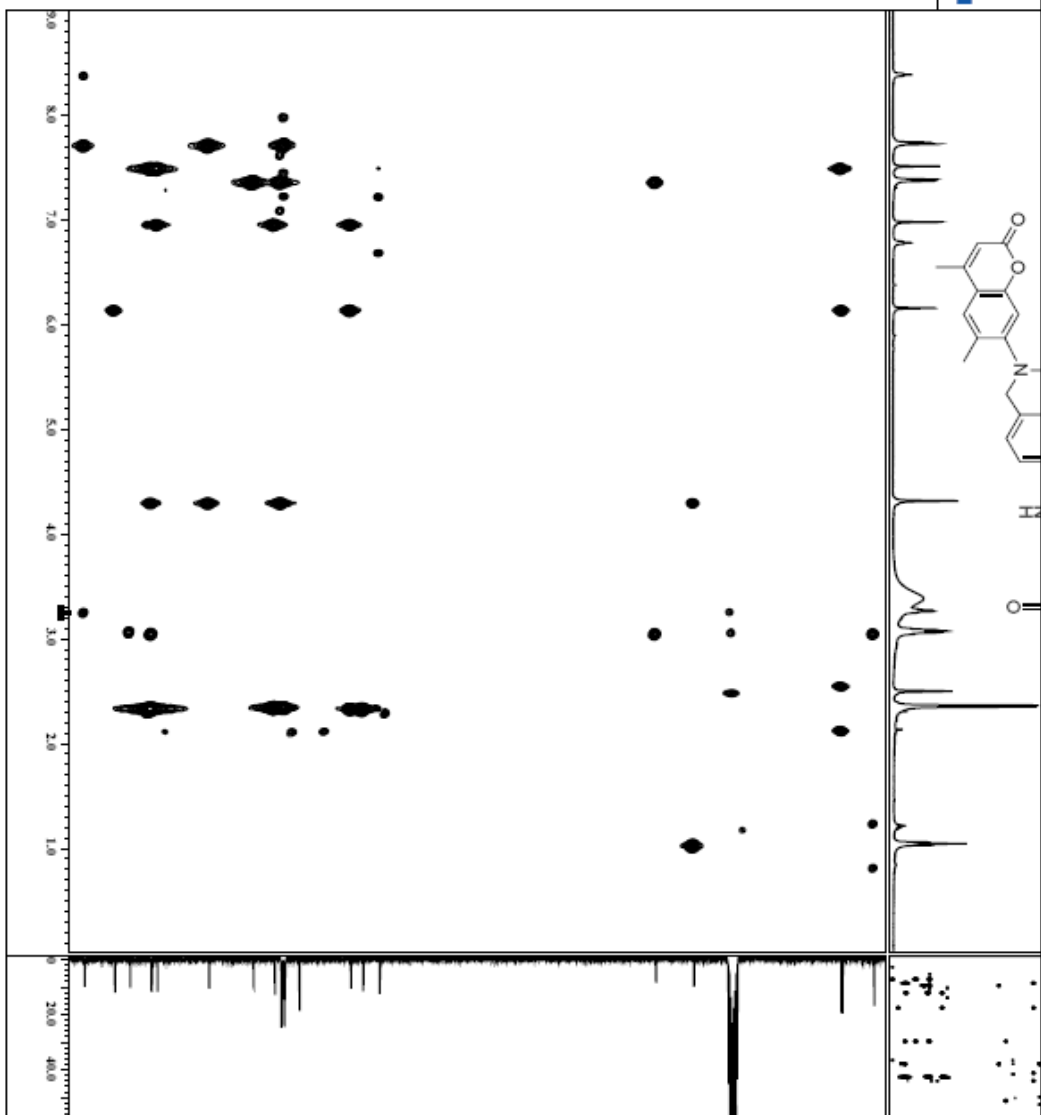


[illegible]

^1H - ^{13}C HMBSC NMR in $\text{DMSO}-d_6$ for compound 4a

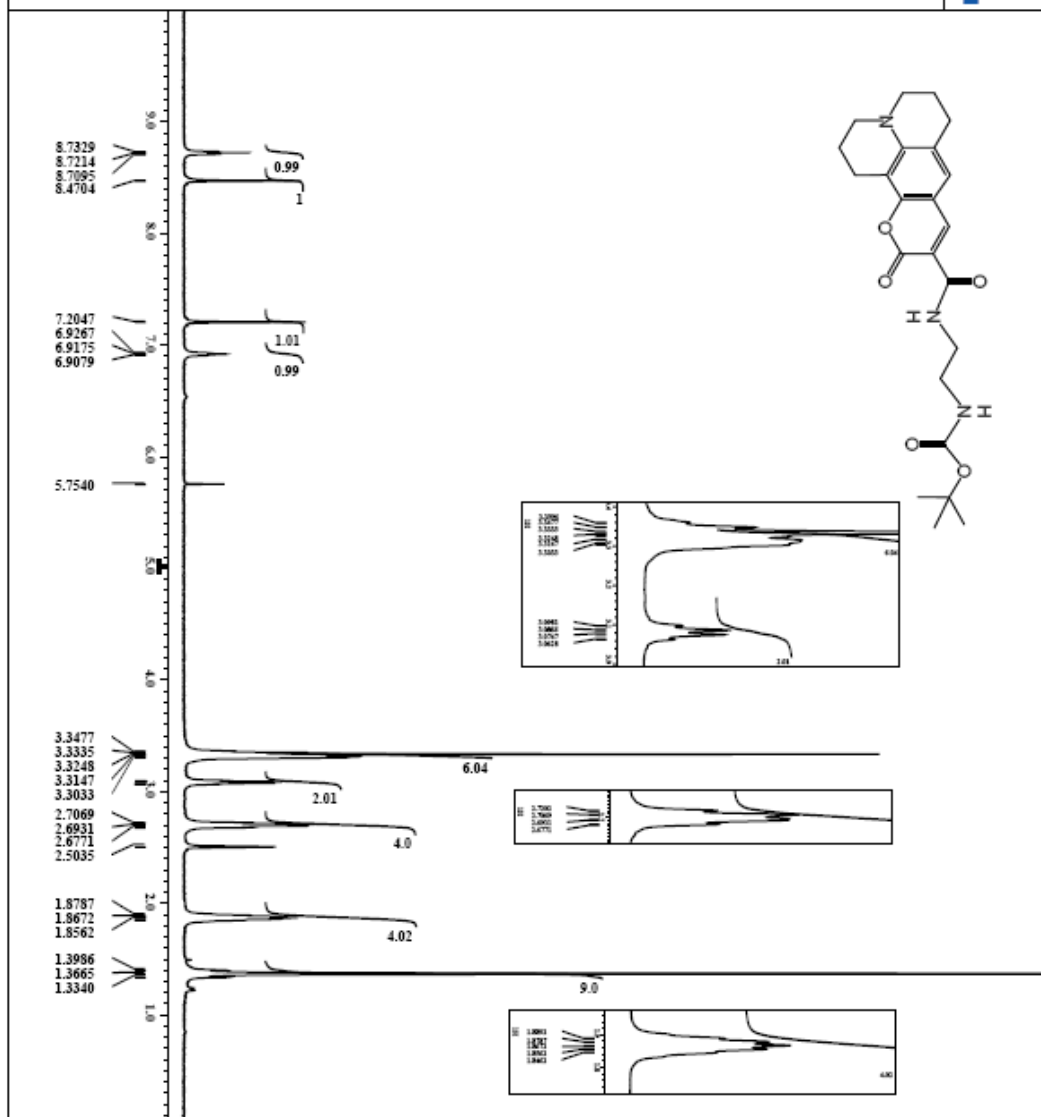


PlateName = 1204_DonorH2_CA_DMSO
 Author = 06113
 Experiment = hmbc_Pfg_vsc2
 Sample_ID = 1204
 Solvent = DMSO-D6
 Acquisition_Time = 5:00:23.005 00:30:13
 Relaxation_Time = 3:00:23.007 21:36:36
 Current_Etane = 3-MOV-2007 21:39:44
 Content = Donor Chd4, as 1115
 Data_Format = 3D BBL BBL
 Data_Type = 2D 3D
 Data_Unit = 13C
 Data_Unit2 = 13C
 Data_Unit3 = 13C
 Dimensions = [paul] [paul]
 Site = 300
 Spectrometer = DELTA2_NMR
 Plate_Acquire = 7.065601317 (300 MHz)
 X_acq_duration = 0.605388816s
 X_domain = 1H
 X_freq = 300.62965502 [MHz]
 X_offset = 4.500751 [ppm]
 X_resolution = 20.48
 X_resolution2 = 1.65183102 [Hz]
 X_resolution3 = 3.38204093 [Hz]
 X_domain2 = 13C
 X_domain3 = 13C
 Y_freq = 75.56823426 [MHz]
 Y_offset = 0.00128 [ppm]
 Y_resolution = 0
 Y_resolution2 = 47.24540397 [Hz]
 Y_resolution3 = 12.094823421 [Hz]
 Y1_domain = 1H
 Y1_freq = 300.62965592 [MHz]
 Y1_offset = 4.500751 [ppm]
 Y1_resolution = 20.48
 Mod_return = 1
 Sca = 59.408
 Total_sca = 17.408
 X_acq_time = 0.605388816s
 X_pulse = 41CB
 Y_acq_time = 13.01 [us]
 Y_pulse = 21.16608 [us]
 Y_acq = 81CB
 Y_pulse2 = 0.75 [us]
 Y_resolution = 0
 Y_resolution2 = 0
 Y_resolution3 = 0
 Data_Preset = PULPROG
 Data_Preset2 = 62.5 [us]
 Qcnd_1_amp = 1 [us]
 Qcnd_1_ph = 60 [us]
 Qcnd_2_amp = 1 [us]
 Qcnd_2_ph = 60 [us]
 Qcnd_3_amp = 1 [us]
 Qcnd_3_ph = 60 [us]
 Qcnd_3_time = 30.18108521 [us]
 Qcnd_3_resolution = 0.1 [us]
 Qcnd_3_resolution2 = 13C = 1.0688.1.08
 Qcnd_3_resolution3 = 13C
 Data_Preset3 = 140 [Hz]
 J_coupling = 140 [Hz]
 J_coupling2 = 81 [Hz]
 Acquire_gain = 50.97142857 [us]
 Relaxation_time = 1.156388816s
 Repeat_time = 1 [us]





Platform = 101, CPMAS 3H/32H NMR
Author = da1ta
Experiment = 3H/32H NMR
Sample = 5
Solvent = DMSO-*d*₆
Creation_time = 21-OCT-2005 11:24:25
Revision_time = 11-NOV-2007 22:26:17
Output_time = 11-NOV-2007 22:32:24
Content = PMOL18 column prod.
Data format = 1D COMPLEX
Data_size = 32768
Data_title = 3H
Data_units = [ppm]
Dimensions = 2D1152x4 500
Spectrometer = DEPTX NMR
Pulld_strength = 11.7473579 [V] (500 MHz)
X_acq_duration = 41.3646974 [s]
X_resolution = 51 [ppm]
X_offset = 51 [ppm]
X_resolution = 32768
X_resolution = 0.22611095 [Hz]
X_resolution = 7.650750751 [Hz]
Modulation = 1
Scan = 32
Total_scan = 32
X_01_v44th = 18.5 [Hz]
X_01_v44th = 18.5 [Hz]
X_01_v44th = 45 [Hz]
X_01_v44th = 0.25 [Hz]
Initial_val = 1 [Hz]
Phase_preserve = 3 [Hz]
Phase_preserve = 1 [Hz]
Phase_preserve = 1 [Hz]
Turn_get = 25 [Hz]
Turn_get = 21 [Hz]



¹³C NMR in DMSO-*d*₆ for compound 5

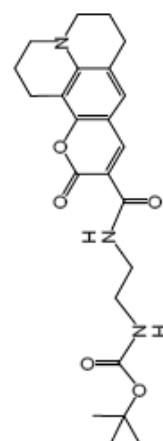
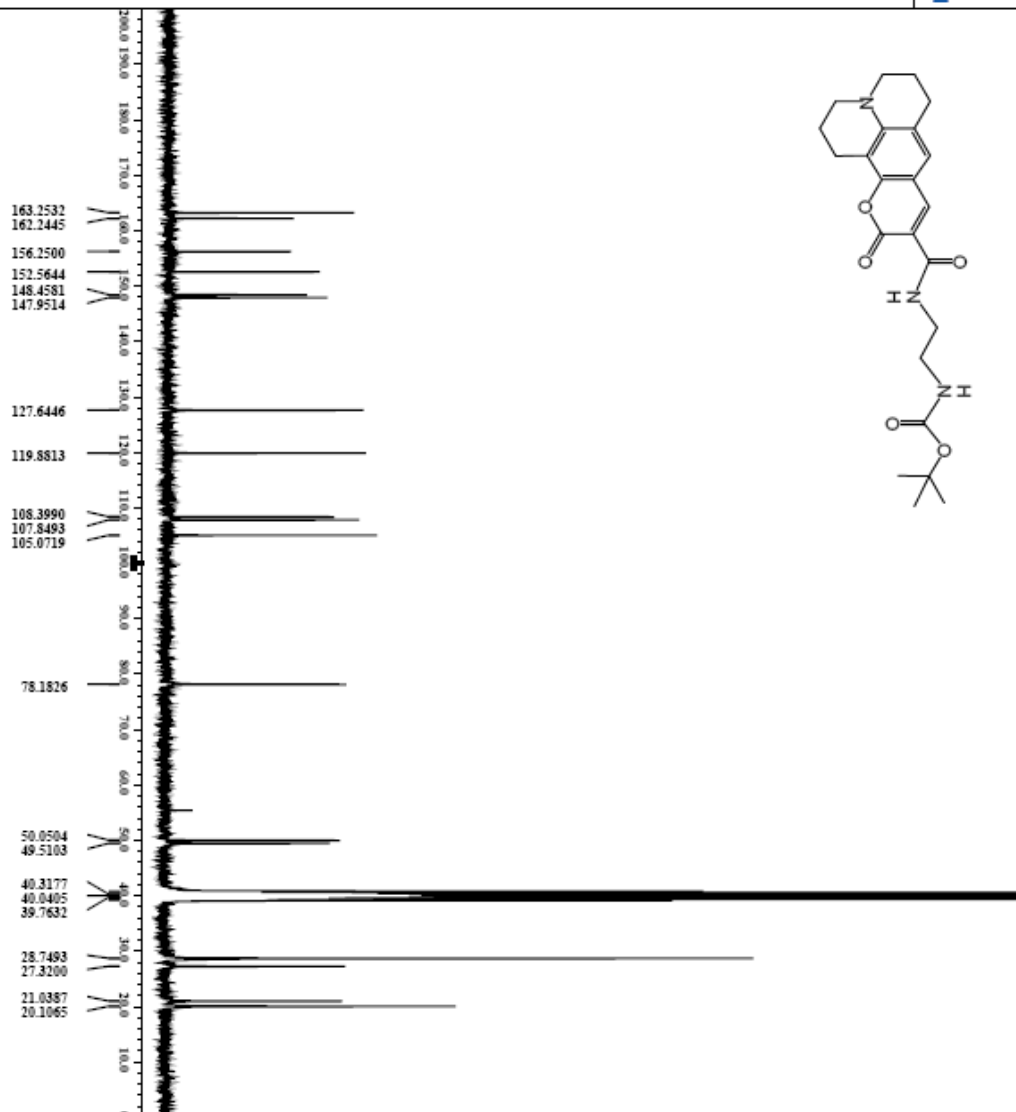
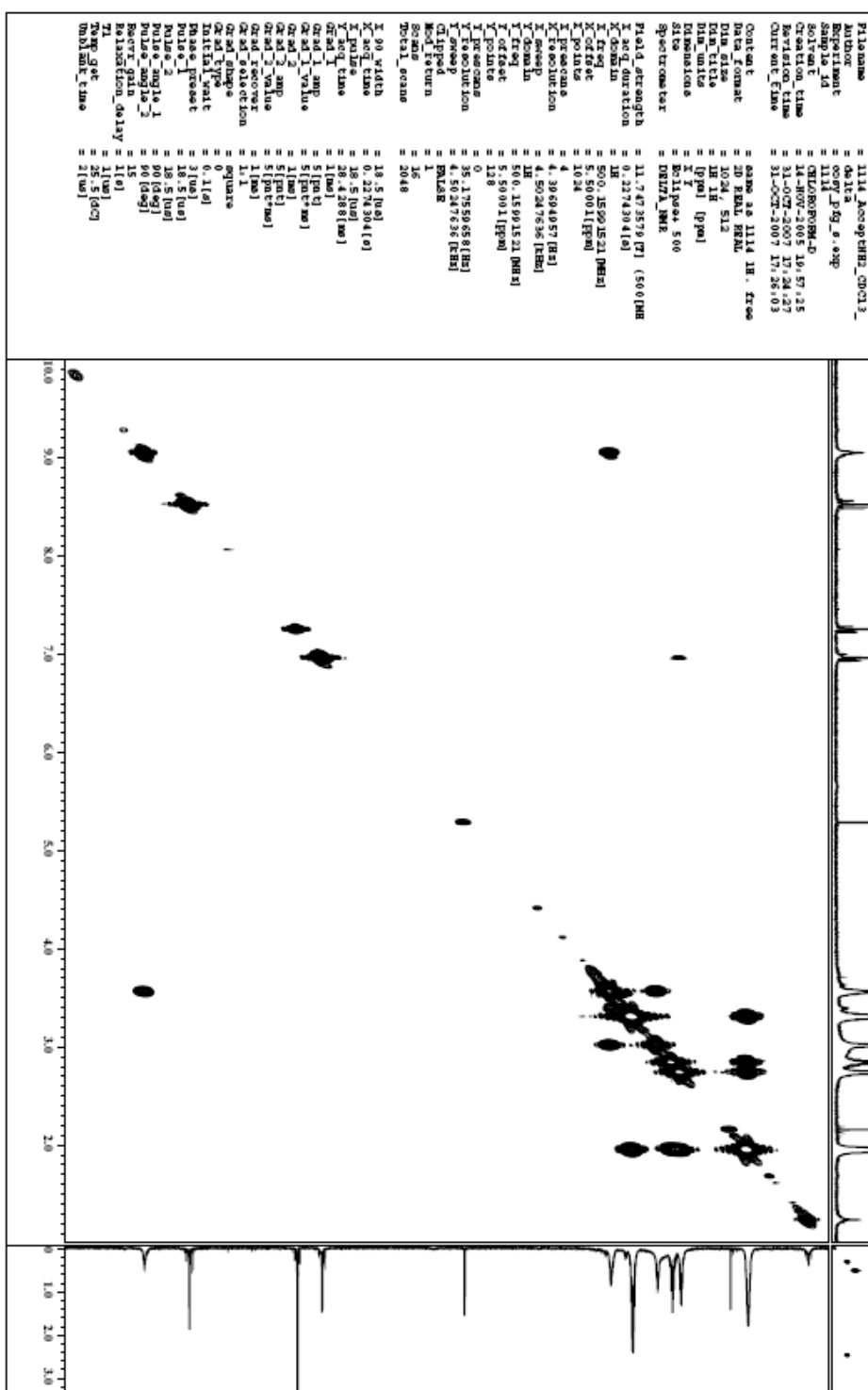
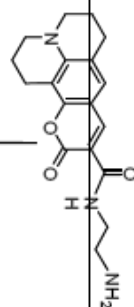


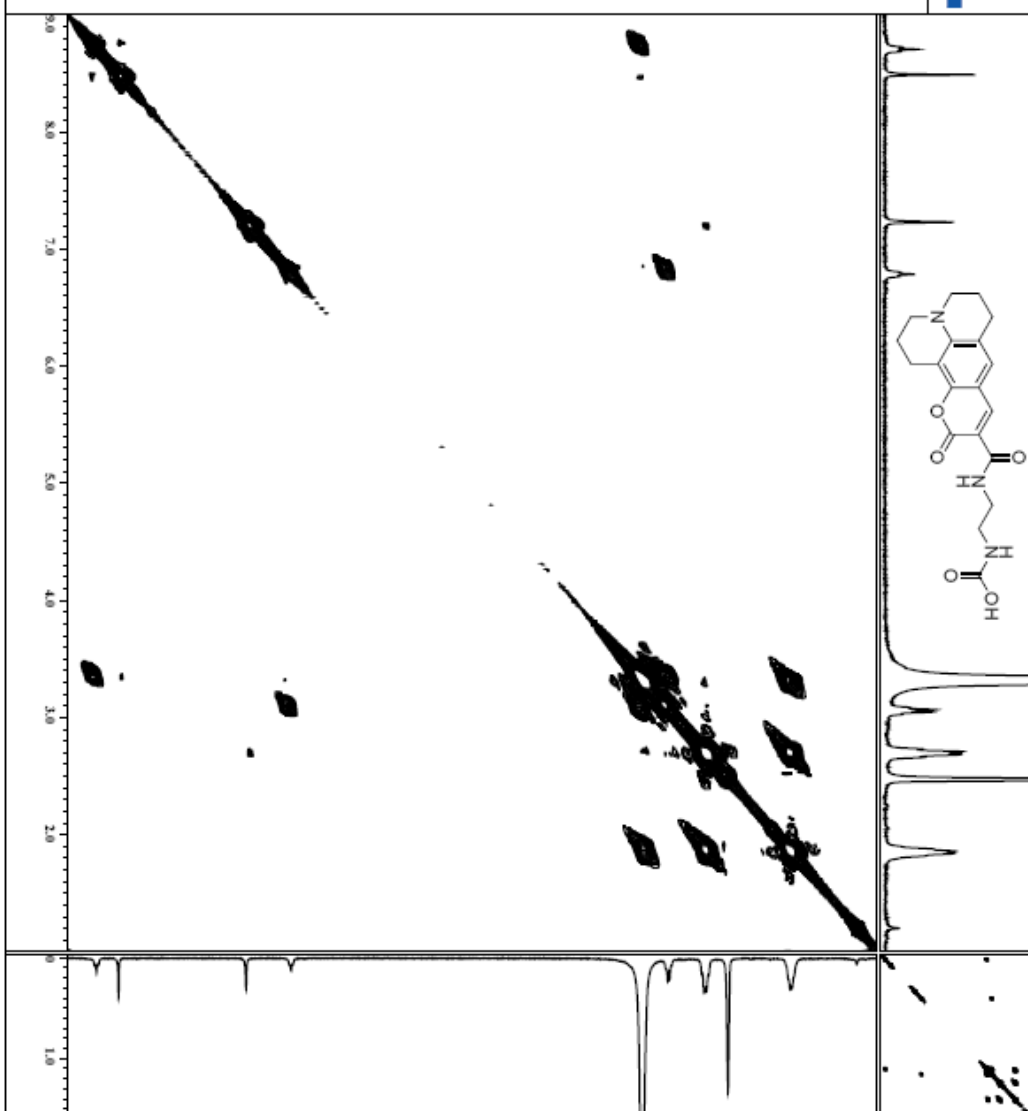
Plate name = 10.21_C0034_3H2C3H4_NH2O
 Author = da.ita
 Experiment = 401qta_pul.oe_dec
 Acquisition time = 09:01:56
 Solvent = DMSO-*d*₆
 Creation time = 22-OCT-2005 09:01:56
 Revision time = 31-OCT-2007 17:11:33
 Current time = 31-OCT-2007 17:14:11
 Content =
 Data directory = 10_C0034_3H2C3H4_NH2O
 Data file = 52428
 Data title = 13C
 Data unit = [ppm]
 Dimensions = 1
 Size of file = 300
 Spectrometer = DRZ750_NMR
 P1, sld, str, angth = 7.058601377 (300 [Hz]
 P1, ang, dur, acton = 2.76824064 [s]
 X, domain = 13C
 X, freq = 125.7624064 [MHz]
 X, offset = 100.1 [ppm]
 X, points = 65538
 X, precursors = 4
 X, resolution = 0.36124027 [Hz]
 X, sweep = 22.6742421 [Hz]
 X, time gain = 300.53065502 [Hz s]
 X, time offset = 5 [ppm]
 Clipped = PALER
 Mod. return = 10
 Acq. time = 5050
 Total scans = 5050
 X, 90 width = 9.75 [us]
 X, 90 time = 2.76824064 [s]
 X, angle = 30 [deg]
 X, gain = 81.00 [1]
 X, phase = 3.33 [deg]
 X, 180 gain = 26.148 [1]
 X, 180 time = 25 [deg]
 X, 180 offset = 90.072
 Decoupling = 7900
 Hetero. pulse = 14.01
 Hetero. time = 21.00
 Hetero. gain = 50
 Hetero. delay = 21.00
 Repetition time = 4.76824064 [s]
 Temp. [deg] = 22.6 [deg]

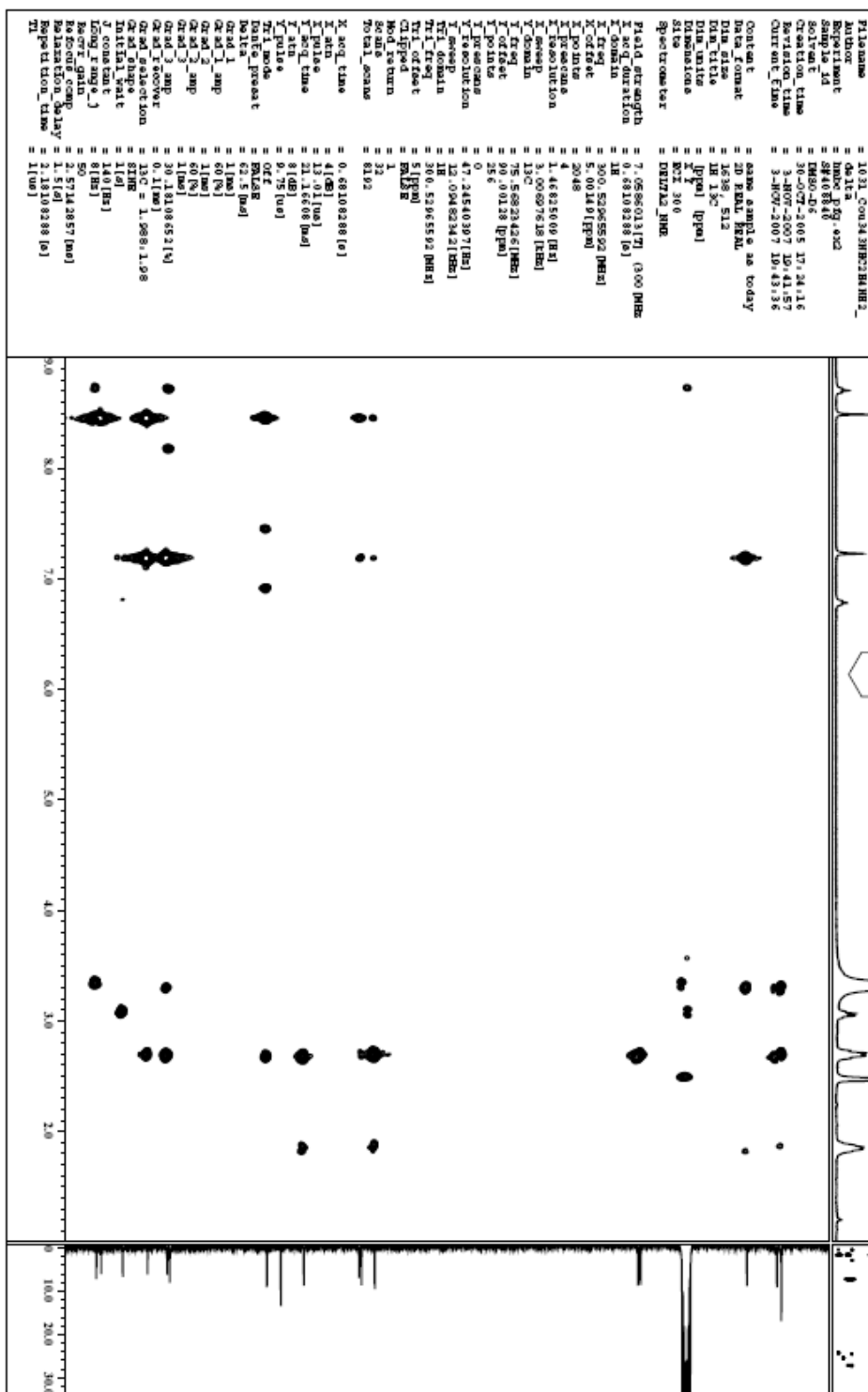
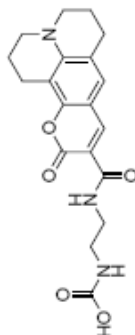








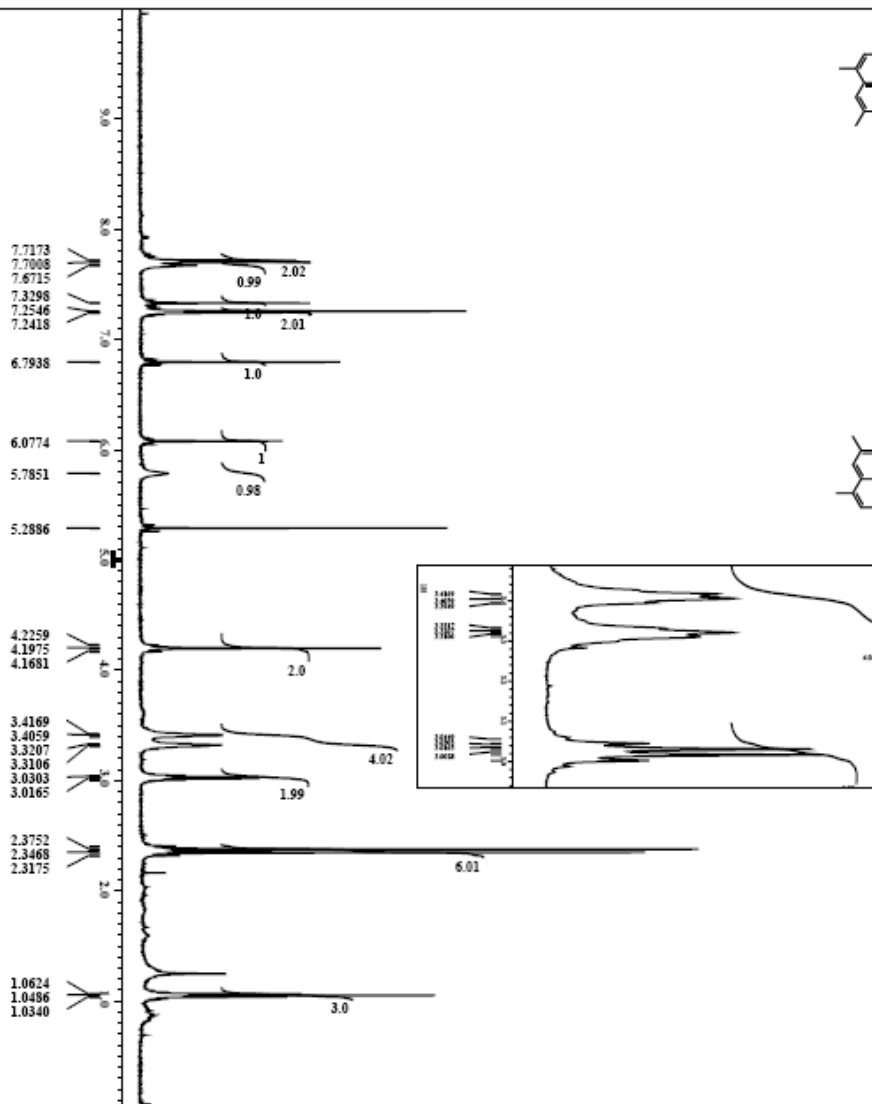
[illegible]



¹H NMR in CDCl₃ for compound 7

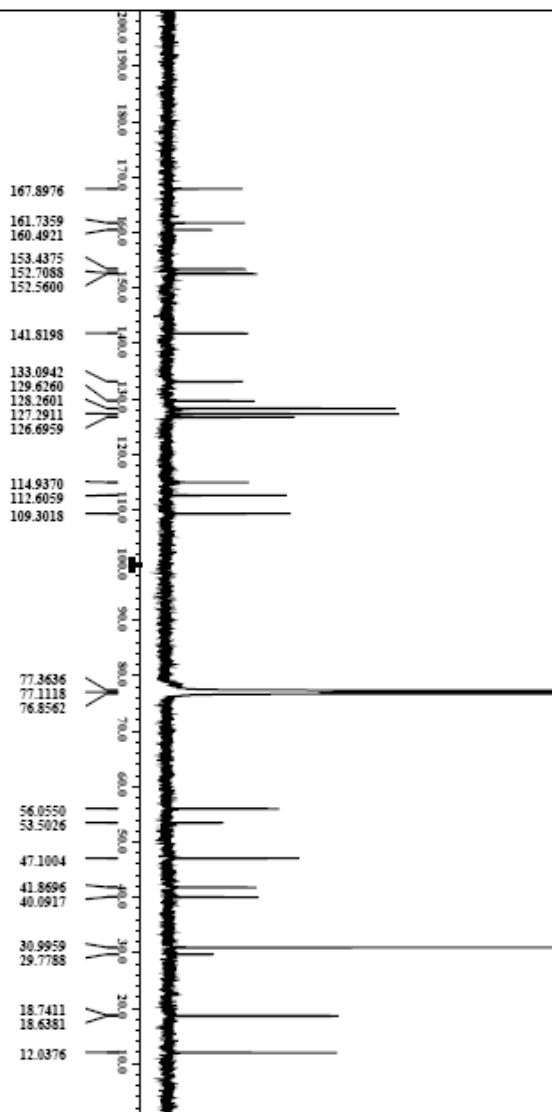
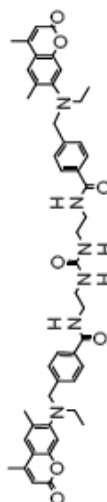


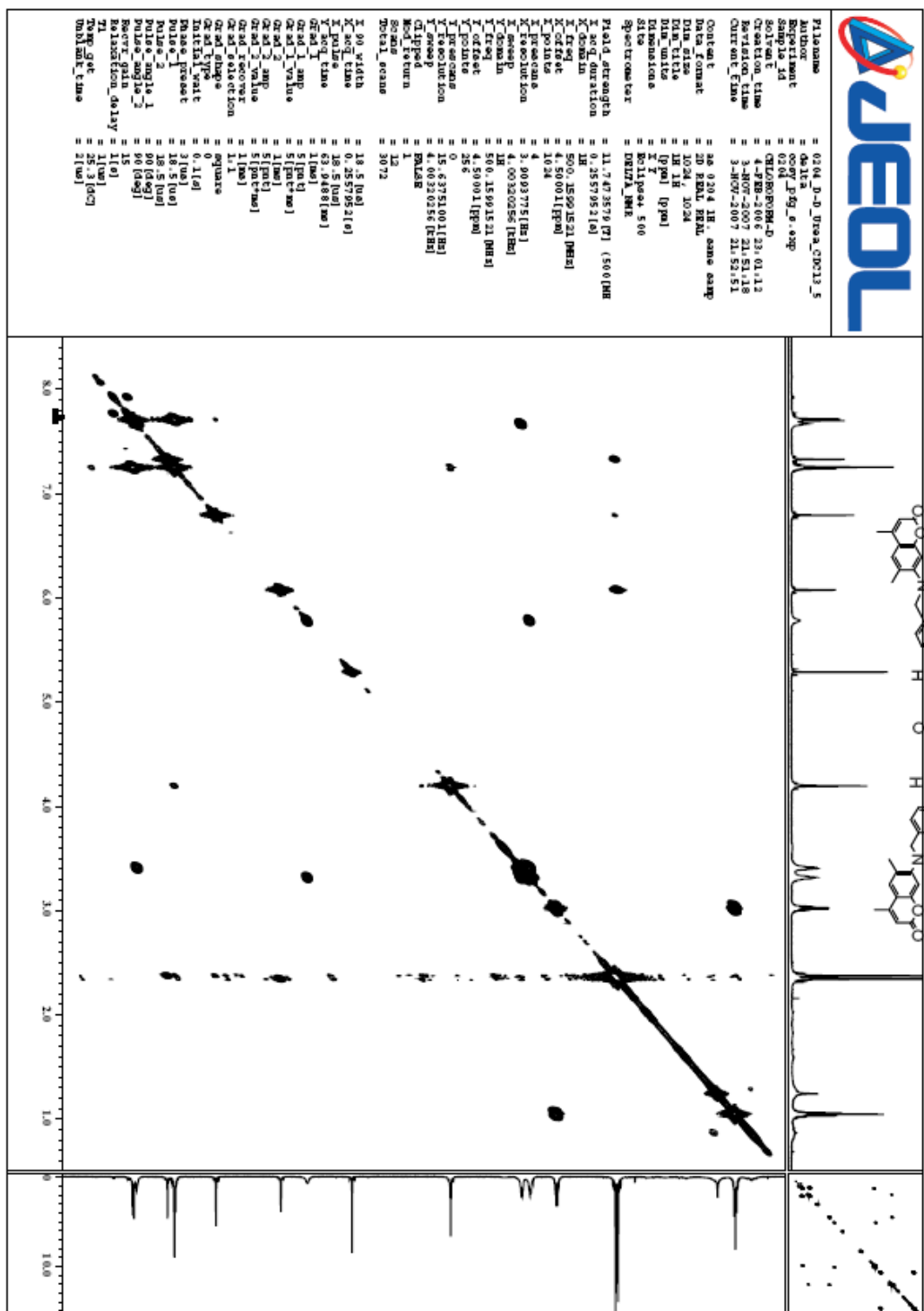
Filename = 0204_D-D_Urea_CDCl3_5
 Author = de la
 SampleName = 0204_D-D_Urea_CDCl3_5
 Solvent = CHLOROFORM-D
 AcquisitionTime = 4-PM-2006 21:52:03
 RelaxationTime = 11-MOV-2007 23:23:25
 CurrentTime = 11-MOV-2007 23:27:54
 Content = same sample as 0121,
 DataFormat = 1D CPMASK
 DataFile = 15384
 DataTitle = 1H
 DataUnit = [ppm]
 Dimensions = 1
 Sites = 1
 Spectrometer = spect-500
 P14.1_frequency = 11.747379 [MHz] (500 MHz)
 P14.1_solvent = 1H
 P14.1_solvent_freq = 500.15901521 [MHz]
 P14.1_freq = 51 [ppm]
 P14.1_offset = 16384
 P14.1_phase = 0
 P14.1_pulseprog = zgpg30
 P14.1_acqtime = 7.50750751 [sec]
 P14.1_f2 = 1
 P14.1_f1 = 24
 P14.1_f0 = 24
 P14.1_offset = 18.5 [ppm]
 P14.1_offset_freq = 2.18234881 [MHz]
 P14.1_offset_time = 45 [sec]
 P14.1_offset_phase = 9.25 [deg]
 P14.1_offset_delay = 31 [sec]
 P14.1_offset_gain = 20
 P14.1_offset_delay = 4 [sec]
 P14.1_offset_gain = 25.2 [dB]
 P14.1_offset_time = 21 [sec]

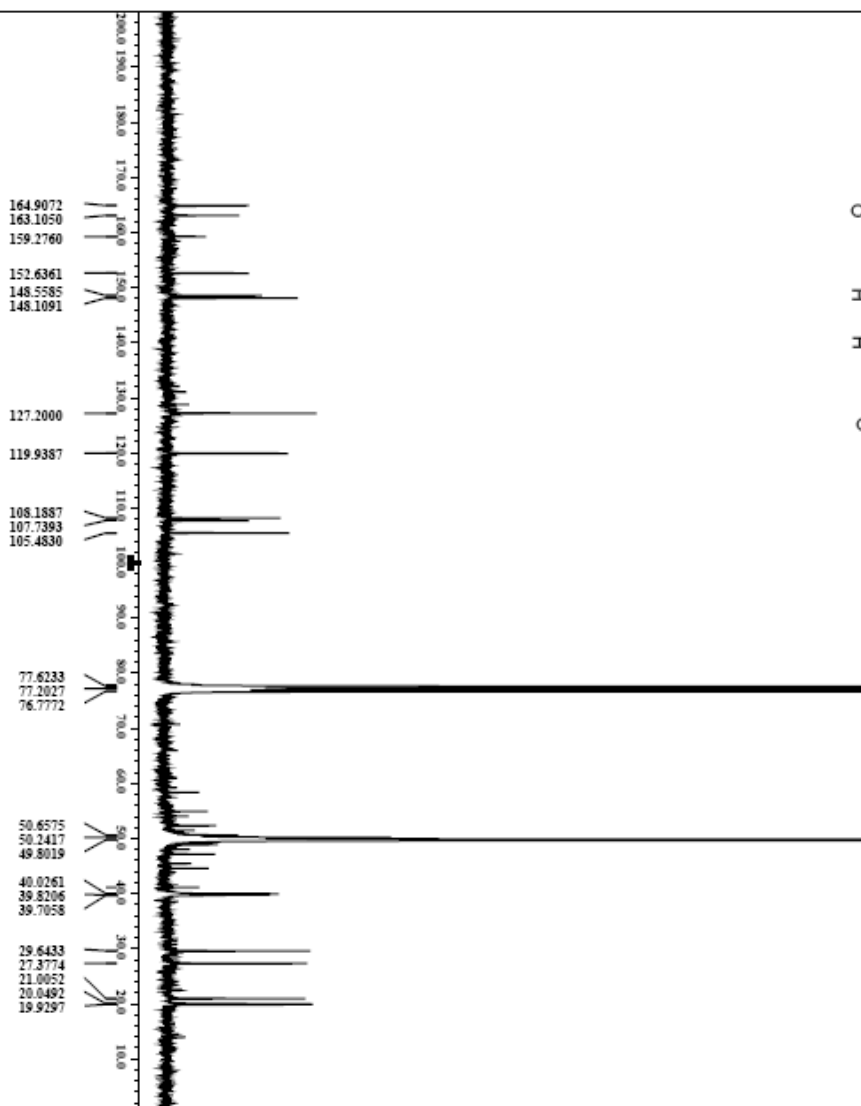
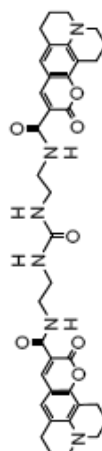


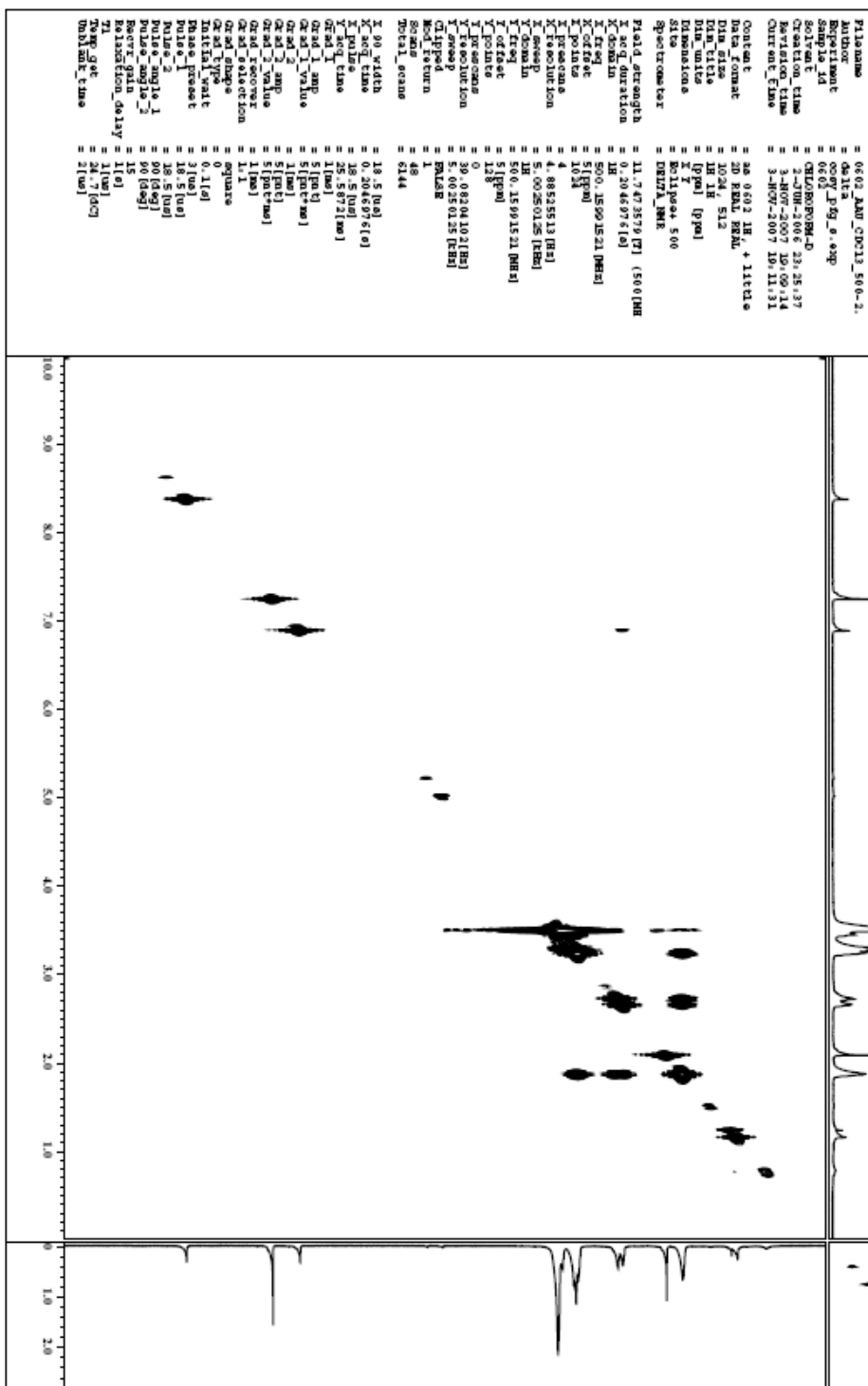
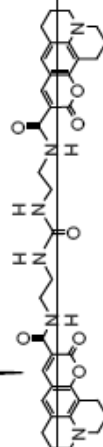
Filename = 0204_D-D_Urea_C0013_1
 Author = da12a
 Experiment = aluq1a_pulse_dec
 Sample_ID = 0204
 Sample_Name = 3-(4-(4-(dimethylamino)-2-methoxyphenyl)-2-methoxyphenyl)-N,N'-bis(4-(dimethylamino)-2-methoxyphenyl)-N,N'-bis(2-methoxyphenyl)urea
 Creation_time = 5-PBB-2006.14.17.4.0
 Revision_time = 3-MOV-2007.21.46.138
 Current_time = 3-MOV-2007.21.50.131
 Contact = NO 0204 HR, O08T, 13h
 Date_of_acq = 2006.14.17.4.0
 Date_time = 05:53:56
 Data_title = 13C
 Data_unit = [ppm]
 Dimensions = 2
 Size = 25211 bytes, 500
 Spectrometer = REBEL_NMR
 F1_acq_length = 11.7473579 [s] (500 MHz)
 F1_acq_duration = 2.0840448 [s]
 F2_acq_length = 13C 765.9748 [MHz]
 F2_acq_duration = 10.0 [ppm]
 F2_offset = 65536
 F2_resolution = 4
 F2_resolution = 0.47983613 [Hz]
 F2_resolution = 21.4465408 [Hz]
 F2_resolution = 500.15091521 [MHz]
 F2_resolution = 5 [ppm]
 F2_resolution = PULPROG
 Mod_resolution = 1
 Mod_resolution = 10790
 Mod_resolution = 10790
 X_90_width = 14.2 [us]
 X_90_time = 2.0840448 [s]
 X_angle = 30 [deg]
 X_offset = 4.7333333 [us]
 X_offset = 3 [us]
 Phase_offset = 30
 Relaxation_delay = 3 [s]
 Temperature = 28.7 [deg]
 Unit_name_time = 21[us]

¹³C NMR in CDCl₃ for compound 7



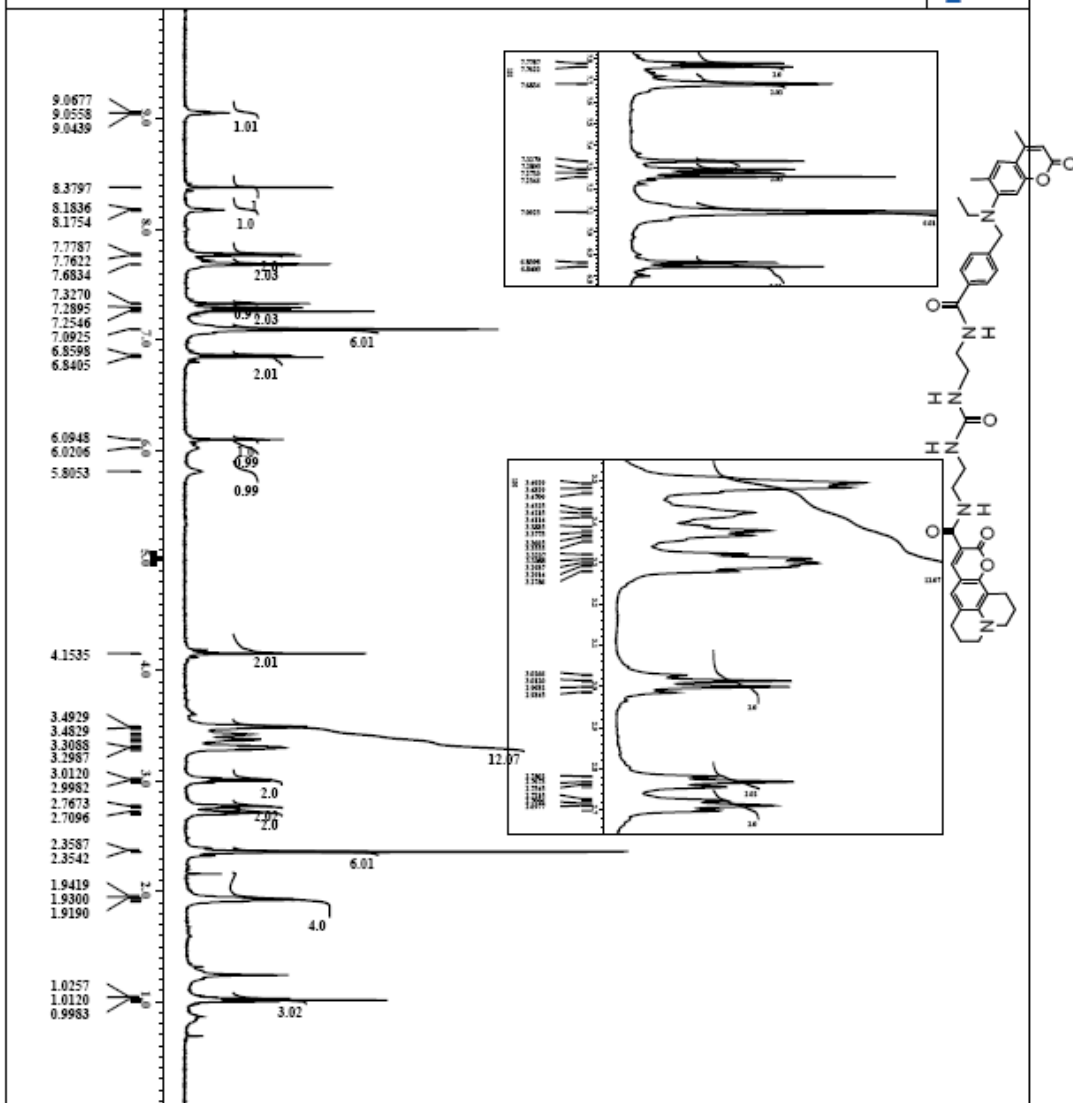




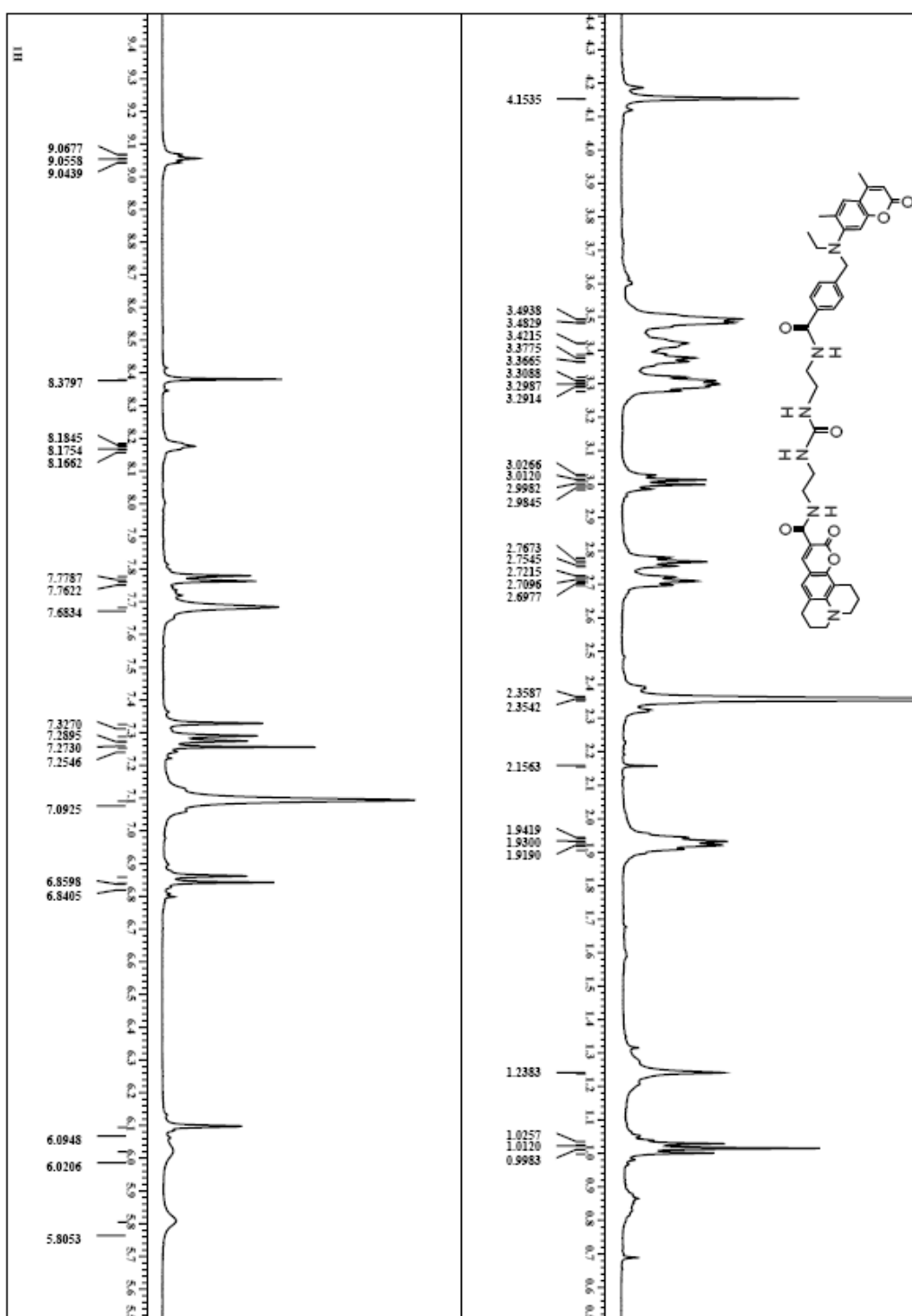




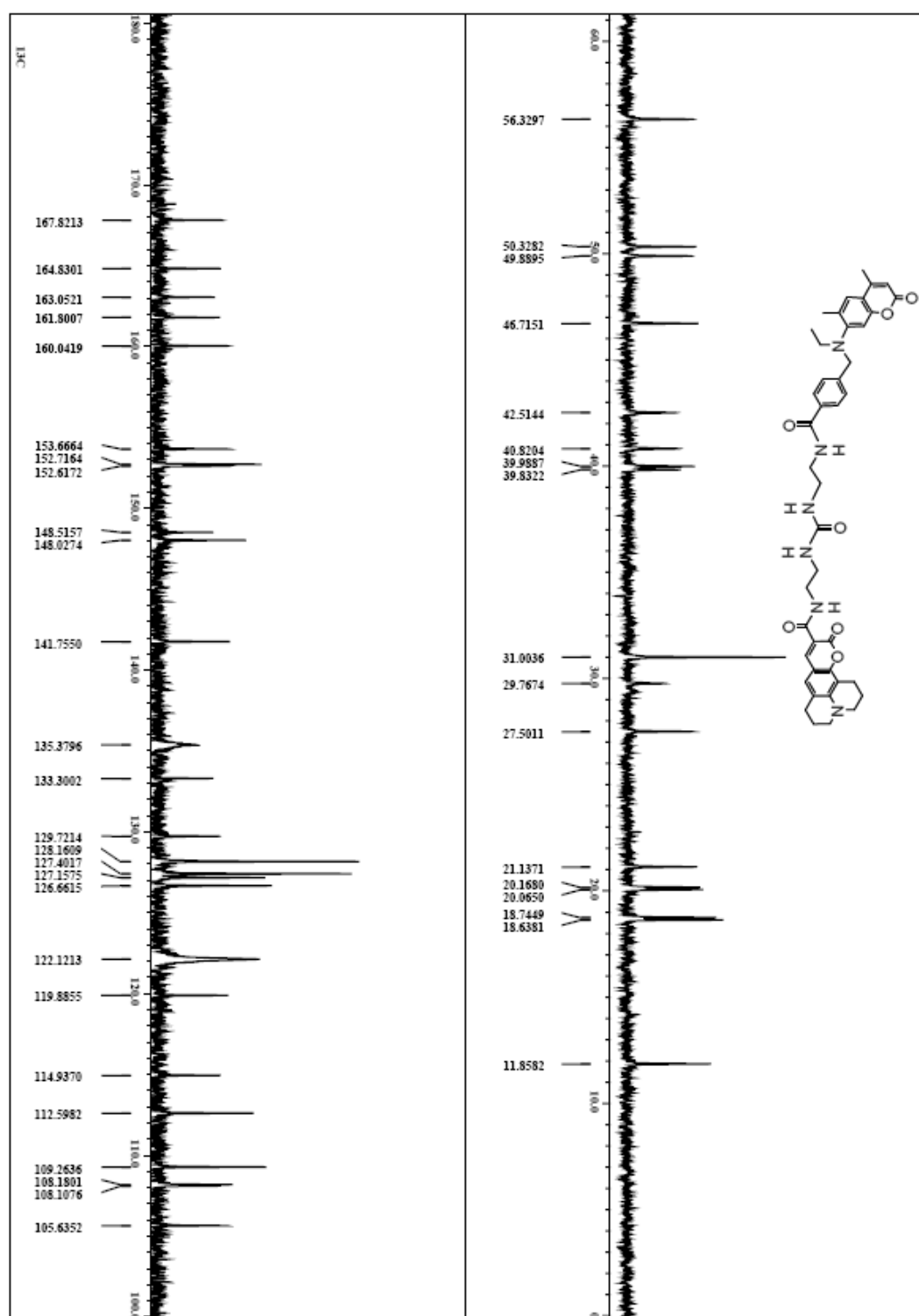
Filename = 0300_D-Altra-92_CDCl3_50
 Author = de1ta
 Experiment = 1D-1H-13C-CP-DEPT-135
 Date_Exp = 2007-03-04
 Date_Recd = 2007-03-04
 Creation_time = 10-MAR-2007 02:06:55
 Revision_time = 11-MAR-2007 23:41:39
 Output_time = 11-MAR-2007 23:44:46
 Content = Bruker 0304 - Column prod
 Data_Format = 1D-CP-DEPT-135
 Data_Size = 16384
 Data_Type = 1H
 Data_Unit = [ppm]
 Data_Units = 1011644.500
 Data_Units = 1011644.500
 Spectrometer = DEPT-135
 P1 (s) = 11.7473579 [s] (500 MHz)
 P2 (s) = 2.1823488 [s]
 P3 (s) = 500.1599151 [MHz]
 P4 (s) = 51 [ppm]
 P5 (s) = 16384
 P6 (s) = 0.4632189 [Hz]
 P7 (s) = 7.5075075 [MHz]
 P8 (s) = 1
 P9 (s) = 24
 P10 (s) = 24
 P11 (s) = 18.5 [Hz]
 P12 (s) = 2.1823488 [s]
 P13 (s) = 45 [Hz]
 P14 (s) = 9.25 [Hz]
 P15 (s) = 1 [Hz]
 P16 (s) = 1 [Hz]
 P17 (s) = 10 [Hz]
 P18 (s) = 4 [Hz]
 P19 (s) = 25 [Hz]
 P20 (s) = 21 [Hz]

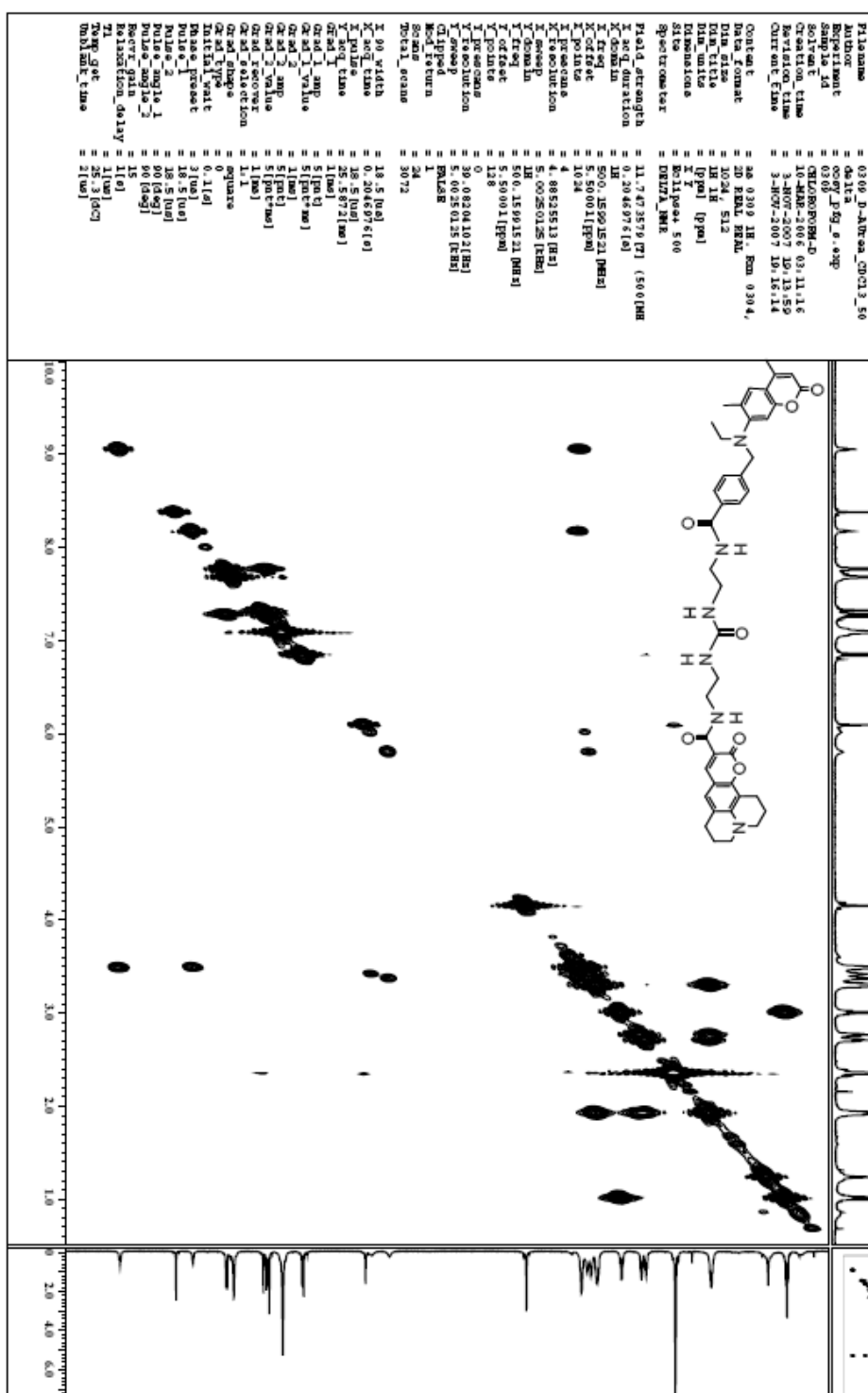


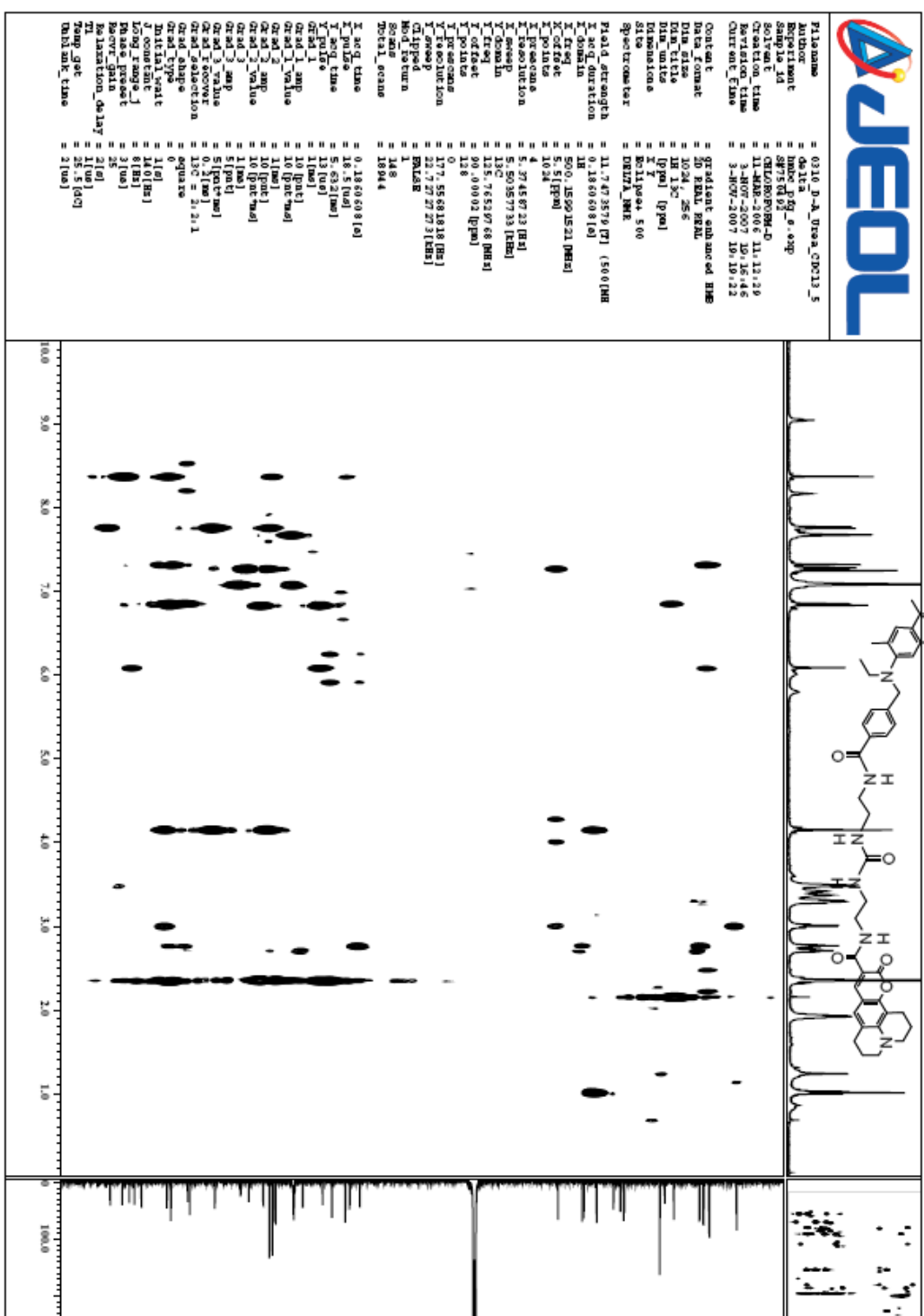
¹H NMR in CDCl₃ for compound 9



¹³C NMR in CDCl₃ for compound 9







¹³C NMR in CDCl₃ for compound 13

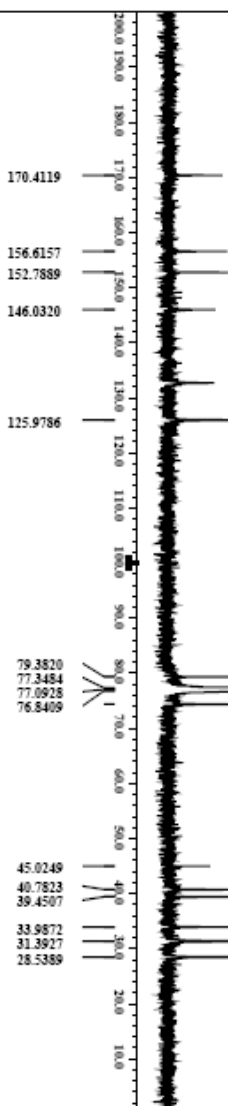
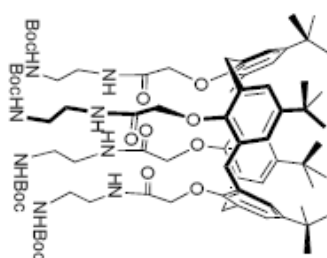


```

P1312300
Name      = 11-173_01_CDCl3_125-5
Date_Exp  = 04-11-2017
Sample    = 13
Solvent    = CHLOROFORM-D
AcqDate    = 8-11-2017 11:15:45
AcqTime    = 4-0007-2007 19:26:32
Current    = 4-0007-2007 19:26:35
Contant    = none 173.01 Hz, conv?
Data_Fomat = 1D CDEXTC
Data_Size  = 65536
Data_Type  = 13C
Data_Units = 1ppm
Dimensions = 2
S1 to      = B011pax 500
Spectrum    = FID13A_NMR

Plot 4: 13C NMR
X_Axis       = 11.732579 [T] (500 MHz)
X_Domain     = 130.464646 [ppm]
X_Trace      = 125.76529768 [MHz]
X_Offset     = 100 [ppm]
X_Points     = 65536
X_Frequency  = 0.47983613 [Hz]
X_SweepRate  = 31.445408 [Hz/s]
X_F1Domain   = 1H
X_F1Freq     = 500.1359521 [MHz]
X_F2Domain   = 13C
X_F2Freq     = 125.76529768 [MHz]
X_F2Domain   = 1
Mod_Freq     = 7843
Total_Points = 14.2 [us]
X_F0_Width   = 2.084048 [Hz]
X_AcqTime    = 30 [sec]
X_Pulse      = 4.7333333 [us]
Initial_Walt = 1 [Hz]
Msc_Cycle    = 1 [us]
Msc_Pulse    = 1 [us]
Msc_Pulse    = 1 [us]
Relaxation_Delay = 2 [sec]
Temp_get_delay = 25.8 [sec]
OnOff_mK_time = 2 [us]

```

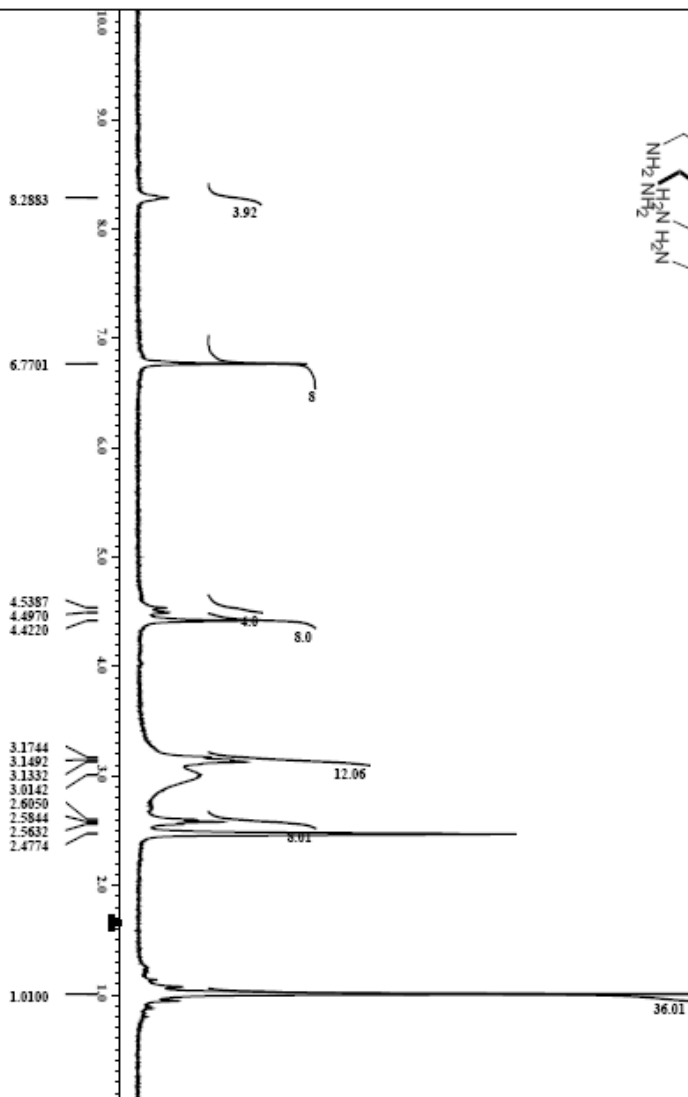
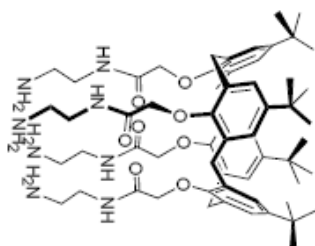


[illegible]

¹H NMR in DMSO-d₆ for compound 14



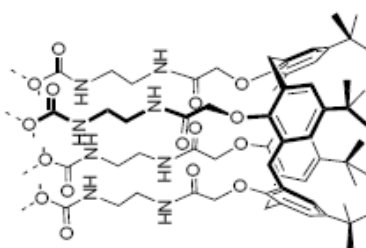
P10name = 11-184_DMSO-300-7.14f
 Author = da.ira_pul.es.ac2
 Experiment = 20mg1s_pulse.ac2
 Sample_id = 20mg1s_pulse.ac2
 Date_acq = 21-MAR-2007 18:23:16
 Acquisition_time = 4-MAR-2007 20:27:02
 Revision_time = 4-MAR-2007 20:27:27
 Overhaul_time = 4-MAR-2007 20:27:27
 Contamt = 40% free H₂O 10.2 mg
 Data format = 1D-CMDSK
 Data_size = 26214
 Data_title = 1H
 Data_units = [ppm]
 Dimensions = 1
 Spectrometer = DELTA_300
 Spectrometer = DELTA_300
 P1014_acq_enh = 7.058601317 (300 MHz
 P1014_acq_function = 5.81435592 [s]
 P1014_acq_gain = 30.5265592 [dB]
 P1014_acq_offset = 51 [ppm]
 P1014_acq_offset = 32.788
 P1014_acq_offset = 0.1716615 [Hz]
 P1014_acq_offset = 63.570786 [kHz]
 P1014_acq_offset = 300.5265592 [MHz]
 P1014_acq_offset = 51 [ppm]
 P1014_acq_offset = 1H
 P1014_acq_offset = 5.2965592 [MHz]
 P1014_acq_offset = 51 [ppm]
 P1014_acq_offset = FALSE
 P1014_acq_offset = 1
 P1014_acq_offset = 24
 P1014_acq_offset = 24
 P1014_acq_offset = 13.01 [Hz]
 P1014_acq_offset = 5.81435592 [s]
 P1014_acq_offset = 45 [deg]
 P1014_acq_offset = 4 [deg]
 P1014_acq_offset = 5.2965592 [MHz]
 P1014_acq_offset = 51 [ppm]
 P1014_acq_offset = FALSE
 P1014_acq_offset = 11 [s]
 P1014_acq_offset = 50 [Hz]
 P1014_acq_offset = 20.91435392 [s]
 P1014_acq_offset = 22.5 [deg]
 P1014_acq_offset = 22.5 [deg]



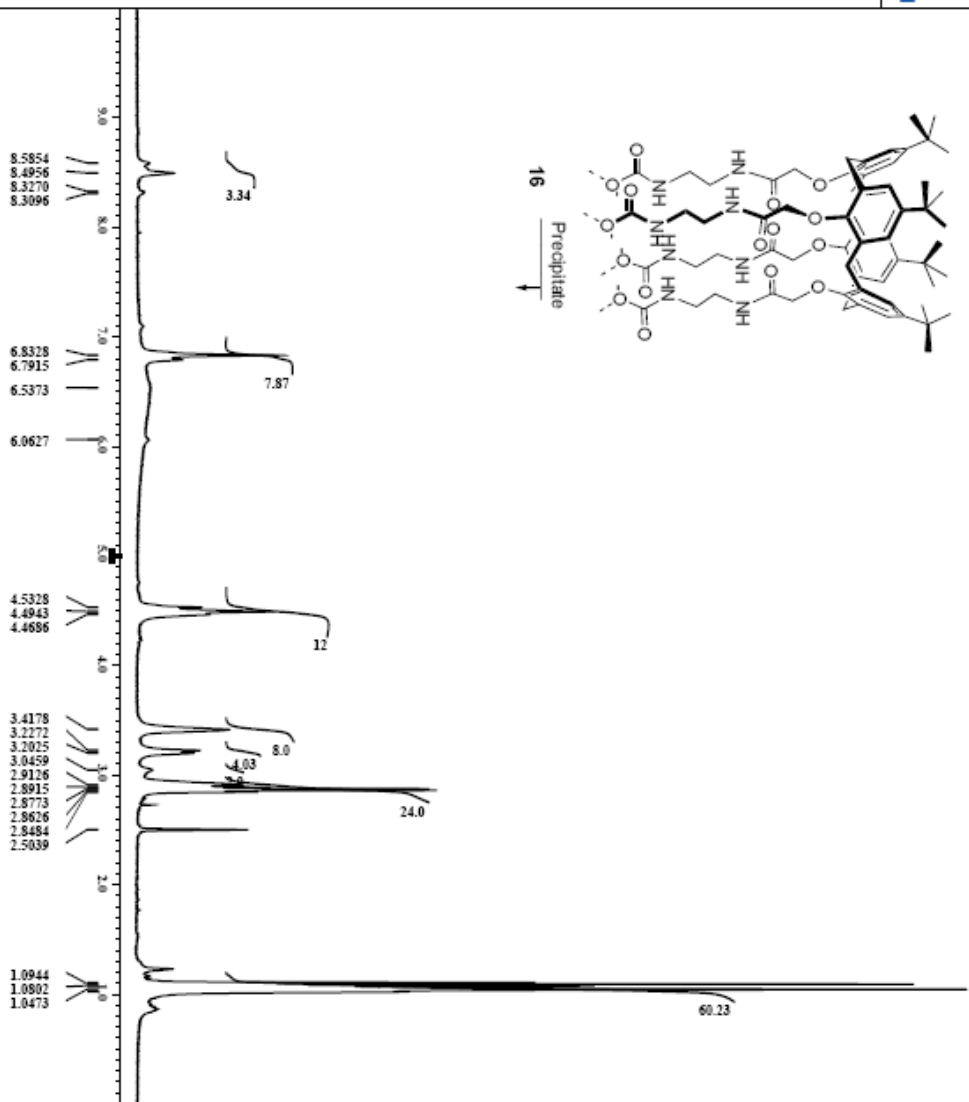
¹H NMR in DMSO-d₆ for compound **16** in the presence of TEA



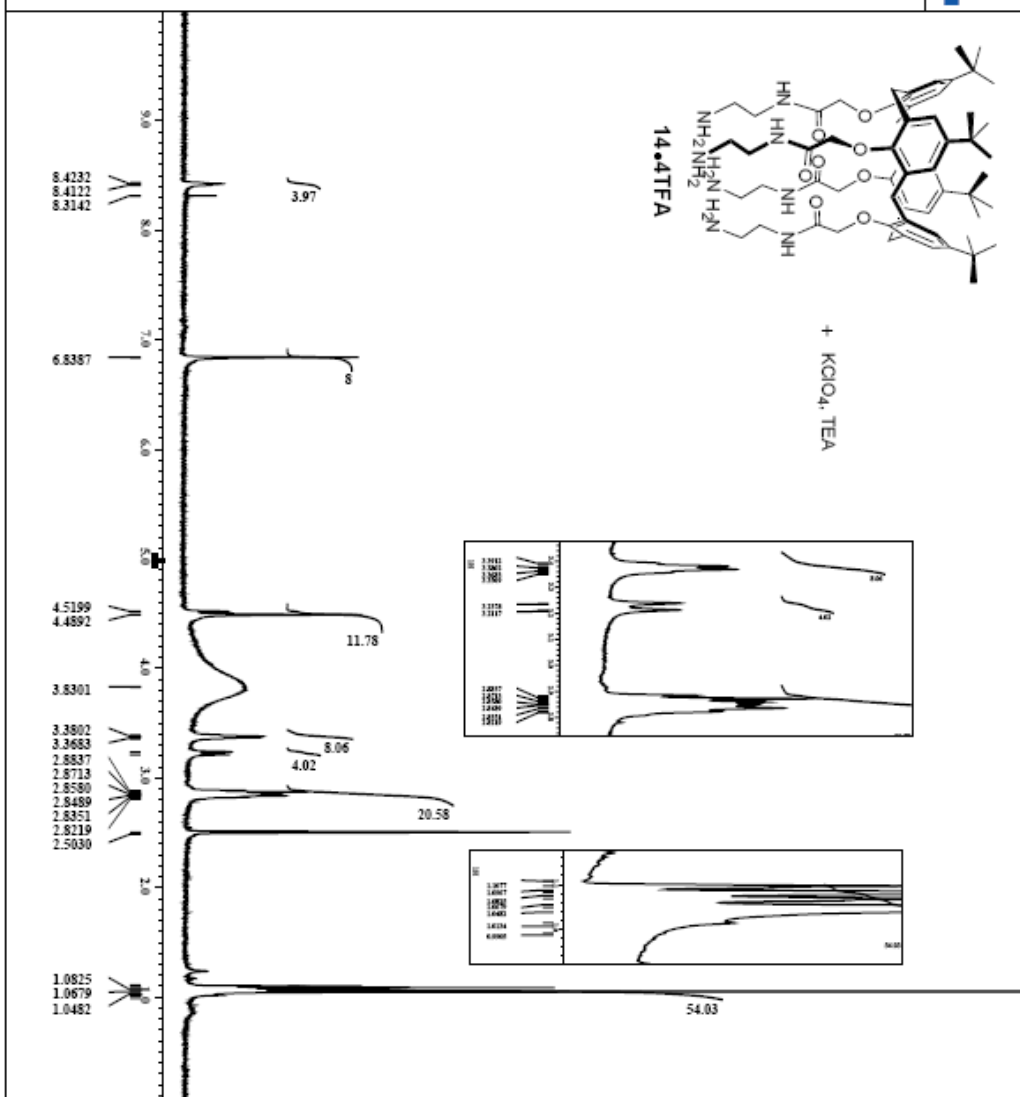
PlateName = 11-158_DMSO_500-5_141
 Author = Orita
 Experiment = 1D 1H NMR
 SampleID = 16
 Solvent = DMSO-d6
 Creation_time = 17-MAY-2007 20:52:07
 Acquisition_time = 5-MAY-2007 18:04:06
 Output_time = 5-MAY-2007 18:04:06
 Content = Free amino carbonate.
 Data format = 1D COMPLEX
 Data file = 11-158.D
 Processing file = 11-158.P
 Dimensions = 512pt x 655pt
 Site = EPR1_NMR
 Spectrometer = Bruker 500
 Proc4_date = 11-24-2007 (P)
 Proc4_time = 11:24:29 (P)
 X_coordination = 50.1591521 (MHz)
 X_freq = 500.1360761 (MHz)
 X_offset = 51 (ppm)
 X_pos = 32768
 X_resolution = 0.2201095 (Hz)
 X_sweep = 7.50750751 (Hz)
 C1ipped = FALSE
 Mod_return = 1
 Name = 16
 Name_prefix = 16
 X_pos_width = 18.5 (Hz)
 X_pos_time = 4.3646761 (s)
 X_angle = 45 (deg)
 X_offset = 1 (Hz)
 Initial wait = 3 (sec)
 Relaxation_delay = 14 (s)
 Delay_time = 25 (sec)
 Delay_time = 25 (sec)



16
Precipitate

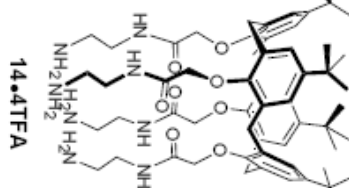










+ Cs⁺Pic⁻, TEA

Chemical structure of **14•4TFA** is shown, which is a complex molecule featuring a central core with multiple amine and amide groups. The structure is labeled **14•4TFA**.

The reaction conditions are specified as Cs^+Pic^- , TEA.

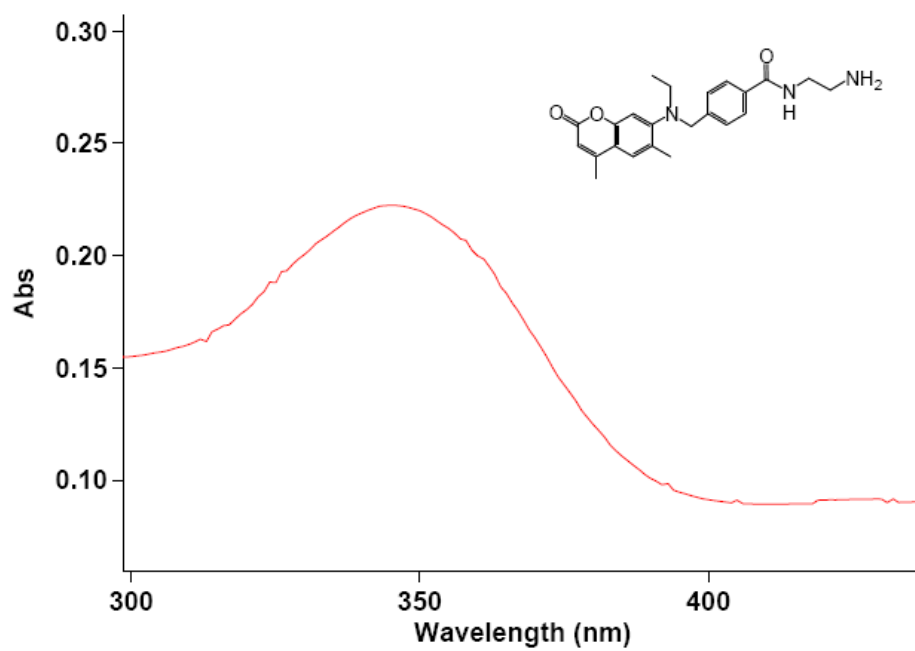
The chemical structure of **14•4TFA** is shown below the reaction conditions. It is a complex molecule with a central core and multiple amine and amide groups. The structure is labeled **14•4TFA**.

APPENDIX B

UV-VIS AND FLUORESCENCE SPECTRA

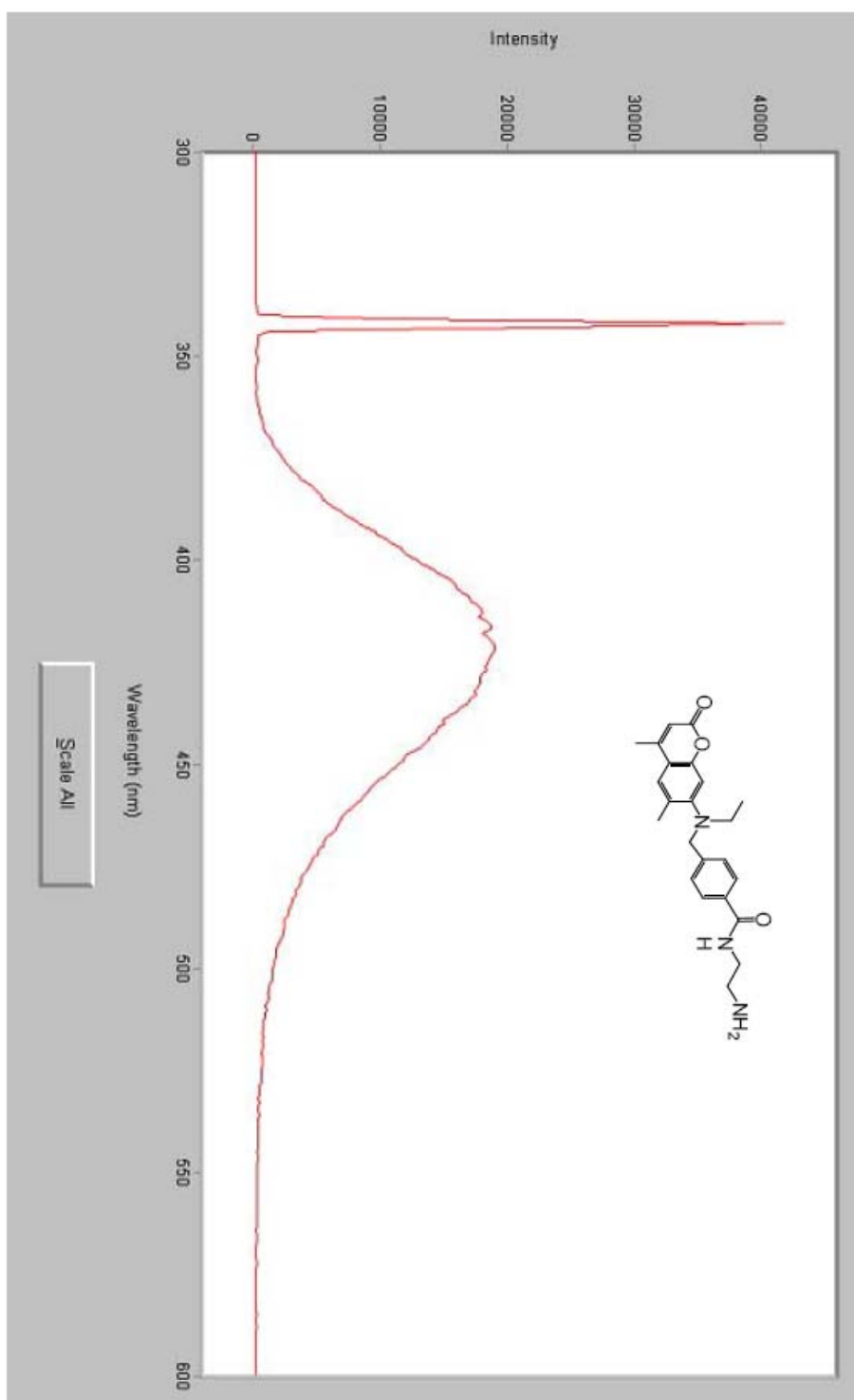
UV-vis Spectrum

Compound **4**: $[c] = 1 \times 10^{-6}$ M, $\lambda_{\text{max}} = 343$ nm



Fluorescence Spectrum:

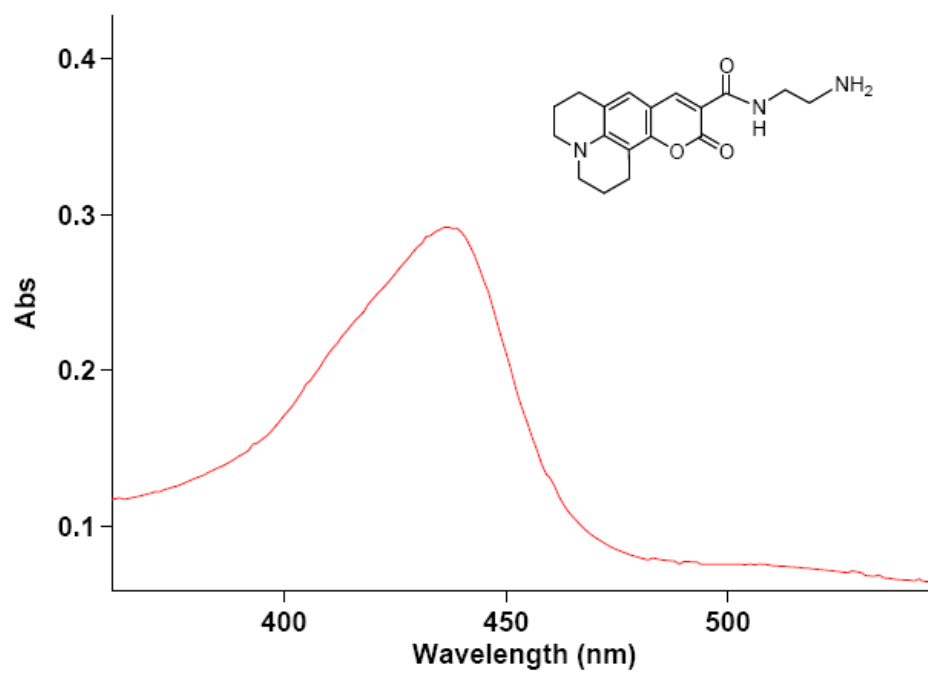
Compound **4**: [c] = 1×10^{-5} M, λ_{ex} = 343 nm, λ_{em} = 425 nm



Scale All

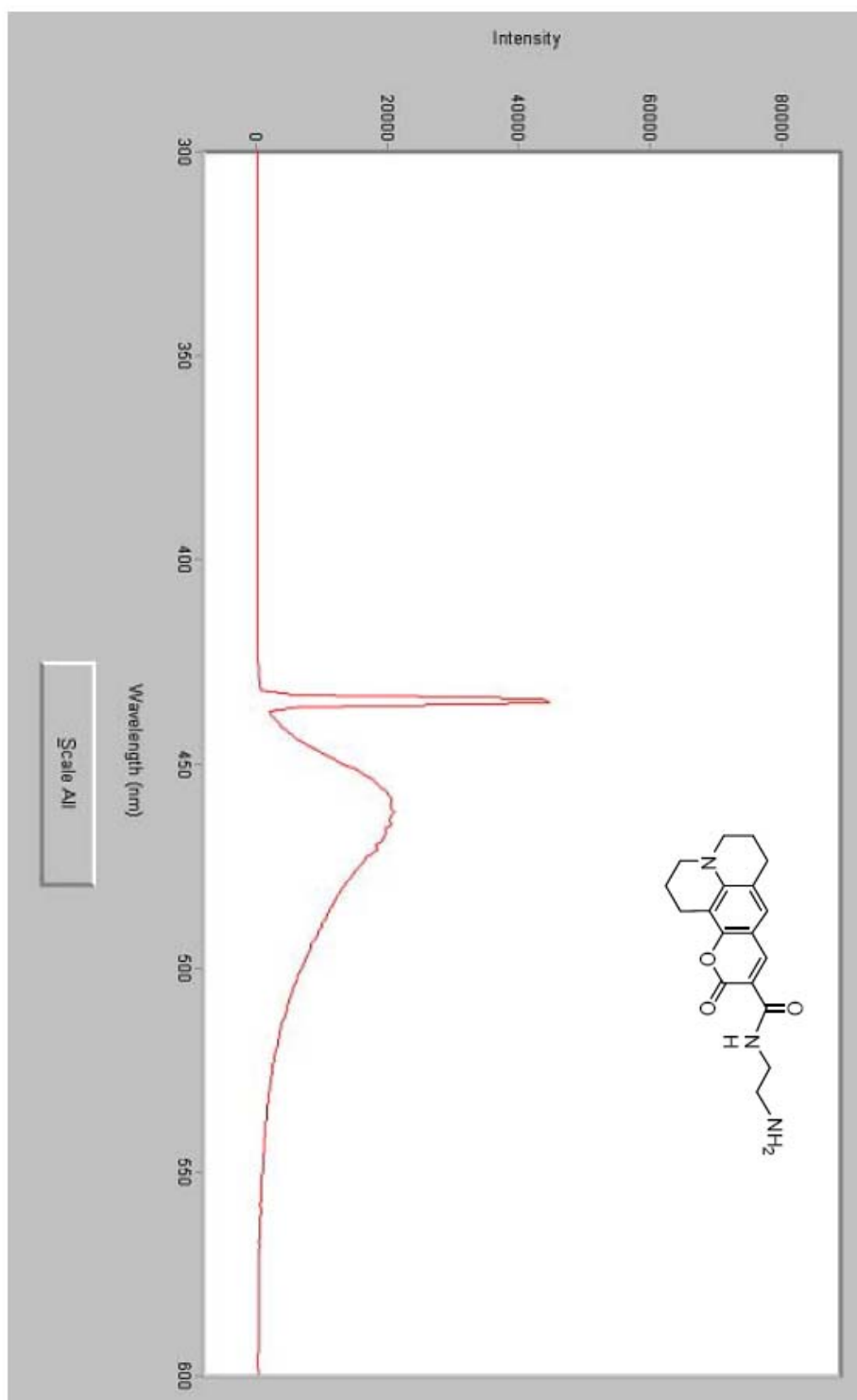
UV-vis Spectrum

Compound 6: $[c] = 1 \times 10^{-6}$ M, $\lambda_{\text{max}} = 435$ nm



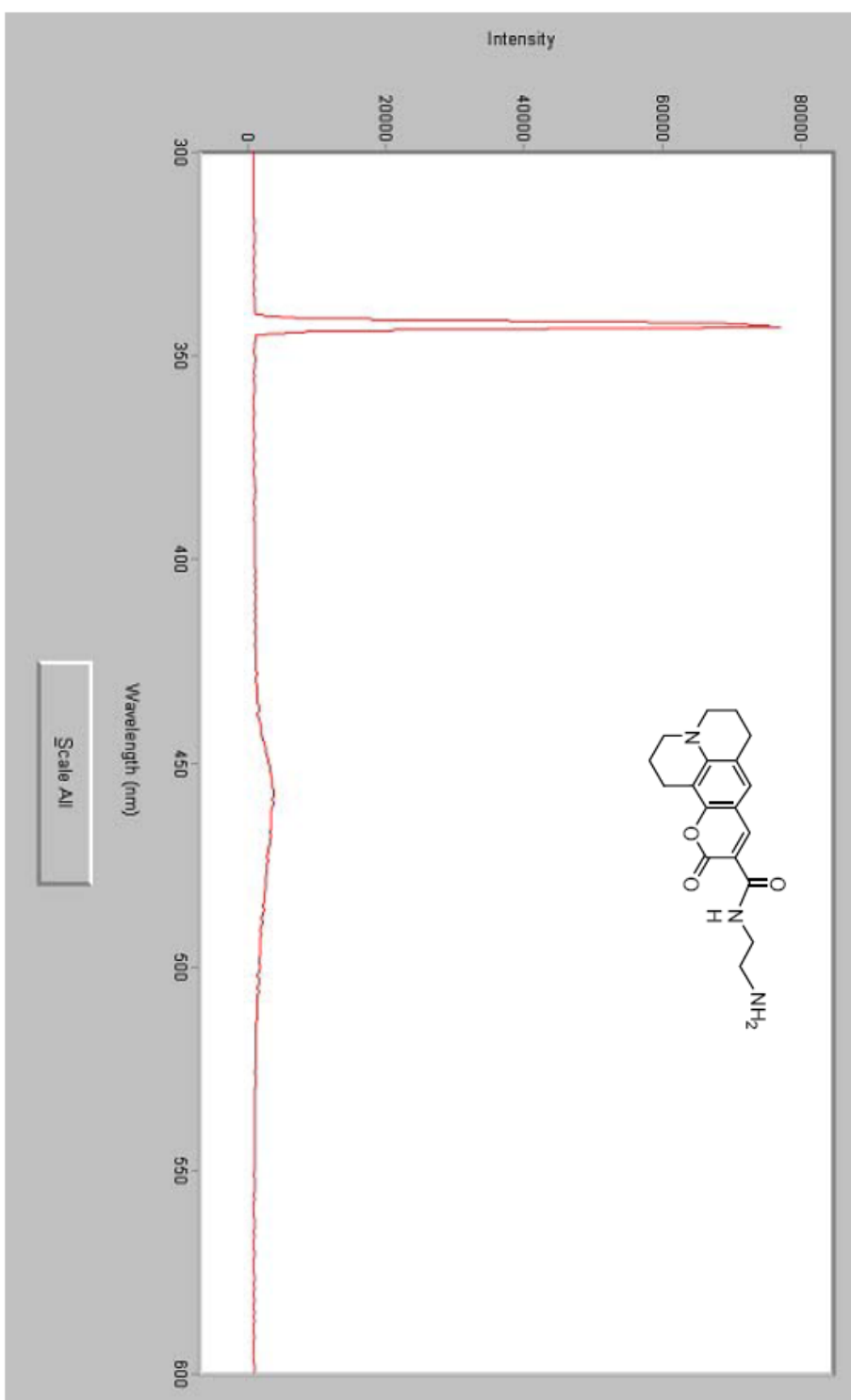
Fluorescence Spectrum:

Compound 6: $[c] = 1 \times 10^{-6}$ M. $\lambda_{ex} = 435$ nm, $\lambda_{em} = 468$ nm



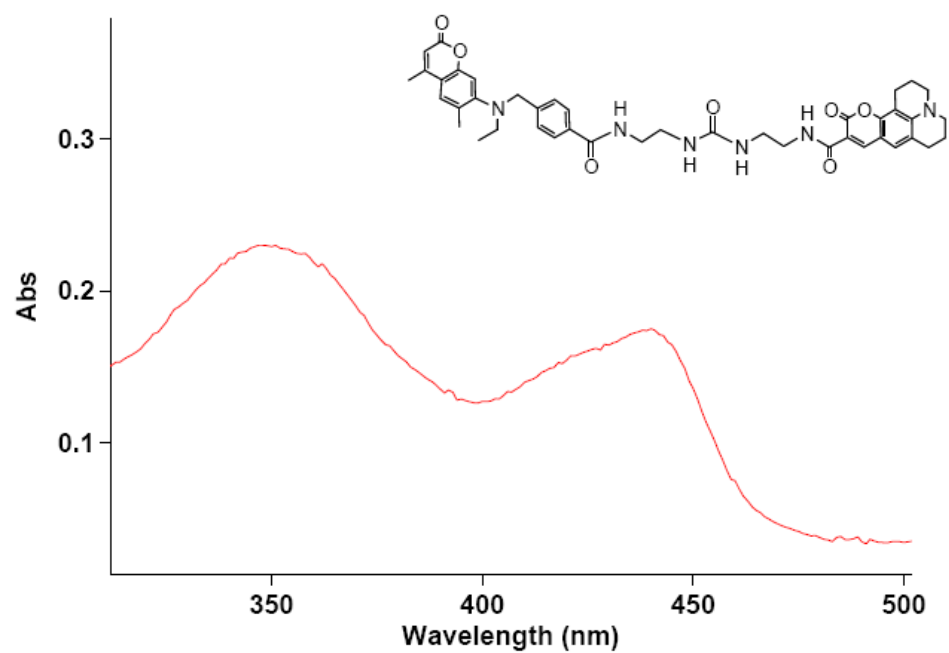
Fluorescence Spectrum:

Compound 6: $[c] = 1 \times 10^{-6}$ M, $\lambda_{ex} = 343$ nm, Emission is weak.



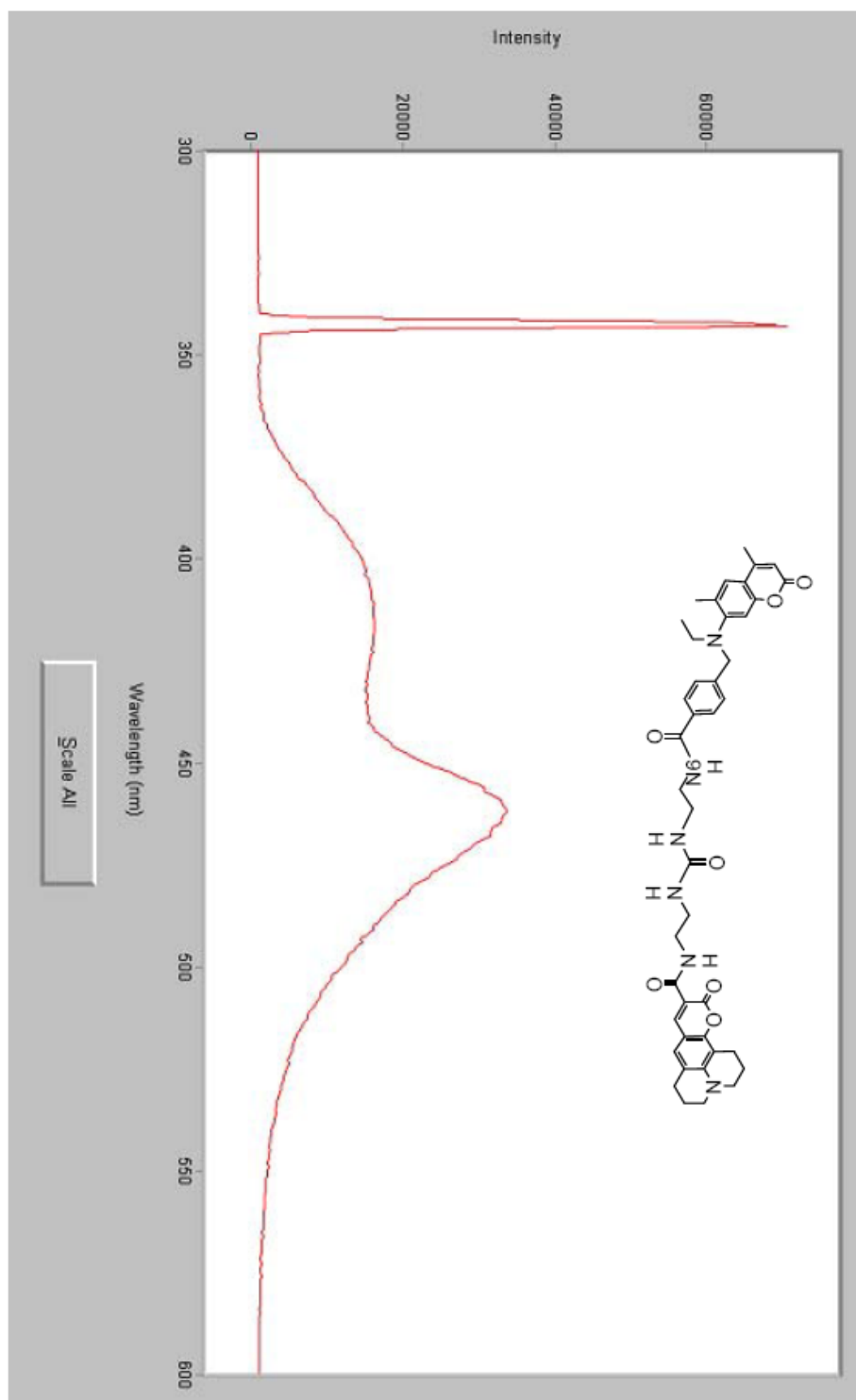
UV-vis Spectrum

Compound **9**: [c] = 1×10^{-5} M, $\lambda_{\text{max}1}$ = 343 nm, $\lambda_{\text{max}2}$ = 438 nm



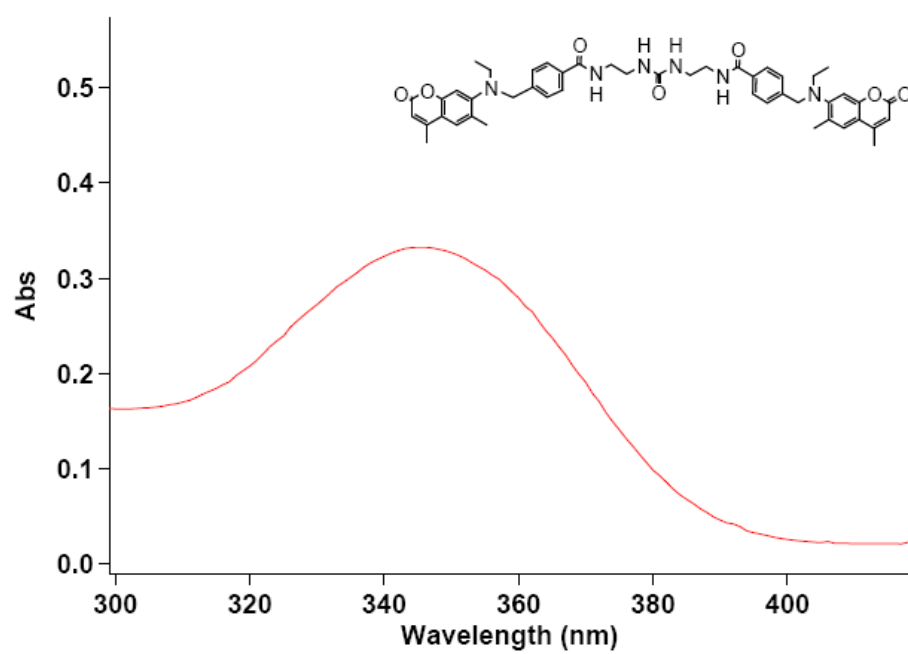
Fluorescence Spectrum:

Compound 9: $[c] = 1 \times 10^{-6}$ M, $\lambda_{ex} = 343$ nm, $\lambda_{em1} = 422$ nm, $\lambda_{em2} = 464$ nm.



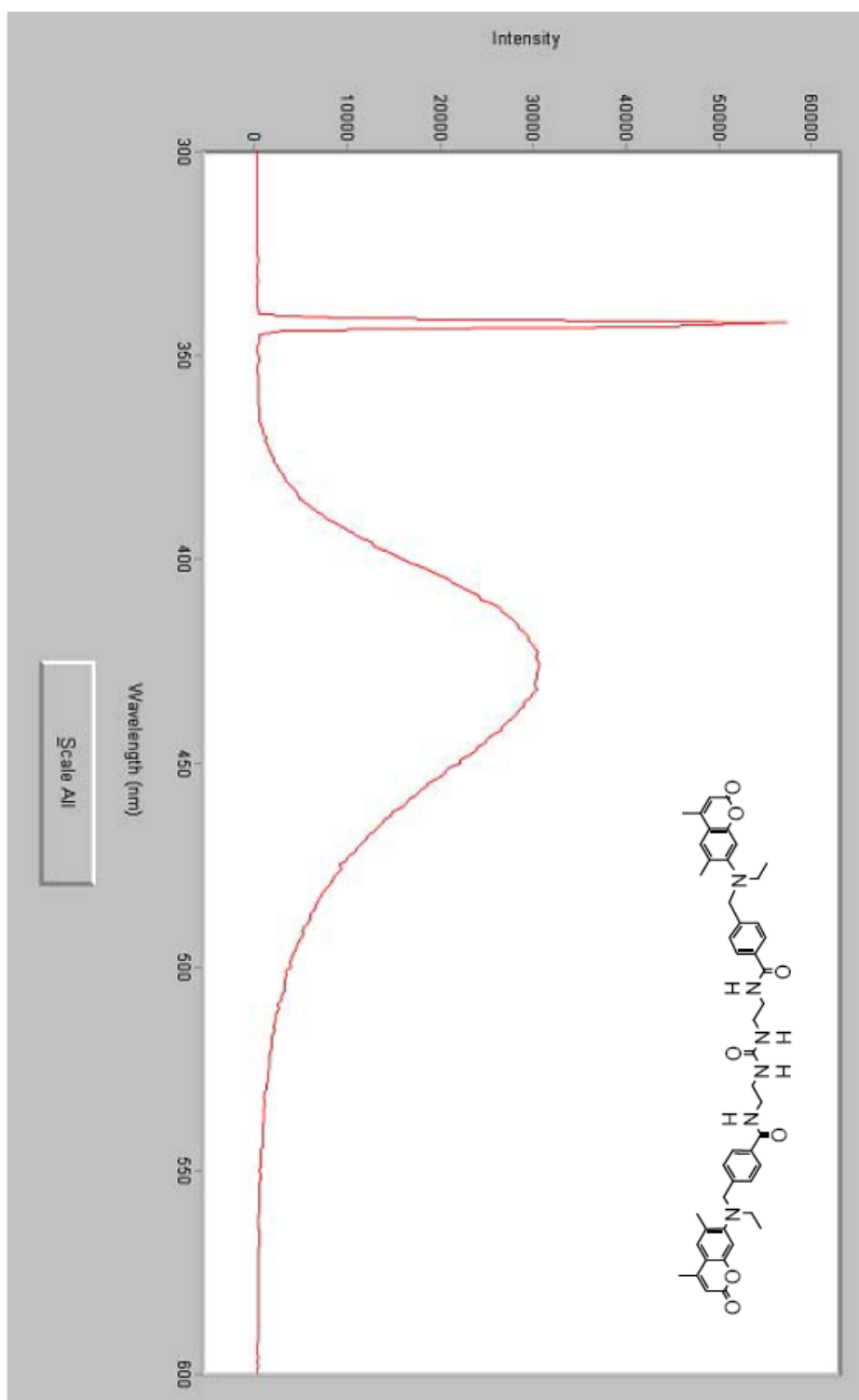
UV-vis Spectrum

Compound 7: $[c] = 1 \times 10^{-6} \text{ M}$, $\lambda_{\text{max}} = 344 \text{ nm}$



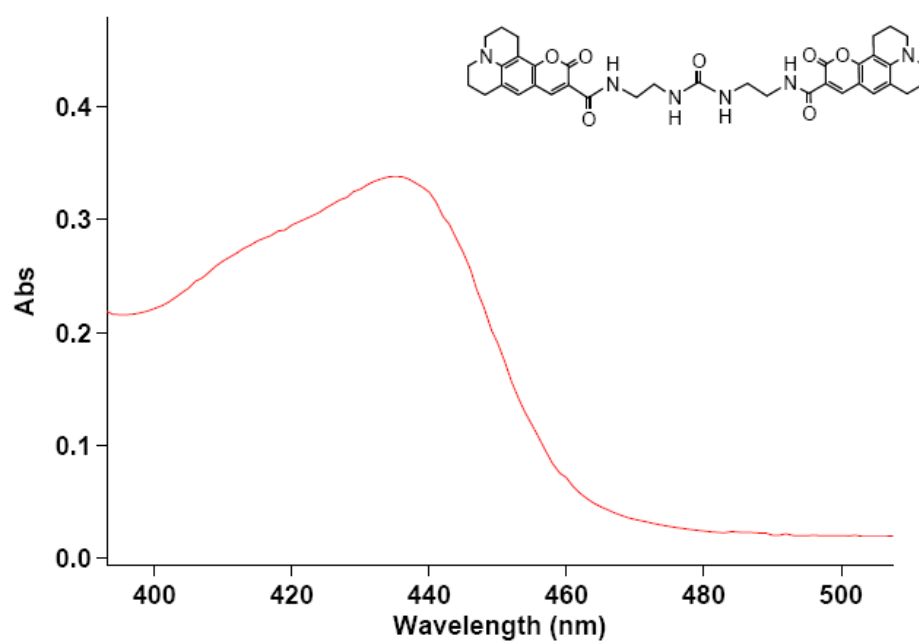
Fluorescence Spectrum:

Compound 7: $[c] = 1 \times 10^{-6}$ M. $\lambda_{ex} = 344$ nm, $\lambda_{em} = 424$ nm



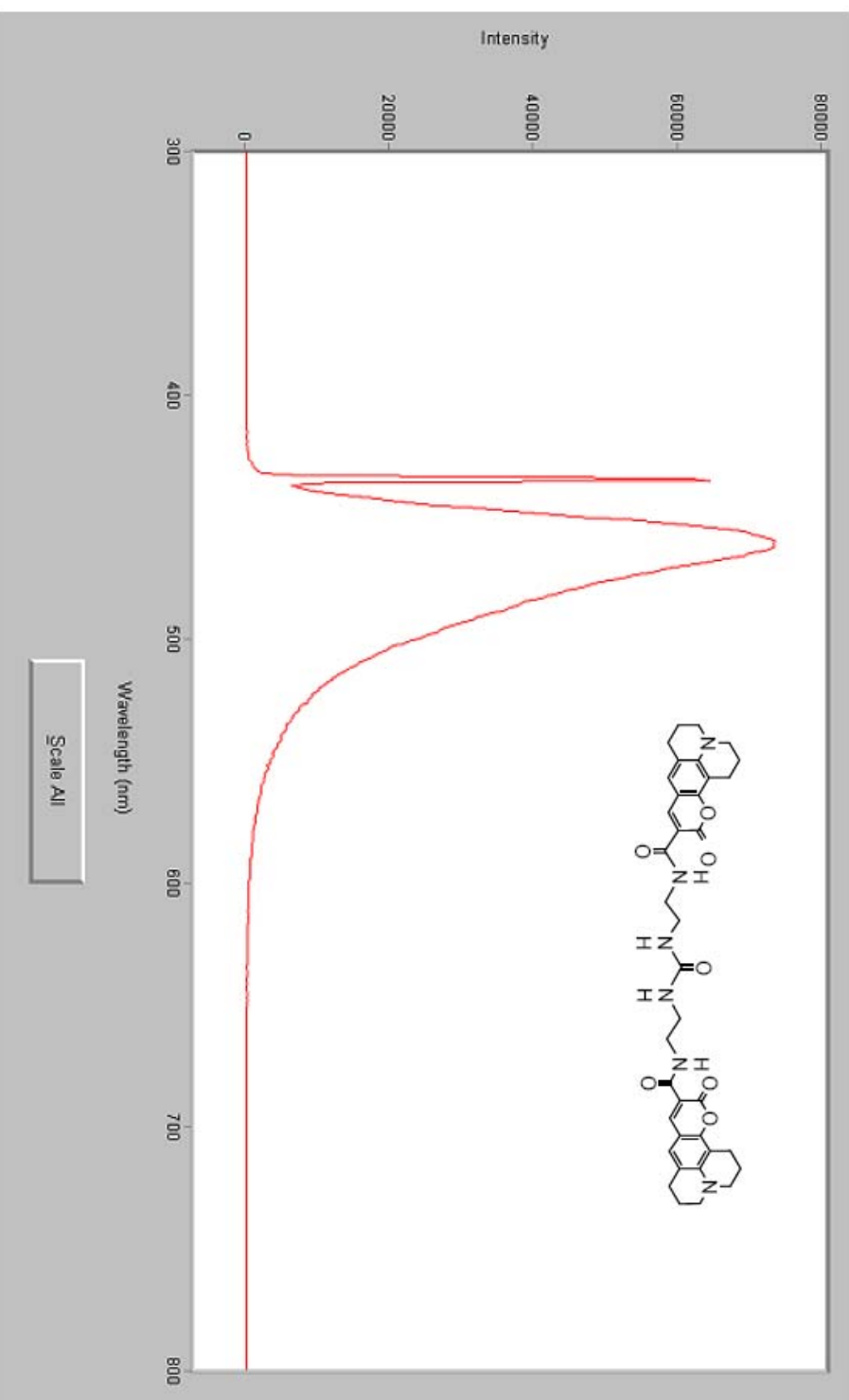
UV-vis Spectrum

Compound **8**: [c] = 1×10^{-6} M, λ_{max} = 435 nm



Fluorescence Spectrum:

Compound 8: $[c] = 1 \times 10^{-5}$ M. $\lambda_{\text{ex}} = 435$ nm, $\lambda_{\text{em}} = 462$ nm



APPENDIX C

TITRATION RESULTS

Titration Results:

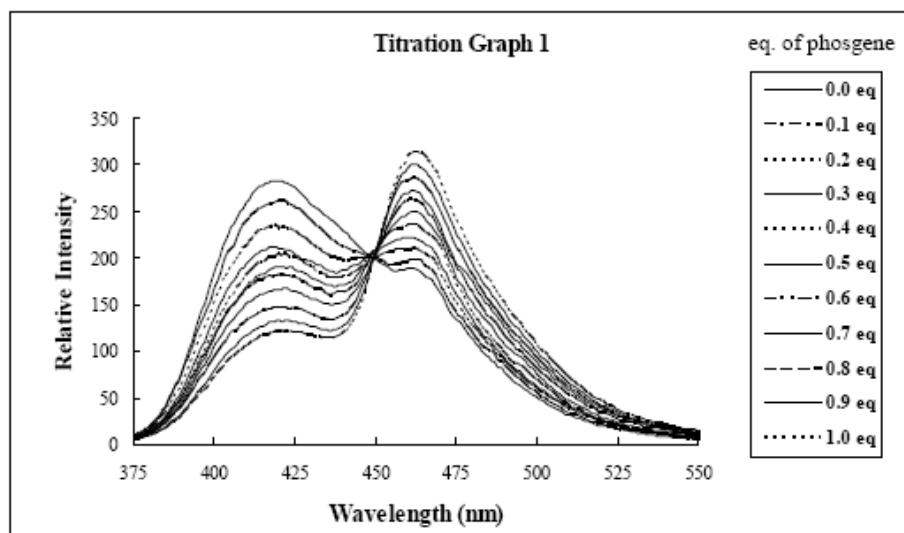


Fig. 1. Fluorescence emission spectra on titration with triphosgene. Coumarins 4 and 6 were mixed in 1:1 ratio at 1×10^{-5} M in CHCl_3 , TEA (10 eq) was added. 1/3 equivalent triphosgene (equal to 1 equivalent phosgene) was added step by step. Aliquots were taken and diluted to 10^{-5} M then emission spectra were recorded. The similar result was shown in 10^{-6} M dilutions.

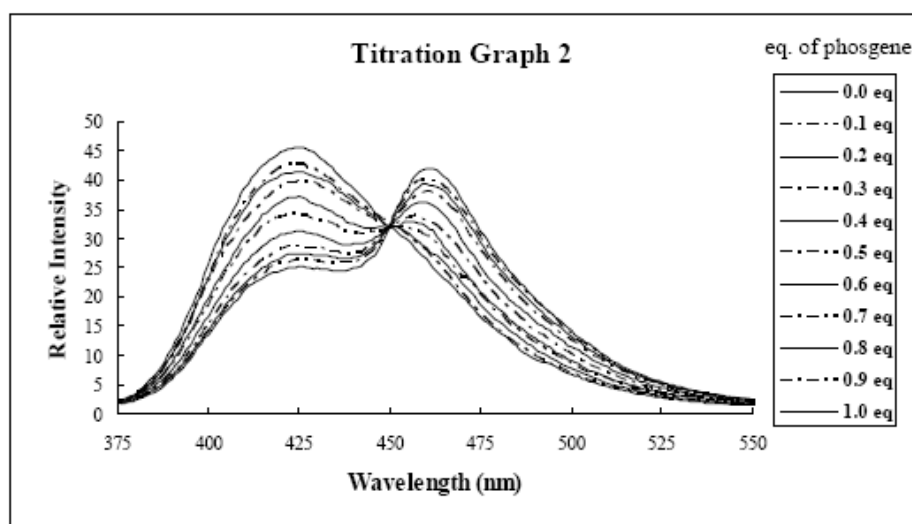


Fig. 2. Fluorescence emission spectra on titration with triphosgene. Coumarins 4 and 6 were mixed in 1:1 ratio at 1×10^{-3} M in CHCl_3 , TEA (10 eq) was added. 1/3 equivalent triphosgene (equal to 1 equivalent phosgene) was added step by step. Aliquots were taken and diluted 10^{-5} M then emission spectra were recorded

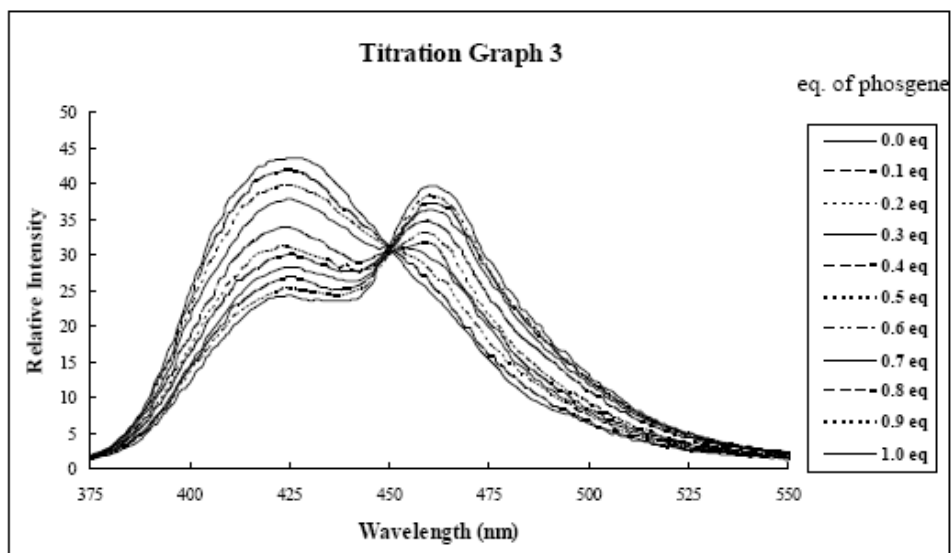


Fig. 3. Fluorescence emission spectra on titration with triphosgene. Coumarins 4 and 6 were mixed in 1:1 ratio at 5×10^{-4} M in CHCl_3 , TEA (10 eq) was added. 1/3 equivalent triphosgene (equal to 1 equivalent phosgene) was added step by step. Aliquots were taken and diluted to 10^{-6} M then emission spectra were recorded

REFERENCES

- (1) Lehn, J.-M. *Pure Appl. Chem.* **1978**, *50*, 871-892.
- (2) Lehn, J.-M. *Angew. Chem., Int. Ed. Engl.* **1988**, *27*, 89-112.
- (3) Lehn, J.-M. *Supramolecular Chemistry. Concepts and Perspectives*; VCH: Weinheim, Germany, 1995.
- (4) Pedersen, C. J. *J. Am. Chem. Soc.* **1967**, *89*, 7017-7036.
- (5) Pedersen, C. J. *Angew. Chem., Int. Ed. Engl.* **1988**, *27*, 1021-1027.
- (6) Dietrich, B.; Lehn, J.-M.; Sauvage, J.-P. *Tetrahedron Lett.* **1969**, *34*, 2885-2888.
- (7) Lehn, J.-M. *Acc. Chem. Res.* **1978**, *11*, 49-57.
- (8) Uekama, K.; Hirayama, F.; Irie, T. *Chem. Rev.* **1998**, *98*, 2045-2076.
- (9) Gutsche, C. D.; Muthukrishnan, R. *J. Org. Chem.* **1978**, *43*, 4905-4906.
- (10) (a) Gutsche, C. D. *Calixarenes Revisited*; The Royal Society of Chemistry: Cambridge, UK, 1998. (b) Asfari, Z.; Böhmer, V.; Harrowfield, J.; Vicens, J. *Calixarene 2001*; Kluwer Academic Publishers: Dordrecht, Netherlands, **2001**.
- (11) Whitesides, G. M.; Grzybowski, B. *Science* **2002**, *295*, 2418-2421.
- (12) Lehninger, A. L. *Biochemistry*, 2nd ed., Worth Publishers Inc.: New York, 1975.
- (13) Cramer, F. *Chaos and Order. The Complex Structure of Living Systems*; VCH: Weinheim, Germany, 1993.

- (14) Prins, L. J.; Reinhoudt, D. N.; Timmerman, P. *Angew. Chem., Int. Ed.* **2001**, *40*, 2382-2426.
- (15) (a) Jorgenson, W. L.; Pranata, J. *J. Am. Chem. Soc.* **1990**, *112*, 2008-2010. (b) Pranata, J.; Wierschke, S. G.; Jorgenson, W. L. *J. Am. Chem. Soc.* **1991**, *113*, 2810-2819.
- (16) (a) Murray, T. J.; Zimmerman, S. C. *J. Am. Chem. Soc.* **1992**, *114*, 4010-4011. (b) Fenlon, E. E.; Murray, T. J.; Baloga, M. H.; Zimmerman, S. C. *J. Org. Chem.* **1993**, *58*, 6625-6628.
- (17) (a) Beijer, F. H.; Kooijman, H.; Spek, A. L.; Sijbesma, R. P.; Meijer, E. W. *Angew. Chem., Int. Ed.* **1998**, *37*, 75-78. (b) Beijer, F. H.; Sijbesma, R. P.; Kooijman, H.; Spek, A. L.; Meijer, E. W. *J. Am. Chem. Soc.* **1998**, *120*, 6761-6769.
- (18) Heinz, T.; Rudkevich, D. M.; Rebek, Jr., J. *Nature* **1998**, *394*, 764-766.
- (19) Wagner, R. W.; Lindsey, J. S. *J. Am. Chem. Soc.* **1994**, *116*, 9759-9760.
- (20) Lehn, J.-M.; Mascal, M.; DeCian, A.; Fischer, J. *J. Chem. Soc., Perkin Trans. 2*, **1992**, 461-467.
- (21) Atwood, J. L.; Davies, J. E. D.; MacNicol, D. D.; Vögtle, F.; Lehn, J.-M. *Comprehensive Supramolecular Chemistry*; Elsevier Science: Oxford, UK, 1996.
- (22) Lehn, J.-M. *Proc. Natl. Acad. Sci. U.S.A.* **2002**, *99*, 4763-4768.
- (23) (a) Silver, A. *The Biology of Cholinesterases*; American Elsevier: New York, 1974, pp. 449-488. (b) Hardman, J. G.; Limbird, L. E.; Gilman, A. G. *The*

- Pharmacological Basis of Therapeutics*; 10th. ed., McGraw-Hill: New York, 2001, pp. 175-191.
- (24) Matsumura, F. *Toxicology of Insecticides*, Plenum: New York, 1975, pp. 67-78.
 - (25) (a) Ashley, J. A.; Lin, C. -H.; Wirsching, P.; Janda, K. D. *Angew. Chem., Int. Ed.* **1999**, 38, 1793-1795. (b) Richardson, S. D. *Chem. Rev.* **2001**, 101, 211-254. (c) Prosnitz, D. *Science* **2005**, 310, 978.
 - (26) (a) Stein, K.; Schwedt, G. *Anal. Chim. Acta* **1993**, 272, 73-81; (b) Ristori, C.; Del Carlo, C.; Martini, M.; Barbaro, A.; Ancarni, A. *Anal. Chim. Acta* **1996**, 325, 151-160.
 - (27) Novak, T. J.; Daasch, L. W.; Epstein, J. *Anal. Chem.* **1979**, 51, 1271-1275.
 - (28) Niewenhuizen, M. S.; Harteveld, J. L. N. *Sens. Actuators B* **1997**, 40, 167-173.
 - (29) Steiner, W. E.; Klopsch, S. J.; English, W. A.; Clowers, B. H.; Hill, H. H. *Anal. Chem.* **2005**, 77, 4792-4799.
 - (30) Sohn, H.; Letant, S.; Sailor, M. J.; Trogler, W. C. *J. Am. Chem. Soc.* **2000**, 122, 5399-5400.
 - (31) De Silva, A. P.; Gunaratne, H. Q. N.; Gunnlaugsson, T.; Huxley, A. J. M.; McCoy, C. P.; Rademacher, J. T.; Ric, T. E. *Chem. Rev.* **1997**, 97, 1515-1566.
 - (32) Van Houten, K. A.; Heath, D. C.; Pilato, R. S. *J. Am. Chem. Soc.* **1998**, 120, 12359-12360.
 - (33) Zhang, S. -W.; Swager, T. *J. Am. Chem. Soc.* **2003**, 125, 3420-3421.
 - (34) Dale, T. J.; Rebek, J. Jr. *J. Am. Chem. Soc.* **2006**, 128, 4500-4501.
 - (35) For some recent reactive sensors which utilize PET or fluorescence resonance

- energy transfer (FRET) see: (a) Zhang, H.; Rudkevich, D. M. *Chem. Commun.* **2007**, 1238-1239. (b) Tal, S.; Salman, H.; Abraham, Y.; Botoshansky, M.; Eichen, Y. *Chem.-Eur. J.* **2006**, *12*, 4858-4864. (c) Albers, A. E.; Okreglak, V. S.; Chang, C. J. *J. Am. Chem. Soc.* **2006**, *128*, 9640-9641. (d) Knapton, D.; Burnworth, M.; Rowan, S. J.; Weder, C. *Angew. Chem., Int. Ed.* **2006**, *45*, 5825-5829.
- (36) Lakowicz, J. R. *Principles of Fluorescence Spectroscopy*; 2nd ed., Plenum Publishing Corp.: New York, 1999.
- (37) (a) Sapsford, K. E.; Berti, L.; Medintz, I. L. *Angew. Chem., Int. Ed.* **2006**, *45*, 4562-4588. (b) Juskowiak, B. *Anal. Chim. Acta* **2006**, *568*, 171-180. (c) Valeur, B. *Molecular Fluorescence. Principles and Applications*; Wiley-VCH: Weinheim, Germany, 2002.
- (38) The US Department of Health and Human Services link: <http://www.bt.cdc.gov/agent/phosgene/basics/facts.asp>.
- (39) (a) Yun, K.-Y.; Baek, W.-W.; Choi, N.-J.; Lee, D.-D.; Kim, J.-C.; Huh, J.-S. *Chem. Sens.* **2004**, *20*, 668-669. (b) Harig, R.; Rusch, P.; Dyer, C.; Jones, A.; Moseley, R.; Truscott, B. *Proc. SPIE-The International Society for Optical Engineering* **2005**, 5995, 599510/1-599510/12. (c) Toon, G. C.; Blavier, J. -F.; Sen, B.; Drouin, B. J. *Geophys. Res. Lett.* **2001**, *28*, 2835-2838. (d) Hill, H. H.; Martin, S. J. *Pure Appl. Chem.* **2002**, *74*, 2281-2291.

- (40) Frye-Mason, G.; Leuschen, M.; Wald, L.; Paul, K.; Hancock, L. F. *Proc. SPIE-The International Society for Optical Engineering* **2005**, 5778, Pt. 1, 337-346.
- (41) (a) Gilat, S. L.; Adronov, A.; Frechet, J. M. J. *Angew. Chem., Int. Ed.* **1999**, 38, 1422-1427. (b) Castellano, R. K.; Craig, S. L.; Nuckolls, C.; Rebek, Jr., J. *J. Am. Chem. Soc.* **2000**, 122, 7876-7882. (c) Kishimoto, A.; Mutai, T.; Araki, K. *Chem. Commun.* **2003**, 742-743.
- (42) (a) Bigi, F.; Maggi, R.; Sartori, G. *Green Chem.* **2000**, 2, 140-148. (b) Cotarca, L.; Delogu, P.; Nardelli, A.; Sunjic, V. *Synthesis* **1996**, 5, 553-576.
- (43) The formation of urea **9** under these conditions was confirmed by ^1H NMR spectroscopy. In addition to **9**, two other, symmetrical ureas **7**, **8** are also formed with two donor or two acceptor fragments. However, they do not emit fluorescence around 464 nm upon excitation at $\lambda = 343$ nm at these concentrations.
- (44) Some possible exceptions could be thionyl chloride (S(O)Cl_2), oxalyl chloride ($(\text{COCl})_2$), or dimethyl carbonate ($(\text{CH}_3\text{CO})_2\text{O}$). However, as liquid at rt, none of them has vapor pressure over 10% of phosgene.
- (45) (a) Stigliani, W. M.; Spiro, T. G.; *Chemistry of the Environment*; 2nd ed., Prentice Hall: Upper Saddle River, USA, 2003, pp. 3-178; (b) Schimel, D. S.; House, J. I.; Hibbard, K. A.; Bousquet, P.; Ciais, P.; Peylin, P.; Braswell, B. H.; Apps, M. J.; Baker, D.; Bondeau, A.; and et al. *Nature* **2001**, 414, 169-172;

- (46) (a) Dell' Amico, D. B.; Calderazzo, F.; Labella, L.; Marchetti, F.; Pampaloni, G. *Chem. Rev.* **2003**, *103*, 3857-3898. (b) McGhee, W. D.; Riley, D.; Christ, K.; Pan, Y.; Parnas, B. *J. Org. Chem.* **1995**, *60*, 2820-2830. (c) Waldman, T. E.; McGhee, W. D. *J. Chem. Soc., Chem. Comm.* **1994**, 957-958. (d) Salvatore, R. N.; Shin, S. I.; Nagle, A. S.; Jung, K. W. *J. Org. Chem.* **2001**, *66*, 1035-1037. (e) Aresta, M.; Quaranta, E. *Tetrahedron* **1992**, *48*, 1515-1530.
- (47) (a) Yamaguchi, T.; Boetje, L. M.; Koval, C. A.; Noble, R. D.; Bowman, C. N. *Ind. Eng. Chem. Res.* **1995**, *34*, 4071-4077. (b) Yamaguchi, T.; Koval, C. A.; Nobel, R. D.; Bowman, C. N. *Chem. Eng. Sci.* **1996**, *51*, 4781-4789. (c) Sada, E.; Kumazawa, H.; Han, Z. *Chem. Eng. J.* **1985**, *31*, 109-115. (d) Kovvali, A. S.; Sirkar, K. K. *Ind. Eng. Chem. Res.* **2001**, *40*, 2502-2511.
- (48) Bates, E. D.; Mayton, R. D.; Ntai, I.; Davis, Jr., J. H. *J. Am. Chem. Soc.* **2002**, *124*, 926-927.
- (49) Ki, C. D.; Oh, C.; Oh, S.-G.; Chang, J. Y. *J. Am. Chem. Soc.* **2002**, *124*, 14838-14839.
- (50) Hampe, E. M.; Rudkevich, D. M. *Tetrahedron* **2003**, *59*, 9619-9625.
- (51) (a) Lehn, J.-M. *Chem.-Eur. J.* **1999**, *5*, 2455-2463. (b) Rowan, S. J.; Cantrill, S. J.; Cousins, G. R. L.; Sanders, J. K. M.; Stoddart, J. F. *Angew. Chem., Int. Ed.* **2002**, *41*, 898-952.
- (52) (a) George, M.; Weiss, R. G. *J. Am. Chem. Soc.* **2001**, *123*, 10393-10394. (b) George, M.; Weiss, R. G. *Langmuir* **2002**, *18*, 7124-7135. (c) Carretti, E.; Dei, L.; Baglioni, P.; Weiss, R. G. *J. Am. Chem. Soc.* **2003**, *125*, 5121-5129. (d)

- George, M.; Weiss, R. G. *Langmuir* **2003**, *19*, 1017-1025. (e) George, M.; Weiss, R. G. *Langmuir* **2003**, *19*, 8168-8176.
- (53) Terech, P.; Weiss, R. G. *Chem. Rev.* **1997**, *97*, 3133–3159.
- (54) Xu, H.; Hampe, E. M.; Rudkevich, D. M. *Chem. Commun.* **2003**, 2828-2829.
- (55) Xu, H.; Rudkevich, D. M. *Chem.-Eur. J.* **2004**, *10*, 5432-5442.
- (56) Rudkevich, D. M.; Xu, H. *Chem. Commun.* **2005**, 2651-2659.
- (57) (a) Steed, J. W.; Atwood, J. L. *Supramolecular Chemistry*; John Wiley & Sons Ltd.: Chichester, UK, 2000. (b) Beer, P. D.; Gale, P. A.; Smith, D. K. *Supramolecular Chemistry*; Oxford University Press: Oxford, UK 1999. (c) Dodziuk, H. *Introduction to Supramolecular Chemistry*; Kluwer Academic Publishers: Dordrecht, Netherlands, 2002.
- (58) *Comprehensive Supramolecular Chemistry; Vol 1. Molecular Recognition: Receptors for Cationic Guests*; Gokel, G. W.; *Vol. 2. Molecular Recognition: Receptors for Molecular Guests*; Vögtle, F.; Elsevier Science: Oxford, UK, 1996.
- (59) Stastny, V.; Rudkevich, D. M. *J. Am. Chem. Soc.* **2007**, *129*, 1018-1019.
- (60) Xu, H.; Rudkevich, D. M. *Org. Lett.* **2005**, *7*, 3223-3226.
- (61) Ciferri, A. *Supramolecular Polymers*; 2nd ed., CRC Press: Boca Raton, USA, 2005.
- (62) Pedersen, C. J.; Frensdorff, H. K. *Angew. Chem., Int. Ed. Engl.* **1972**, *11*, 16-25.

- (63) (a) Arnaud-Neu, F.; Collins, E. M.; Deasy, M.; Ferguson, G.; Harris, S. J.; Kaitner, B.; Lough, A. J.; McKervey, M. A.; Marques, E.; Ruhl, B. L.; and et al. *J. Am. Chem. Soc.* **1989**, *111*, 8681-8691.
- (64) a) Gutsche, C. D.; Iqbal, M. *Org. Synth.* **1990**, *68*, 234-237; (b) Gutsche, C. D.; Levine, J. A.; Sujeeth, P. K. *J. Org. Chem.* **1985**, *50*, 5802-5806.
- (65) Yamada, A.; Murase, T.; Kikukawa, K.; Matsuda, T.; Shinkai, S. *Chem. Lett.* **1990**, 455-458.
- (66) (a) Liu, Y.; Jessop, P. G.; Cunningham, M.; Eckert, C. A.; Liotta, C. L. *Science* **2006**, *313*, 958-960. (b) Jessop, P. G.; Heldebrant, D. J.; Li, X.; Eckert, C. A.; Liotta, C. L. *Nature* **2005**, *436*, 1102.
- (67) (a) Ballivet-Tkatchenko, D.; Camy, S.; Condoret, J. S. *Environ. Chem.* **2005**, 541-552. (b) Beckman, E. J. *Chem. Commun.* **2004**, 1885-1886.
- (68) McKervey, M. A.; Seward, E. M.; Ferguson, G.; Ruhl, B.; Harris, S. J. *J. Chem. Soc., Chem. Commun.* **1985**, *7*, 386-388.
- (69) Arduini, A.; Pochini, A.; Reverberi, S.; Ungaro, R. *J. Chem. Soc., Chem. Commun.* **1984**, 981.

BIOGRAPHICAL INFORMATION

Hexiang Zhang, born in 1979 in Tangshan, Hebei Province, P.R.China, obtained his B.S. in 2001 from Dalian University of Technology, Dalian, China. He came to The United States in 2004 and began his M.S. study at the University of Texas at Arlington under the supervision of Professor Dmitry. M. Rudkevich. He received his M.S. degree in Chemistry in 2007. His research interests are in supramolecular chemistry on carbon dioxide.